SEQUENCE STRATIGRAPHY OF THE LATE PLEISTOCENE - HOLOCENE DEPOSITS ON THE NORTHWESTERN MARGIN OF THE SOUTH CASPIAN BASIN

A Thesis

by

OGTAY RASIM RAHMANOV

Submitted to the Office of Graduate Studies of
Texas A&M University
in partial fulfillment of the requirements for the degree of

MASTER OF SCIENCE

August 2003

Major Subject: Geophysics

SEQUENCE STRATIGRAPHY OF THE LATE PLEISTOCENE - HOLOCENE DEPOSITS ON THE NORTHWESTERN MARGIN OF THE SOUTH CASPIAN BASIN

A Thesis

by

OGTAY RASIM RAHMANOV

Submitted to Texas A&M University
in partial fulfillment of the requirements
for the degree of

MASTER OF SCIENCE

Approved as to style and content by:

Joel S. Watkins (Chair of Committee)	Luc T. Ikelle (Member)
Duane A. McVay (Member)	Andrew Hajash (Head of Department)

August 2003

Major Subject: Geophysics

ABSTRACT

Sequence Stratigraphy of the Late Pleistocene - Holocene Deposits on the Northwestern Margin of the South Caspian Basin. (August 2003)

Ogtay Rasim Rahmanov, B.S., Azerbaijan State Oil Academy

Chair of Advisory Committee: Dr. Joel S. Watkins

Interpretation of 900 km of a closely spaced grid of high-resolution seismic profiles over the northwestern margin of South Caspian Basin (SCB) allows recognition and study of six late Pleistocene - Holocene depositional sequences.

Sequence stratigraphy analysis of sedimentary strata from 117,000 years B.P. to present led to the identification of a highstand systems tract, two transgressive systems tracts and six lowstand systems tracts. Each systems tract is characterized by specific seismic facies. Diverse depositional processes on the northwestern margin of the SCB are suggested by the thirteen seismic facies patterns recognized in the study area. Two distinct progradational complexes were interpreted within Sequence III and Sequences IV and V in the northeastern and northwestern parts of the study area, respectively. Stratigraphic interpretation of the sequences provided important information on parameters that control depositional architectures, such as lake level fluctuations, tectonic dynamics, and sediment supply.

High sedimentation rates combined with a series of high-frequency and high-amplitude lake-level fluctuations, abrupt changes at the shelf edge, abnormally high formation pressure, and high tectonic activity during Quaternary time resulted in the

development of a variety of complex geologic drilling hazards. I distinguished three types of hazards as a result of this study: mud volcanoes, sediment instability, and shallow gas.

The 2D high-resolution seismic dataset from the northwestern margin of the SCB allowed more detailed seismic sequence stratigraphic analysis in the study area than has previously been attempted. In particular, it has a clear application in deciphering sediment supply and relative lake level changes as well as tectonic relationship of the northwestern shelf margin of the SCB.

Results of this work led us towards better understanding of recent depositional history, improved our knowledge of the nature of the basin tectonics, climate history and styles of and controls on sedimentation processes within a sequence stratigraphic framework during the late Pleistocene-Holocene time.

DEDICATION

I dedicate this thesis to my wife **Aynur** and daughter **Aydan**.

ACKNOWLEDGEMENTS

I would like to express my sincere appreciation to my committee chairman, Dr. Joel Watkins for his guidance, support and encouragement during my graduate study at Texas A & M and preparation of this thesis.

I would like to thank Dr. Luc Ikelle and Dr. Duane McVay for their advice and suggestions, and for their service as members of my graduate advisory committee.

I am very grateful to all my friends, particularly Nazim Abdullayev and Hasan Asgarov for their help and advice during my attendance of this university.

Moreover, I wish to acknowledge the BP for providing scholarship and the data for this study. Special thanks go to Neil Piggott and Greg Riley for pioneering and founding of this scholarship program.

Finally, I don’t have words to express my thanks to Aynur, my wife. Your love, support and patience during this whole experience were just what I needed. I will always be grateful to you for your willingness to endure and sacrifice.

TABLE OF CONTENTS

CHAPTER Page

LIST OF FIGURES

FIGURE Page

FIGURE Page

LIST OF TABLES

CHAPTER I

INTRODUCTION

The Caspian Sea is the largest inland water body of the world, which is situated in the south-central Eurasia. The Caspian Sea can be divided into three discrete basins with completely different origins based on the physico-geographical characteristics (Figure 1.1). These are the North Caspian Basin, which is a shallow water area, the Central Caspian basin and the South Caspian Basin. The border between the North Caspian Basin and the Central Caspian Basin runs over the Mangyshlak Meganticline. The Central and South Caspian Basins (SCB) are separated by the Apsheron Sill, beneath which the giant Azeri-Chirag-Guneshli "megastructure" is being developed.

The SCB is located between 36.5°N to 40°N latitude and 48°E to 53°E longitude. The SCB is occupies an area approximately of 120,000 km^2. The SCB is surrounded by mountainous regions and lies in an intermediate position between the Greater and Lesser Caucasus to the west, the Kopet Dag Mountains to the east, and the Talysh Mountains to the southwest, and is bordered to the south by the Iranian blocks with the Albors belt. The northern margin of the SCB is defined by the Apsheron Sill, a linear anticlinal structure that coincides with a seismically active zone extending from the Caucasus Mountains in the west to the Kopet Dag Mountains in the east (Mangino and Priestley, 1998).

This thesis follows the style and format of the American Association of Petroleum Geologists Bulletin.

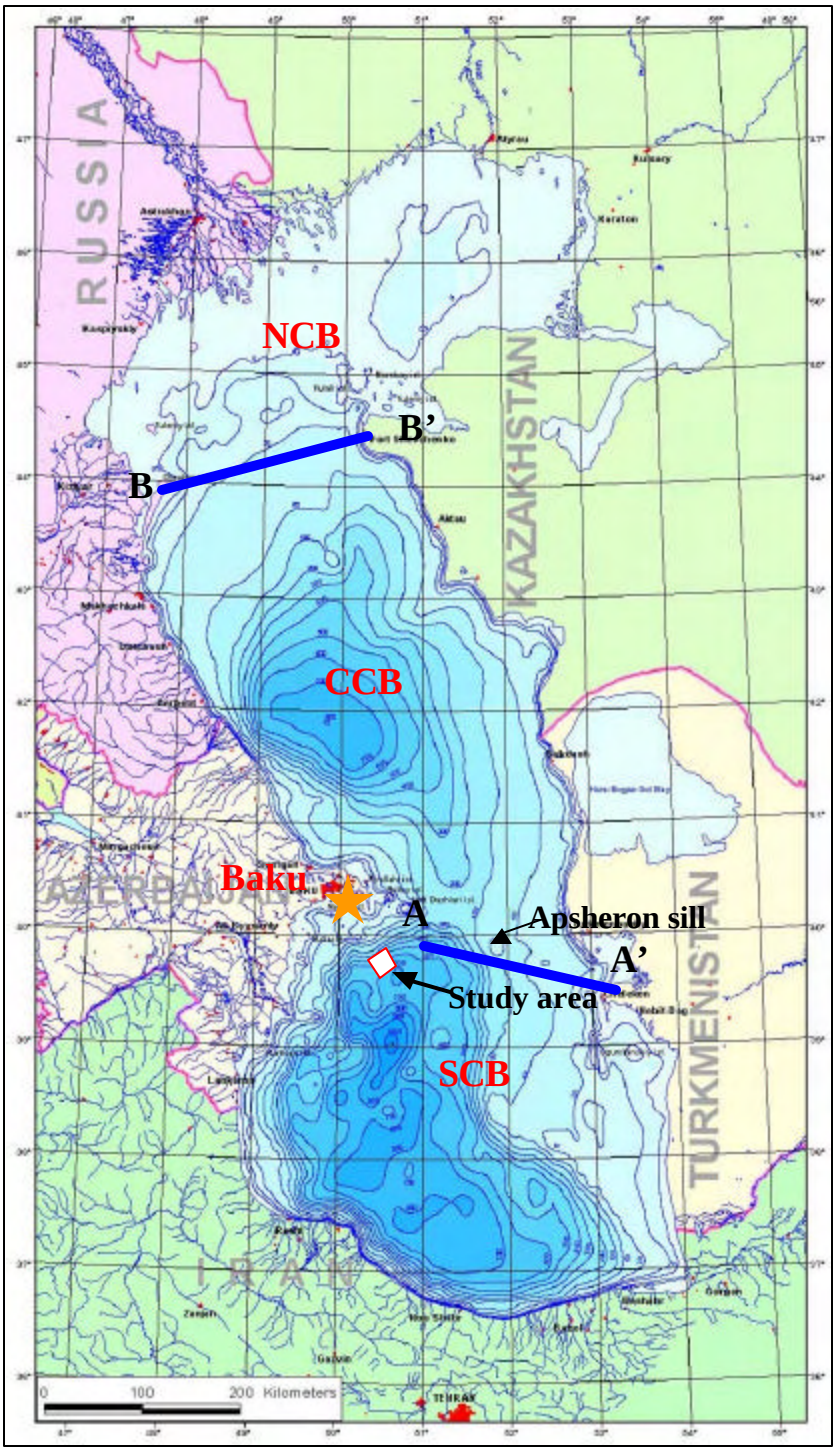

Figure 1.1. Location of the study area. SCB=South Caspian Basin; CCB= Central Caspian Basin; NCB=North Caspian Basin; AA'=border line between SCB and CCB; BB'=border line between CCB and NCB (modified from http://scf.usc.edu/~bagirov/azeri.htm).

The SCB is an old and prolific hydrocarbon producing basin. The largest fields are Azeri-Chirag-Guneshli (combined recoverable reserves 5.3 billion bbl of oil), Neft Dashlary (1.2 billion bbl) and Shah Deniz (35 TCF of gas) (Belopolsky and Talwani, 2000).

The study area is located on the continental shelf and slope on the northwestern margin, adjacent to the deepest part of the SCB, approximately 80 km southeast of Baku, Azerbaijan (Figure 1.1). The water depths range from 33 m to 455 m.

The study area is characterized by a gently dipping (~ 0.25 to 0.5 degree) shelf to the north and west, and a moderately dipping (~ 1.5 to 2.0 degree) slope region to the south and southwest beyond the shelf edge. An extensive region of mass wasting underlies the eastern portion of the study area. Slopes within the region of mass wasting locally exceed 20 degrees with average slopes typically in excess of 5 degrees (Figure 1.2).

High sedimentation rates combined with a series of high-frequency and high-amplitude lake-level fluctuations, abrupt changes at the shelf edge, abnormally high formation pressure, and high tectonic activity during Quaternary time resulted in the development of a variety of complex geologic drilling hazards.

This project involved the seismic sequence stratigraphy analysis of the Quaternary deposits in the continental shelf and slope in order to obtain a better understanding of the depositional history. The study of the recent depositional history expands knowledge of the nature of the basin tectonics, climate history and styles of and controls on sedimentation within a sequence stratigraphic framework during the

Quaternary. This study also carried out more detailed seismic sequence stratigraphic analysis in the study area than has previously been attempted. It has clear application in deciphering sediment supply and relative lake level changes as well as tectonic relationship of the northwestern shelf margin of the SCB.

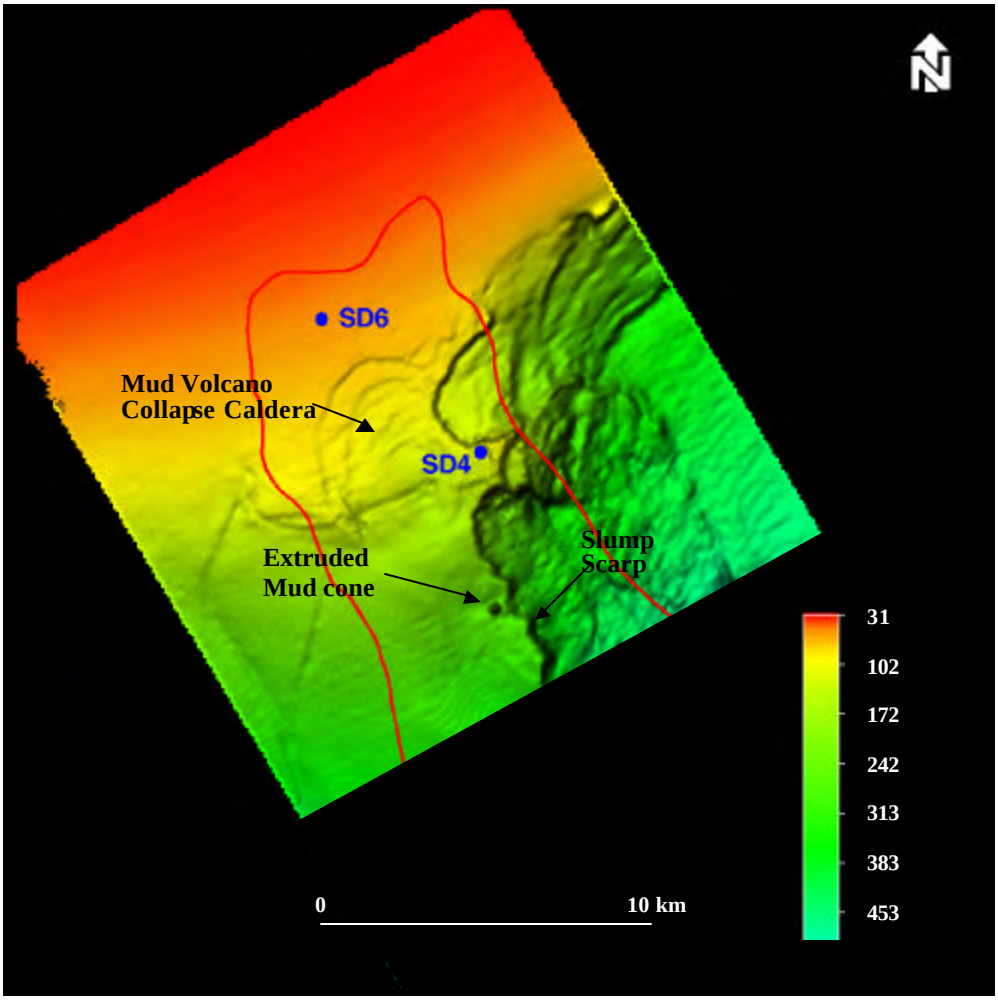

Figure 1.2. Bathymetry map of the study area, showing general slope to the southeast, mud volcano features and the significant mass wasting and slumping that has occurred in the eastern/southeastern part. Depth ranges from 30 to 455 m (red shallow). SD4 and SD6 are well locations (modified from Fowler et al., 2000).

Objectives

The main purpose of this study is to evaluate and demonstrate a sequence stratigraphic model of the Quaternary deposits in the continental shelf and slope on the northwestern margin of the SCB. The study of the recent depositional history allows us to expand knowledge of the nature of the basin tectonic, climate history and the styles of and controls on sedimentation within a sequence stratigraphic framework during the Quaternary.

Location

The study area covers approximately 400 km^2 located on the northwestern margin, adjacent to the deepest part of the SCB, approximately 80 km southeast of Baku, Azerbaijan with water depth ranging from 33 to 455m (Figure 1.1).

Data Quality

The data set for this study was provided by BP Exploration Operating Company and comprised the 1997 Regional 2D high-resolution seismic survey and stratigraphic ages from boreholes. The study used 1x1 km grid of high-resolution 2D seismic lines covers an area of 400 km^2 (Figure 1.3). More than 40 seismic lines were interpreted include about 900 km. The seismic dip orientation is northwest-southeast and the strike orientation is southwest-northeast. Seismic survey was shot and processed by Ensign

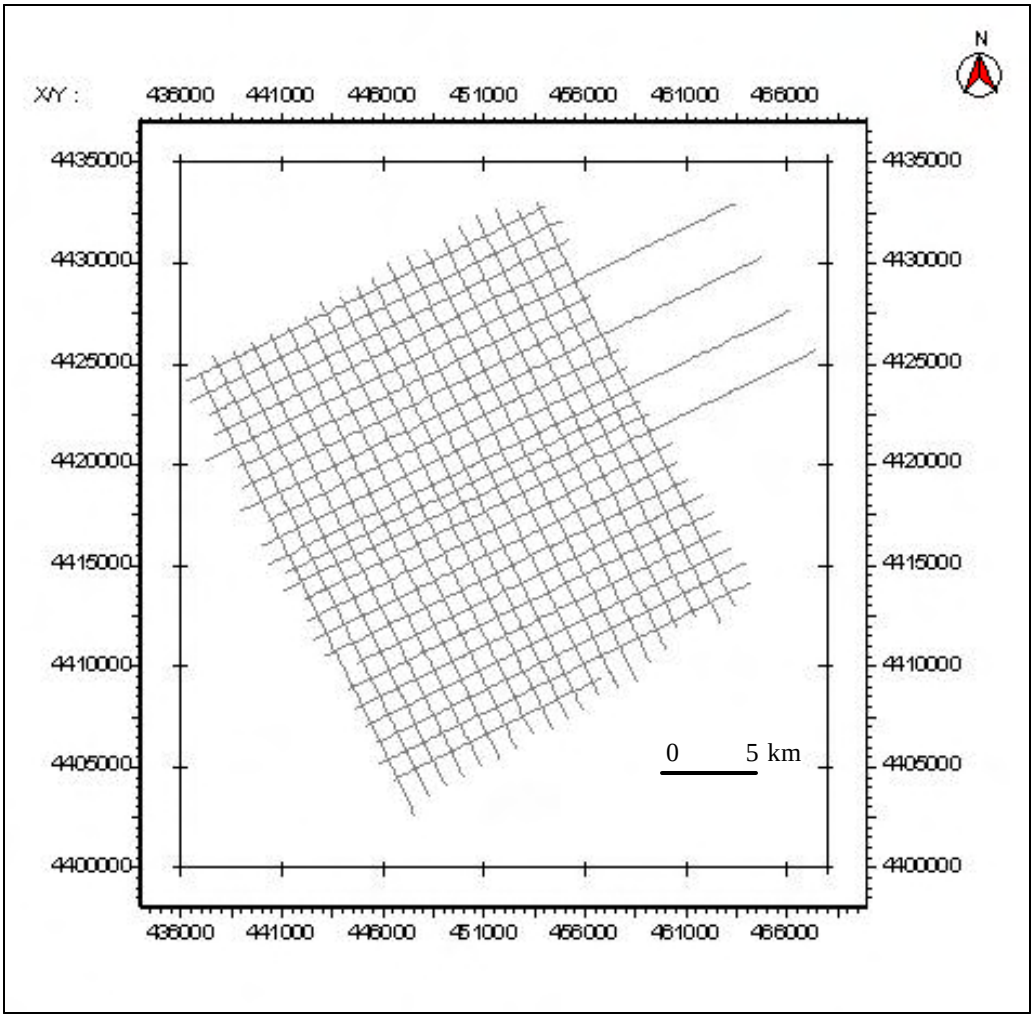

Figure 1.3. Basemap of the study area. The spacing grade of the seismic lines is 1 km.

Geophysics Limited in 1997. The record length of the data is 2.0 seconds and sample interval is 1 ms. Detailed acquisition parameters of time migrated seismic data are listed in Table 1.1. The reflection quality of the data is very good and faults and stratigraphic picks for horizons are easily recognizable. Seismic interpretation and seismic facies analysis are performed using The Kingdom Suite software version 7.2, which has been licensed to Texas A&M University by Seismic Micro-Technology, Inc.

Table 1.1. Detailed acquisition parameters of the study area.

Streamer	
Streamer Length	600 m (ITI streamer)
Number of Channels	48 per streamer
Group Length/Interval	12.5 m
Streamer Depth	3 m
Inline near offset distance	40-60 m
Source	
Source size	150 cubic inches, single GI gun
Operating Pressure	2000 PSI
Source Interval	12.5 m
Source Depth	3 m
Recording System	
Recording System	OYO-DAS 1
Recording Format	SEGD
Recording Length	2.0 seconds
Sample Interval	1 ms.

Stratigraphic ages from borehole samples have been dated using the radioisotope ^{14}Carbon-dating technique provided by BP Exploration Operating Company. Borehole information was used in this study to correlate seismic horizons to stratigraphic ages. Correlation of seismic horizons to regional stratigraphy is shown in Table 1.2.

Table 1.2. Correlation of seismic horizons to regional stratigraphy.

Period	Epoch	Time Startigraphical Unit		Approximate Age, BP	Seismic Horizon No.
QUATERNARY	Holo-cene	Novocaspian		10200	IV
	PLEISTOCENE	Kvalyn	Upper	26350	V
			Lower	51000	IV III
		Khazar	Upper	71000 117000	II I
			Lower		

Previous Studies

One of the first geological and stratigraphic interpretations of Quaternary sediments in the SCB has been provided by Lebedev (1987), based on shallow seismic profiles from the 1970's.

Comprehensive analysis of seismic stratigraphy in the SCB was first laid out by Mamedov (1992) that subdivided Tertiary deposits into several distinct seismic packages based on the major scale internal characteristics.

Bozkurt et al. (1997) interpreted the Pleistocene Paleo-Amu Darya shelf margin complex in the Turkmenistan sector of the SCB and identified several seismic sequences linked to fluctuations in the lake level of the Caspian Sea.

Work by Abdullayev (2000) documents the stratigraphic architecture of the Upper Pliocene and Quaternary sediments of the SCB. Abdullayev has identified a series of distinct depositional episodes and established the linkage between phases of sediment input and the distribution of depositional environments, controlled by the interplay between tectonic and climatic factors. This study shows that seismic stratigraphy works well on the Post-Productive Series, where all elements of shelf-margin to basin-floor deposition are present and readily identifiable, quite unlike the underlying Productive Series.

CHAPTER II

BACKGROUND

Tectonic Setting

The area of study is on the western shelf and slope of the SCB and lies on the Greater Caucasus – Kopet Dag portion of the southern margin of active plate convergence known as the Alpine – Himalayan orogenic belt (Kosarev and Yablonskaya, 1994).

Zonenshain and Le Pichon (1986) indicate that the semicontinuous series of mountain ranges of the Alpine – Himalayan belt result from the continental collision of the African, Arabian and Indian plates with the Eurasian plate.

The regional geologic history of the SCB relates to the Paleo Tethys Ocean. Lebedev et al. (1987) established that in the Middle Jurassic time the whole area of the Caspian Sea was part of a marine basin. It appears from the reconstruction of Philip et al. (1989) that during Jurassic, Cretaceous and Palaeogenic times subduction of the Tethys ocean occurred to the south of the Turkish, Lesser Caucasian and Iranian continental blocks. A marginal sea developed between these blocks and the Russian Platform. The Red Sea opened during the Middle-Late Miocene and the Arabian Plate began to move toward the north with respect to Africa. That caused a loss of area of the Paleo Tethys Ocean (Figure 2.1, Philip et al., 1989). Zonenshain and Le Pichon (1986) and Philip et al. (1989) theorized that after Tethys closed (at about 20 Ma), subduction shifted to the northern boundary of the marginal sea. Volcanism developed to the north of the new

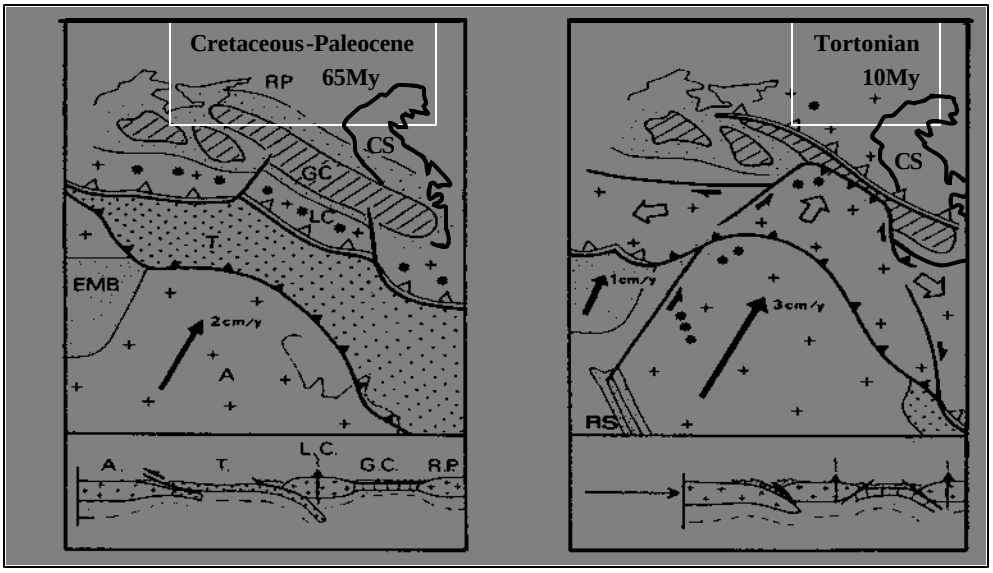

Figure 2.1. Geodynamics of the Caspian region. T=Tethys; CS=Caspian Sea; A=Arabian Plate; GC=Greater Caucasus; LC=Lesser Caucasus; RP=Russian Platform; EMB=Mediterranean basin; RS=Red Sea (modified from Philip et al., 1989).

subduction zone. The old marginal basin was rapidly shortened and was closed at the northern border of the Lesser Caucasus.

Kosarev and Yablonskaya (1994) indicate that separation of the Caspian Sea from the Black Sea area occurred during Middle Pliocene time. It has remained isolated from open marine influence for the entire Pliocene interval. Reynolds et al. (1998) and Jones and Simmons (1997) recognized the isolated nature of the SCB in the latest Miocene by a dramatic fall in sea level that left the SCB as a small, entirely isolated basin. Closure of the marginal sea left a relic oceanic crust underlying part of the Black Sea and SCB. Oceanic crust that underlies the SCB extends west to the Azerbaijan coast and northward beneath the Apsheron Sill. Thickness of the oceanic crust is 6 to 7 km in

the middle of the basin. Evidence for the presence of oceanic crust comes from seismic refraction and gravity data (Zonenshain and Le Pichon, 1986).

Continental collision, as observed at present, was characterized by the drift to the north of the Arabian plate and the lateral ejection of the Anatolian plate to the west and of the Iranian plate to the east (Figure 2.2, Philip et al., 1989).

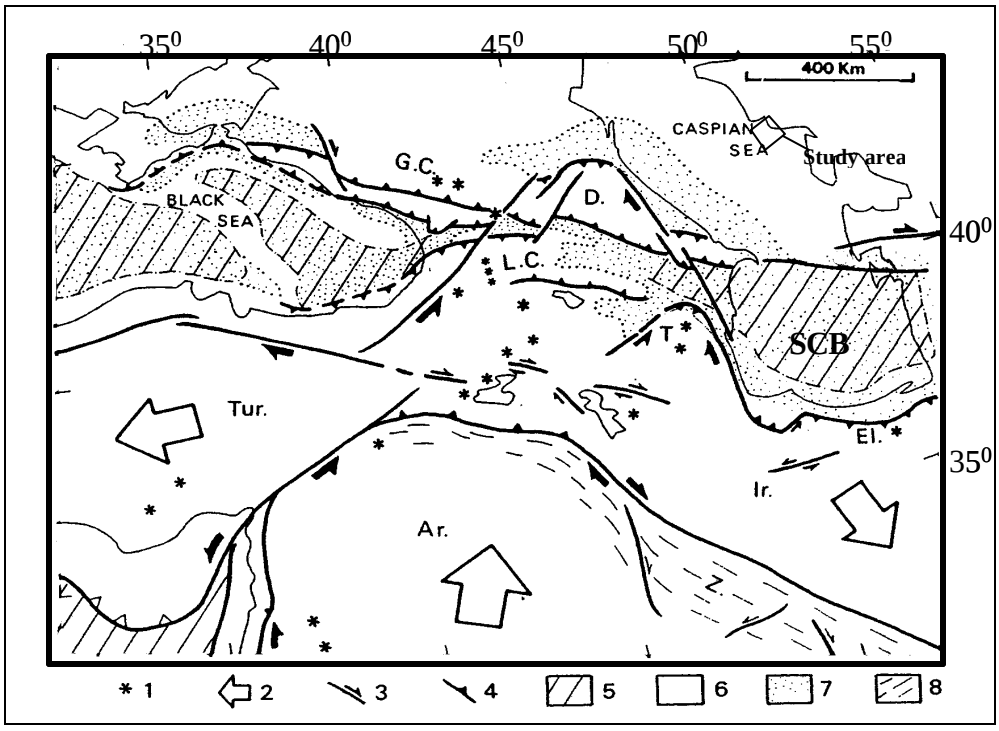

Figure 2.2. Present-day tectonic features. 1=Recent volcanoes; 2=Relative motion with respect to Eurasia; 3=Major strike-slip faults; 4=Major thrust faults; 5=Oceanic or intermediate crust; 6=Continental crust; 7=Sedimentary basins; 8=Recent folding; GC=Great Caucasus; LC=Lesser Caucasus; T=Talesh; El=Elbroz; Ir=Iranian Block; Ar=Arabian Plate; Tur=Turkish Block; SCB=South Caspain Basin (modified from Philip et al., 1989).

Abrams and Narimanov (1997) suggest that closure of the marginal sea and collision by late Miocene-Pliocene was accompanied by regional uplift and subsidence of the South Caspian oceanic crust, which led to the deposition of deltaic and lacusrine sediments. Large volumes of sediment influx up to 1300 m/m.y. were initiated by orogenic uplift of the surrounding land areas following the collision. The thickness of these sediments ranges from 10 to 15 km thickness near the basin edges and reaches more than 20 km in the deepest part of the basin.

Shale cored anticlinal folds formed within this sediment cover during Pliocene-Pleistocene folding episode. The folding was caused by regional compressional tectonics, differential loading and shale mobilization. These factors, as well as generation of hydrocarbons, led to mud diapirism and formation of mud volcanoes that actively seep (Guliev and Feizullayev, 1996).

Regional Stratigraphy

The stratigraphy of the SCB has been established on the basis of outcrop and deep exploration wells from the Upper Cretaceous to recent periods (Narimanov et al., 1998).

The Tertiary sedimentary section of the SCB is characterized by rapid deposition of thick sections of fluvial, deltaic and lacustrine sediment with the maximum thickness of the reservoir succession, known as the “Productive Series,” exceeding 4000 m. The main hydrocarbon-bearing formation within the SCB is the Middle Pliocene Productive

Series (Abrams and Narimanov, 1997). Traditionally, the Productive Series in the SCB is considered to have been delivered by three major river systems: the Paleo-Volga, the Paleo-Kura and the Paleo-Amu Darya. The interplay of these river systems is the most important factor for lithology distribution in the SCB. The Paleo-Kura and the Paleo-Amu Darya river systems transported sediment from the relatively local Kopet Dag, Talysh, Lesser Caucasus and Greater Caucasus mountain ranges. Much of this sediment is lithic rich and of poor reservoir quality. In contrast, the Paleo-Volga system is thought to have delivered a much more significant volume of high-quality reservoir into the SCB, with a longer sediment transport pathway that traverses the entire North Caspian Basin and Central Caspian Basin, from a sediment provenance region on the Russian Platform. The thick Productive Series interval drilled in the Azeri-Ghirag-Guneshli and Shah Deniz fields has been identified as being principally sourced by the Paleo-Volga River.

The deposits of the Productive Series are devoid of fauna and flora; as a consequence, their stratigraphic position is determined by faunal characteristics of the underlying Pontian and overlying Akchagyl stages. In Soviet literature stratigraphic divisions such as series are divided into a succession of “suites,” rather than formations (Reynolds et al., 1998). The Productive Series is divided into lower and upper substages and into several suites according to lithological composition. Interbedded open lacustrine shales vertically separate reservoirs. Frequent and large fluctuations in lake level associated with a low depositional gradient are thought to have resulted in laterally

extensive sand sheets and laterally extensive lacustrine shales (Buryakovsky et al., 2001).

The early Productive Series is dominated by quartz and minor sedimentary rock fragments typical of the Paleo-Volga provenance to the north. The late Productive Series contains less quartz, more feldspar, and fragments of both sedimentary and volcanic rock fragments more typical of sediments transmitted by the Paleo-Kura in the west (Abrams and Narimanov, 1997; Ruehlman et al., 1995).

The Upper Pliocene, which includes the Akchagyl and Apsheron stages, overlies the Productive Series. According to Narimanov (1993) this time is characterized by a large expansion of the basin along with intensive tectonic activity and onset of mud volcanoes. Kosarev and Yablonskaya (1994) and Narimanov (1990) recognized that during the Upper Pliocene time two major Akchagyl and Apsheron transgressions occurred. The Akchagyl transgression took place 2 to 3 Ma and the Apsheron occurred 0.7 to 2.0 Ma. During the Apsheron time, sea level was no more than 50 m, and it flooded a smaller area than did the Akchagyl transgression. At the end of the Apsheron time, a deep regression took place. The late Pliocene is marked by a flooding surface, a return to marine conditions and deposition of mudstone that acts as a seal to the Productive Series reservoir rocks. The Quaternary sediment overlying these rocks is the object of the study.

The Pleistocene-Pliocene boundary proposed by Narimanov (1990) coincides with the top of the Apsheron and the base of Tyurkyan Formation (0.95 to 1.07 Ma) of the SCB. The Quaternary history of the Caspian Sea is characterized by numerous

changes in lake level. The Quaternary stratigraphy of the SCB includes cyclic deposition sequences bounded by lowstand erosional unconformities. The Quaternary sequences resulted almost exclusively from alternating periods of increased and decreased sedimentation, associated with climate-driven fluctuations of the lake level (Kosarev and Yablonskaya, 1994). Detailed stratigraphic subdivision and correlation of the Quaternary deposits have been based on effects of climatic changes. The main feature of the SCB evolution in the upper Pliocene and Pleistocene ages is the sequence of repeated transgressions and regressions, with lake level fluctuations ranging up to 170 to 190 m in the Pleistocene. During the Pleistocene period three principal transgressions occurred; these are Baku, Khazar and Khvalyn, which were separated by Urunjik, Singil and Atelian regressions (Figure 2.3, Kosarev and Yablonskaya, 1994).

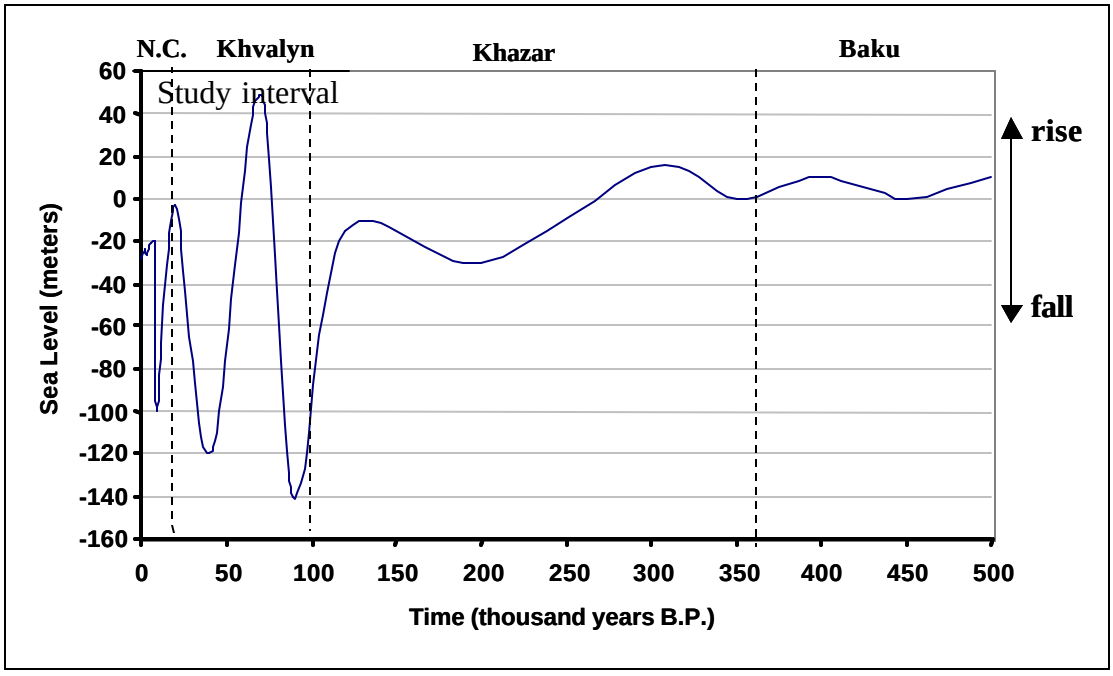

Figure 2.3. Relative change of Caspian Sea level between present day to 500,000 years B.P. (constructed from Kosarev and Yablonskaya, 1994).

The first transgressive peaks during the Novocaspian time are dated at about 9 ka B.P., when the sea surface was approximately at 25 m below sea level. This time corresponds to the beginning of the Holocene stage (Kosarev and Yablonskaya, 1994).

The fluctuations of the lake level exert a dominant control on the style and complexity of sedimentation, environment of deposition and organic life.

Geologic Drilling Hazards

This thesis also addresses geologic drilling hazards in the study area. Geologic drilling hazards are defined as a range of natural geological phenomena, existing or potential, which may affect the safety and would repress the development of petroleum provinces (Burdick and Richmond, 1982).

Based on geologic criteria, Bouma (1981) divided geologic drilling hazards into the following categories: seismicity and active faulting, near-surface fracturing of rocks, volcanism, sediment instability, erosion and sedimentation, ice scouring, permafrost and clathrates.

The SCB has a variety of complex geologic drilling hazards and active geological processes. A great concentration of geologic drilling hazards is present in the study area (Figure 2.4). Because of the relevance to the study area, some of the categories and processes from this group will be discussed in detail. These are mud volcanoes, sediment instability and shallow gas.

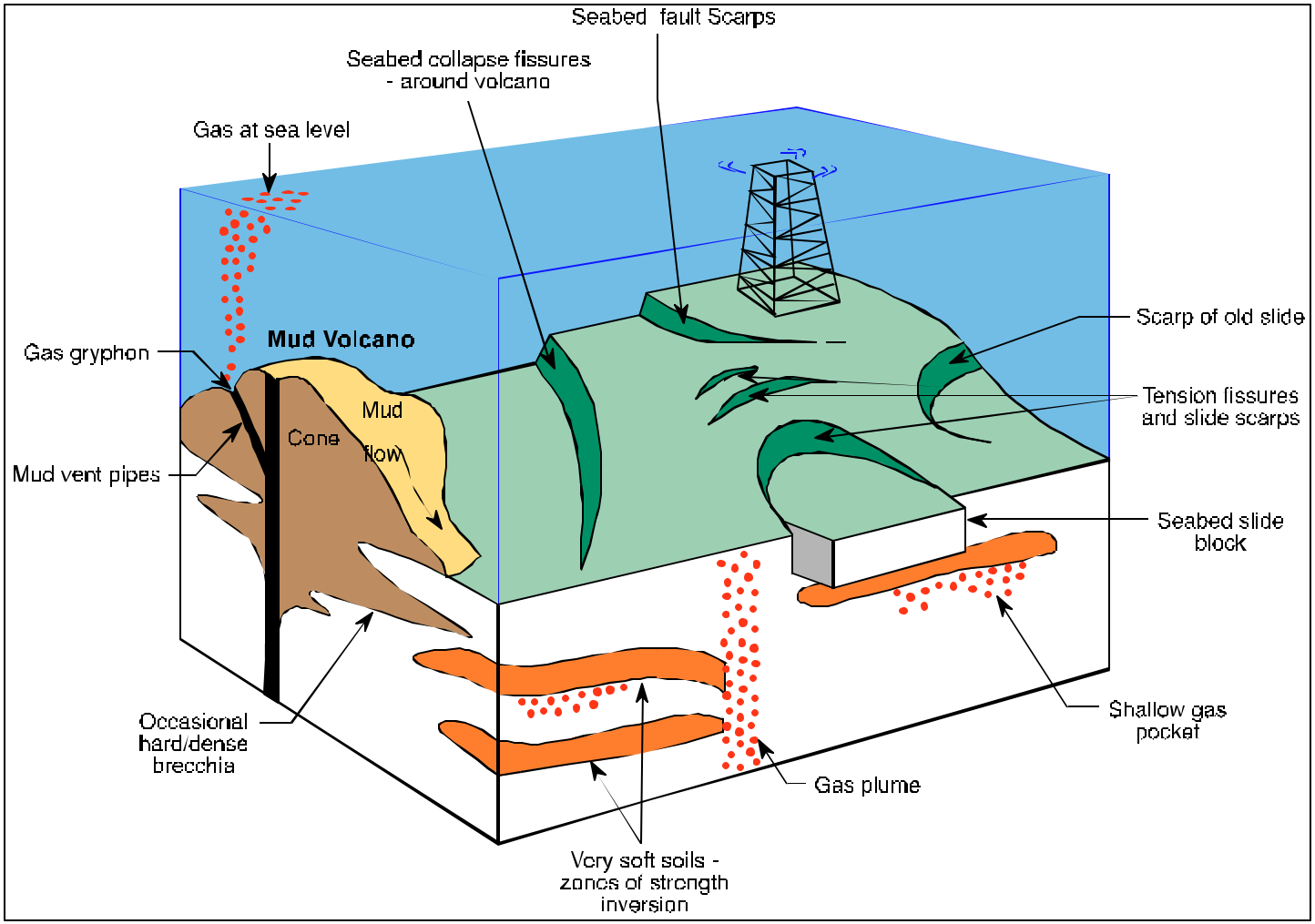

Figure 2.4. Generalized diagram showing a variety of complex geologic drilling hazards within a study area (modified from Nicholas et al., 2000).

Mud volcanoes

One of the characteristic features of Quaternary of the SCB is the abundance of mud volcanism. Mud volcanoes are considered hazardous to offshore facilities sited in volcanic mud areas. Mud flowing downhill along the slopes of a volcano can damage offshore structures, because mud volcanoes are usually associated with hydrocarbon fields (Lerche et al., 1997).

The SCB is a unique area where many mud volcanoes are concentrated. More than 300 mud volcanoes have already been recognized worldwide. However, the greatest concentration and most spectacular development of mud volcanoes are in Azerbaijan where there are over 220 of them (Rahmanov, 1987). Figure 2.5 shows a map of the distribution of mud volcanoes in the SCB.

Mud volcanoes usually form mounded or cone-like structures of varying size. They take the shape of circles, ellipsoids, calderas and truncated cones up to 500 m high and several kilometers wide. Mud volcanoes form from the accumulation of mud and clasts ejected through migration pathways along lines of weakness usually associated with faults for the release of pressure from overpressure zones up to 10 km deep (Guliyev and Feizullayev, 1996). The vented fluid can be composed of mud, clasts, brine, oil and/or gas. The venting style can vary from violent explosions of gas and mud to placid or gentle extrusions and can often vary from periods of activity to dormancy (MacDonald et al., 2000). The presence of the fluidized mud and free gas is clearly defined in the seismic data by the number of mud volcanoes that reach the seabed, as imaged on Figure 2.6. Guliyev and Feizullayev (1996) described the mud volcanoes as

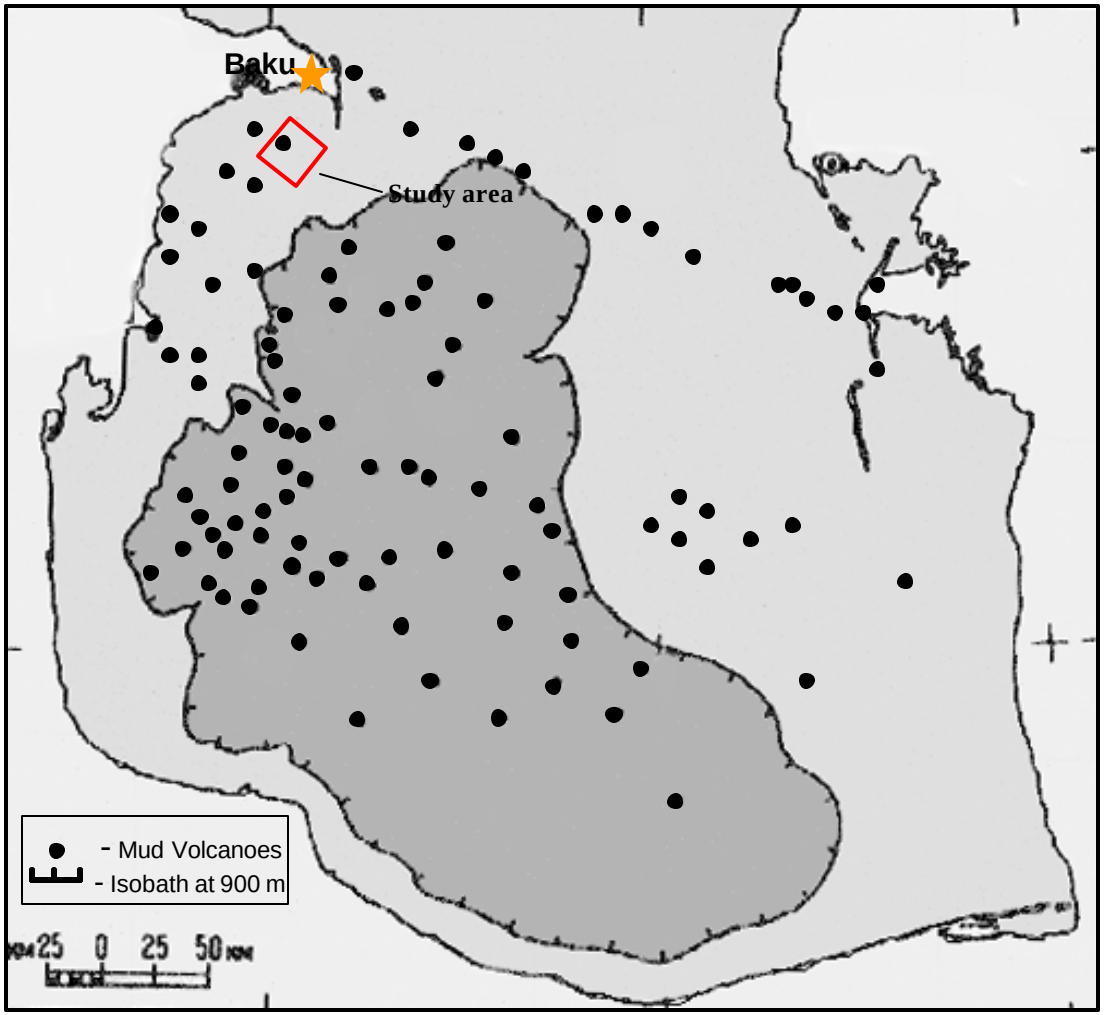

Figure 2.5. Distribution of mud volcanoes in the SCB (modified from Guliyev and Feizullayev, 1996).

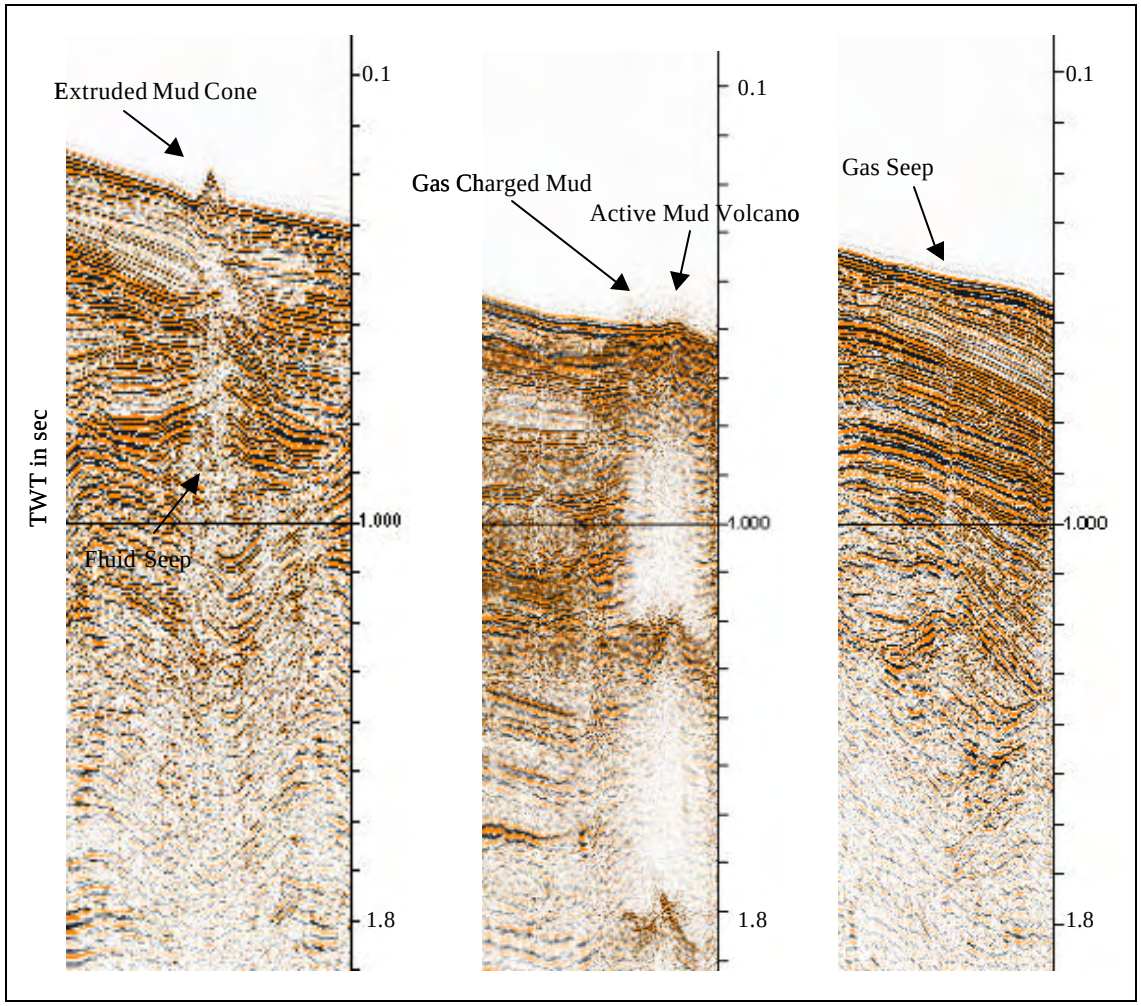

Figure 2.6. Presence of the fluidized mud and free gas is clearly defined in the study area by the number of mud volcanoes that reach the seabed.

not just simply point from which composition of mud, brine, gas or/and oil are actively flowing, but rather expressions of very deep-seated buildup of pressure far below the zones of hydrocarbon accumulation.

Lebedev et al. (1987) distinguished two types of mud volcanoes in the SCB. The first type is linked with faults in anticlinal and diapiric uplifts. This type of mud volcano usually forms a cone-like structure at the crest. The second type is linked with faults not only on the uplifts but also between them. Volcanoes of this type are dikes or stocks intruding into the sedimentary strata. Such volcanoes form a relatively small cone made up of mud-volcano products on the sea floor (Figure 2.7).

Observation of mud volcanoes over many years in Azerbaijan has enabled three characteristics of eruption activity to be recognized (Fowler et al., 2000):

(1) Explosive/Effusive – Explosions accompanied by the eruption of large volumes of argilaceous ground mass and rock fragments to form a “breccia” with or without ignited emission of a powerful stream of gas.
(2) Effusive – Ejection of mud-volcano breccia without intensive gas emissions.
(3) Extrusive – Very slow extrusion of breccia with insignificant emission of gas.

The main development factors of mud volcanism in the SCB are thick sections of Cenozoic deposits, the presence of a large volume of plastic shales, the presence of brine and hydrocarbon accumulations with abnormally high formation pressure, and high tectonic activity. The spatial relationship between mud volcanism and anticlinal growth

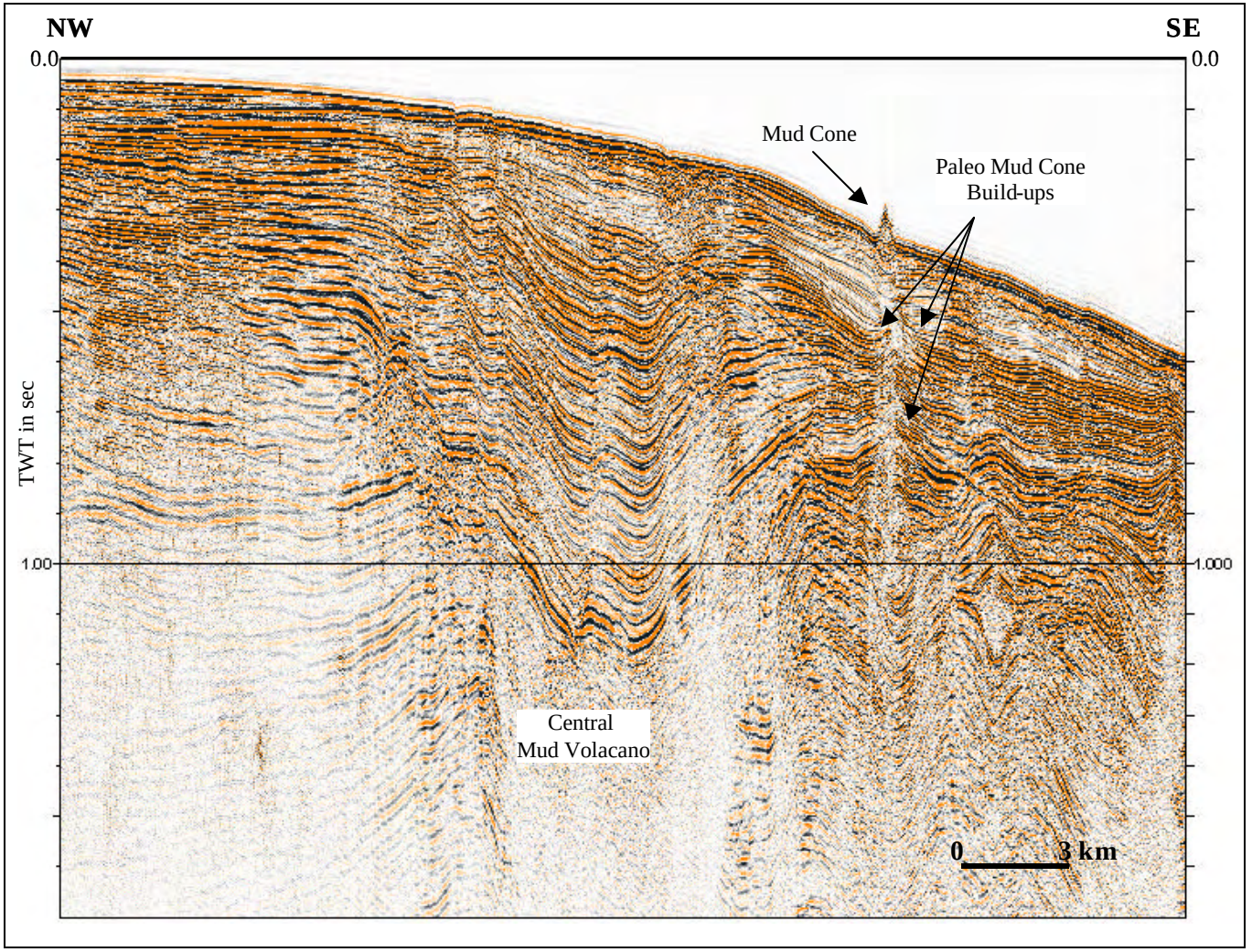

Figure 2.7. Seismic section shows the different style and geometry of the mud volcanoes that occur within the study area.

in the SCB is well-documented (Lebedev et al., 1987; Guliyev and Feizullayev, 1996). The thickness of Quaternary sediments reaches 2000 m, and basin subsidence during Quaternary period could be 1500 m. Such rapid sediment deposition led to the creation of zones with abnormally high formation pressure, which promoted the formation of mud volcanoes. Mud volcanoes became active in the Akchagyl time, but their major phase of activity is considered to have occurred during Quaternary, which nicely correlates with the period of active subsidence of the SCB (Lebedev et al., 1987).

In Azerbaijan the debris from the volcanoes contains clasts with ages from Cretaceous through Neogene. The main source for muds is predominantly the Maykop Formation (Oligocene-Miocene age), which is also the main hydrocarbon source in the SCB (Guliyev and Feizullayev, 1996).

Sediment instability

The other main geologic drilling hazard in the study area within Quaternary strata is sediment instability.

Mass transport is a serious hazard for bottom-founded structures and facilities because of the high contrasts in load-bearing capacities that exist between the failure zone and surrounding sediments (Bouma, 1981; Burdick and Richmond, 1982).

Sediment movement may cause loss of support for artificial structures and pipelines. Before any bottom-supported structures are recommended, the possibility of slope failure should be carefully assessed through geological and geophysical studies (Burdick and Richmond, 1982).

Sediment instability includes such processes as sliding, slumping, sediment creeps, liquefaction, and instabilities resulting from low degrees of consolidation, seeps, gas-charged sediments, tectonic activity, and diapirism (Bouma, 1981).

Sliding, slumping and sediment creep are types of downslope movements of sediments caused by gravity-driven processes. Sliding is defined as translational movement of rigid or semiconsolidated sediments along discrete shear planes subparallel to underlying beds. Slumping is a rotational movement of sediment failure along a discrete shear surface. Sediment creep means slow, nearly continuous downslope movement of top layers of an unconsolidated sediment unit (Burdick and Richmond, 1982).

These processes are greatly affected by the sedimentation rate. The high rates of sedimentation occasionally may restrain proper sediment dewatering processes and cause sediment material to be unconsolidated. Such sediments will have high pore pressure, reflecting high water content and low shear strength. Therefore, this layer of sediments becomes a potential sliding surface for overlaying normally compacted sediments (Bouma, 1981).

Evidence of historic sediment instability and mass wasting phenomena on the northwestern margin of the SCB has long been recognized (Lebedev et al., 1987). High sedimentation rates combined with high bathymetric gradients, tectonic instability, mud volcano activity and lake level fluctuations have caused extensive sediment instability and mass wasting phenomena during the area's geological history (Fowler et al., 2000).

The location of the study area on the continental shelf and slope on the northwestern margin of the SCB is important to the formation of mass wasting or sediment instability zones in the form of slides, slumps, and viscous debris flows for several reasons. In this environment of high sedimentation rates, abrupt changes in seabed at the shelf edge can cause rapid changes in the location, style and geometry of sediment accumulation. The reason for this could be the shelf/slope transition, sensitivity to fluctuations in lake level and sediment influx. This geologic environment is fundamentally unstable, which can result in the formation of slope failure along the shelf/slope transition. Sliding and slumping in this environment can form as a result of high sedimentation rates basinward of the shelf edge, enhanced subsidence rates, sediment unconsolidation and rapid progradation (Fowler et al., 2000).

The presence of sediment instability along shelf margins is well-documented in geologically similar environments such as the northern Gulf Coast Basin, which is characterized by high rates of sedimentation and enhanced subsidence rates (Edwards, 2000).

The study area reveals a suite of mass wasting and sediment instability that has affected an area of at least 140 km^2 in the eastern/southeastern part and, probably, a more extensive area to the northeast. Slumping generally occurred in the upper slope area, and detached slump materials rotated and were displaced downslope onto the middle of a lower slope. In addition, varying portions of the slump masses were further liquefied and transported basinward to deepwater as debris flows (Figure 2.8). Major debris flows can be seen, as well as slumping blocks where activation of shear planes has permitted rotational block faulting with the result that large, intact blocks of sediments have moved downslope without collapsing into a chaotic flow.

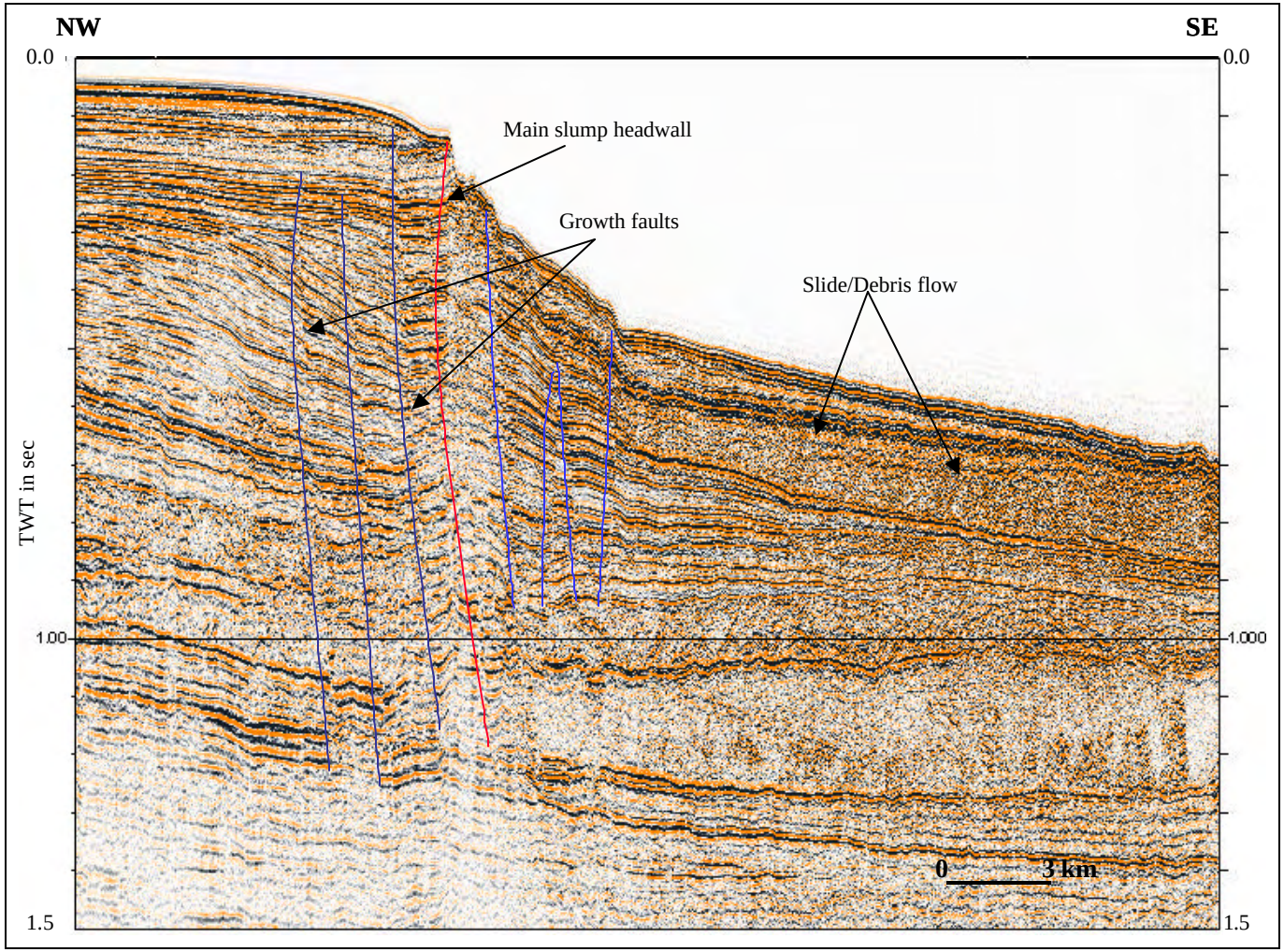

Figure 2.8. Sediment instability features in the study area.

Shallow gas

The presence of abundant shallow gas in the SCB has been documented by Lebedev et al. (1987) and Guliyev and Feizullayev (1996).

Shallow gas has the ability to alter the geotechnical, physical properties and behavior of the marine sediment in which they are present. This can have decisive significance for geophysical modeling studies and engineering applications, such as foundation design for offshore facilities (Murphy et al., 2002).

An extensive record of the well-control incidents in the SCB reflects encounters with shallow gas, and rigs have been lost due to blowouts and subsequent explosions.

Three main types of hazard are caused by shallow gas: gas-charged sediments, shallow-gas drilling hazards, and gas seeps (Bouma, 1981).

Gas-charged sediments were defined by Richmond and Burdick (1982) as "zones of unconsolidated to semiconsolidated sediments saturated with interstitial gas under normal to near-normal pressures."

Gas-charged sediment zones can pose an awkward drilling hazard because the load-bearing capacity usually differs greatly between these zones and surrounding sediments. The presence of gas may contribute to sediment instability by decreasing the shear strength of the sediments (Burdick and Richmond, 1982).

Shallow-gas zones are defined as accumulations of gas in shallow marine sediment with possible abnormal pore pressure. This gas may be of biogenic origin or gas that migrated from a deeper hydrocarbon reservoir and became trapped by structural or stratigraphic unconformity in near-surface rocks. Drilling through shallow-gas zones

may be dangerous because high-pressure gas may cause blowouts (Richmond and Burdick, 1982).

Gas seeps themselves do not create a geologic drilling hazard, but they indicate weaker zones that can be hazardous. Drilling through a fault along which gas migrates from a deeper pressurized gas zones may be a reason for blowout (Bouma, 1981).

The SCB contains a large distribution of shallow free gas and gas seeps. These features were originally inferred from the acoustic anomalies found on seismic data (Lebedev et al., 1987).

According to Lebedev et al. (1987), the factors that create favorable conditions for shallow gas in the SCB are high sedimentation rate, enormous thickness of sedimentary cover, abnormally high pressures, low heat flow, faulting and fracturing of the sedimentary cover and high tectonic activity.

The geology of the study area and analysis of free gas in the SCB suggest that the gases come from a wide variety of sources and a wide depth interval of generation and migration. Guliyev and Feizullayev (1996) recognized that in the SCB the main potential source of gas in shallow marine sediments can originate from biogenic or thermogenic sources. Biogenic gas originates from bacterial degradation of organic material at low temperatures and usually occurs in areas where sedimentation rates are high. Thermogenic gas is formed from high-temperature degradation and cracking of organic matter at considerable burial depths and requires migration pathways to reach the shallow marine sediments (Murphy et al., 2002).

High-resolution, 2D seismic data acquired across the study area have proven the existence of widespread seismic anomalies that are similar to features described from other regions and indicative of the presence of shallow gas in the sediment (Figure 2.9, Carlson et al., 1985).

Some of the common types of seismic responses associated with shallow free gas, which are present in the study area within Quaternary strata, are bright spots (anomalously high amplitude), phase reversal (negative reflection coefficient), velocity pull-down effects and acoustic blanking (strong masking of the underlying reflectors). Each one of these responses produces a different appearance on seismic data.

The most evident gas-related feature observed on the seismic profiles is bright spots. These appear as high amplitude events, as results of the large impedance contrast between gas and surrounding shallow sediments. Bright spots created by shallow gas can be distinguished from other bright-spot creating phenomena by a phase reversal associated with the event (Anderson and Bryant, 1990).

Acoustic blanking is another type of seismic anomaly created by shallow gas, which appears as a diffuse and chaotic seismic facies masking nearly all other reflections (Murphy et al., 2002). It most likely occurs when interstitial gas bubbles in the sediment absorb seismic energy, and results in the rapid attenuation or loss of the seismic wave energy (Anderson and Bryant, 1990).

The type of anomaly referred to as “velocity sag” is apparently caused by the lower compressional velocity of gas-charged zones than that of the same seismic wave traveling through normal sediments (Carlson et al., 1985).

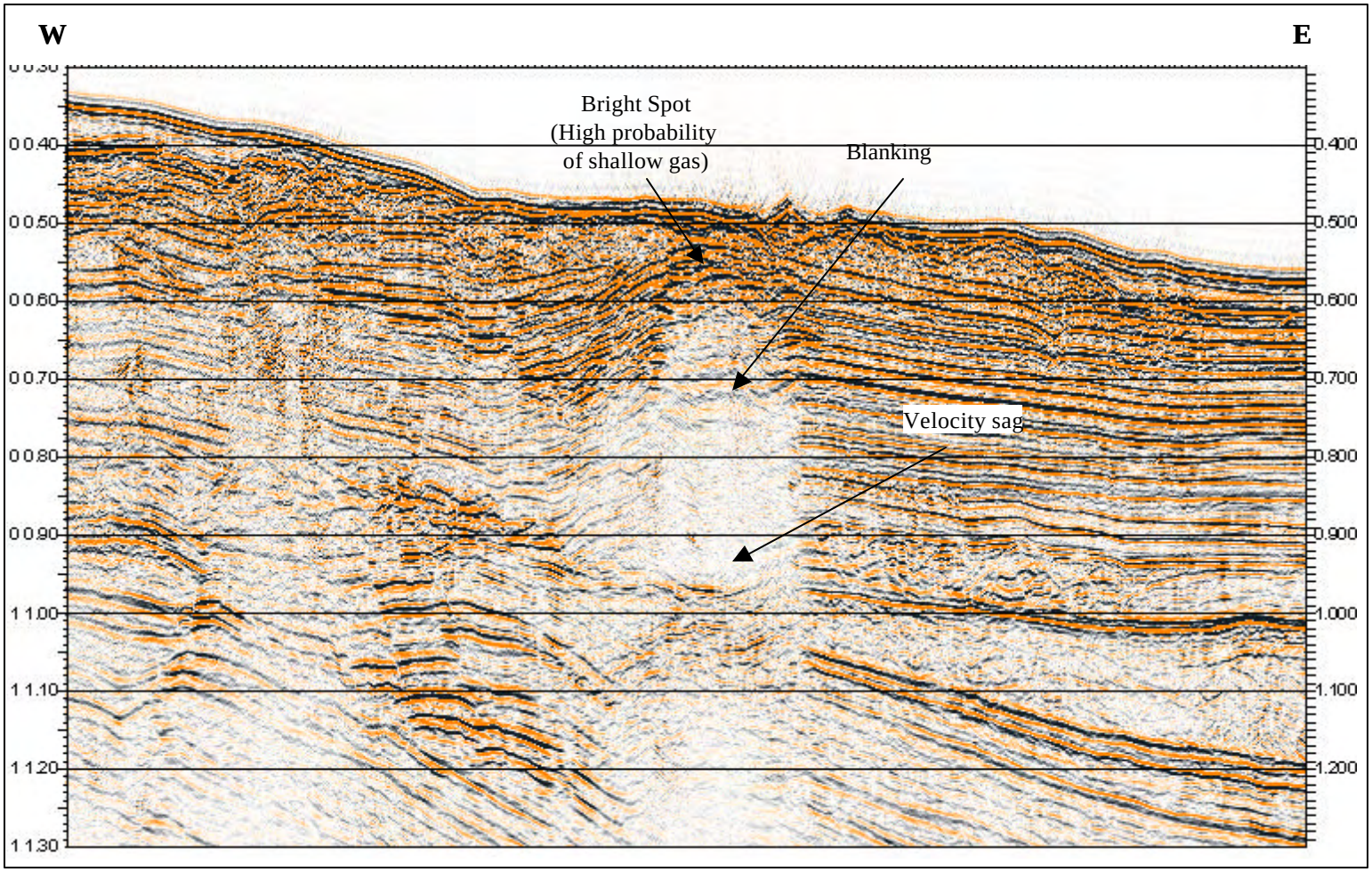

Figure 2.9. Bright spot and associated acoustic blanking are the most evident gas-related features observed on the seismic lines.

Significance of This Study

This project involved the study of the late Pleistocene-Holocene deposits in the continental shelf and slope on the northwestern margin of the SCB. The study of the recent depositional history expands the knowledge of the nature of the basin tectonics, climate history and styles of and controls on sedimentation within a sequence stratigraphic framework during the late Pleistocene-Holocene time.

Sequence stratigraphic interpretation gives important information on parameters that control depositional architectures, such as lake level fluctuation, tectonic dynamics and sediment supply.

The isolation of the SCB from the Tethys open-marine environment during the Middle Pliocene has given rise to rapid fluctuations in the lake level (Nummedal, 1999). The main controls on lake level and sediment supply are therefore likely to be interplay of climate and tectonics. Changes in lake level have a major impact on the rate of sediment supply, accommodation space and depositional environments.

The late Pleistocene-Holocene sedimentary strata of the SCB has clearly defined shelf margin and slope environments identifiable on seismic. Mapping of those sedimentary complexes helped to explain their spatial distribution and tie their onsets to dated lake level changes.

To do this, time horizons, faults, seismic facies and seismic sequence stratigraphy relations of the area are mapped and interpreted using 2D, high-resolution seismic and borehole datasets. Information gained from structural interpretation, seismic

facies and sequence stratigraphic analysis are used to acquire a better understanding of the depositional history of key sequences in the Quaternary interval.

The 2D high-resolution seismic and borehole dataset from the northwestern shelf margin of the SCB allows more detailed seismic-sequence stratigraphic analysis in the study area than has previously been attempted. In particular, it has a clear application in deciphering sediment supply and relative lake level changes as well as the tectonic relationship of the northwestern shelf margin of the SCB.

CHAPTER III

METHODOLOGY

Seismic Stratigraphy

The seismic data have been interpreted according to the basic seismic stratigraphic techniques described by Vail et al. (1977) and Vail (1987).

In this study I followed a procedure that involved three principal stages: (1) seismic sequence analysis, (2) seismic facies analysis and (3) interpretation of depositional environments.

Seismic sequence analysis divides the seismic section into a series of genetic reflection packages separated by surfaces of discontinuity defined by systematic reflection terminations. These packages of reflection are interpreted as depositional sequences consisting of genetically related strata and bounded at top and base by time hiatuses, which are normally important unconformities, or their correlative conformities (Mitchum et al., 1977).

Six erosional surfaces have been defined and mapped throughout the study area; these are designated by numbers from I to VI in order of decreasing age. The erosional surfaces have been interpreted as sequence boundaries. A seismic profile through a relatively undisturbed area illustrates the six sequence boundaries (Figure 3.1). The termination of reflections at an unconformity is the principal evidence of the presence of a sequence boundary. Reflection termination patterns interpreted as stratal terminations include onlap, downlap, erosional truncation, toplap and apparent

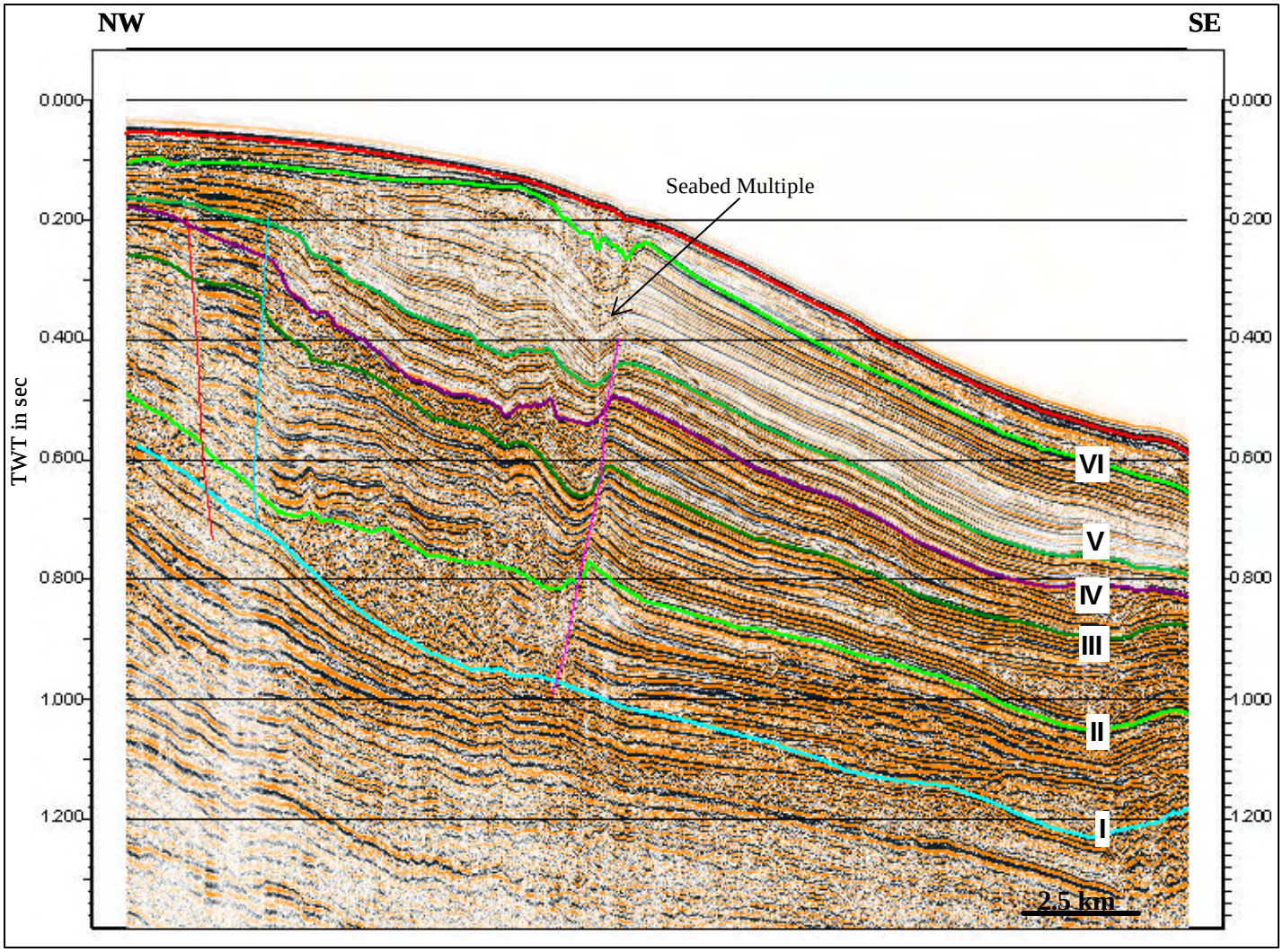

Figure 3.1. Dip-oriented seismic line showing six sequence boundaries defined in this study.

truncation (Figure 3.2, Vail, 1987). Two of these sequence boundaries are distributed throughout the study area and four of them are limited to the eastern/southeastern part as a result of mass wasting and sediment instability. Time structure maps of all six sequence boundaries have been generated. These structure maps provide information regarding the distribution of the depositional surfaces and structural characteristics that can be defined and correlated in the study area.

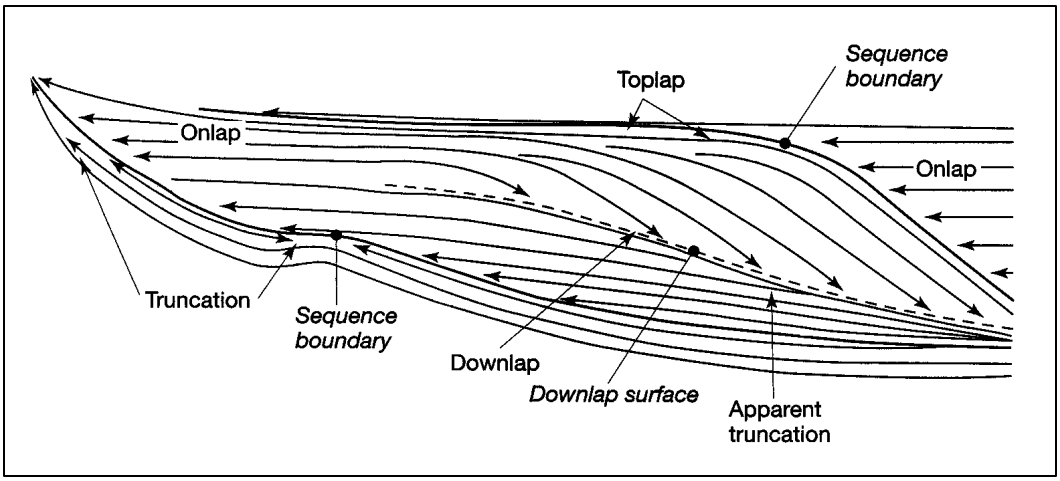

Figure 3.2. Diagram illustrating sequence boundaries, downlap surfaces, and various kinds of reflection terminations (from Vail, 1987).

Seismic stratigraphic analysis is also applied to interpretation of ancient sea-level changes. Through recognition of the reflection pattern of sedimentation above the unconformity from the seismic response such that relative vertical changes in sea level or at least their effects on coastal onlap patterns can be recognized and measured.

After seismic sequences are defined, further interpretation of a sequence comprises seismic facies analysis. Seismic facies analyse have been used for many years

to describe the geology of the subsurface based on delineation of seismic reflection parameters including amplitude, reflection geometry continuity, reflection terminations, reflection configuration and three-dimensional external forms. After seismic facies units are recognized, their limits defined and areal associations mapped, they are interpreted to express certain stratification, lithologic, and depositional features of the deposits that generated the reflections. In this study, interpretation of seismic facies is based on an assumption that the depositional setting is a shelf- to- slope setting.

Sequence Stratigraphy

Sequence stratigraphy study (Van Wagoner et al., 1988; Vail and Wornard, 1991; Emery and Myers, 1996; Posamentier et al., 1988, and many others) provides concepts applicable to the stratigraphic analysis of late Quaternary deposits from the northwestern margin of the SCB.

Sequence stratigraphy is “the study of rock relationships within a chronostratigraphic framework of repetitive, genetically related strata bounded by surfaces of erosion or nondeposition, or their correlative conformities” (Van Wagoner et al., 1988). Sequences and their stratal patterns are interpreted to form in response to the interaction of four major factors such as eustatic change of sea level, climate, sediment supply and tectonic subsidence (Van Wagoner et al., 1988).

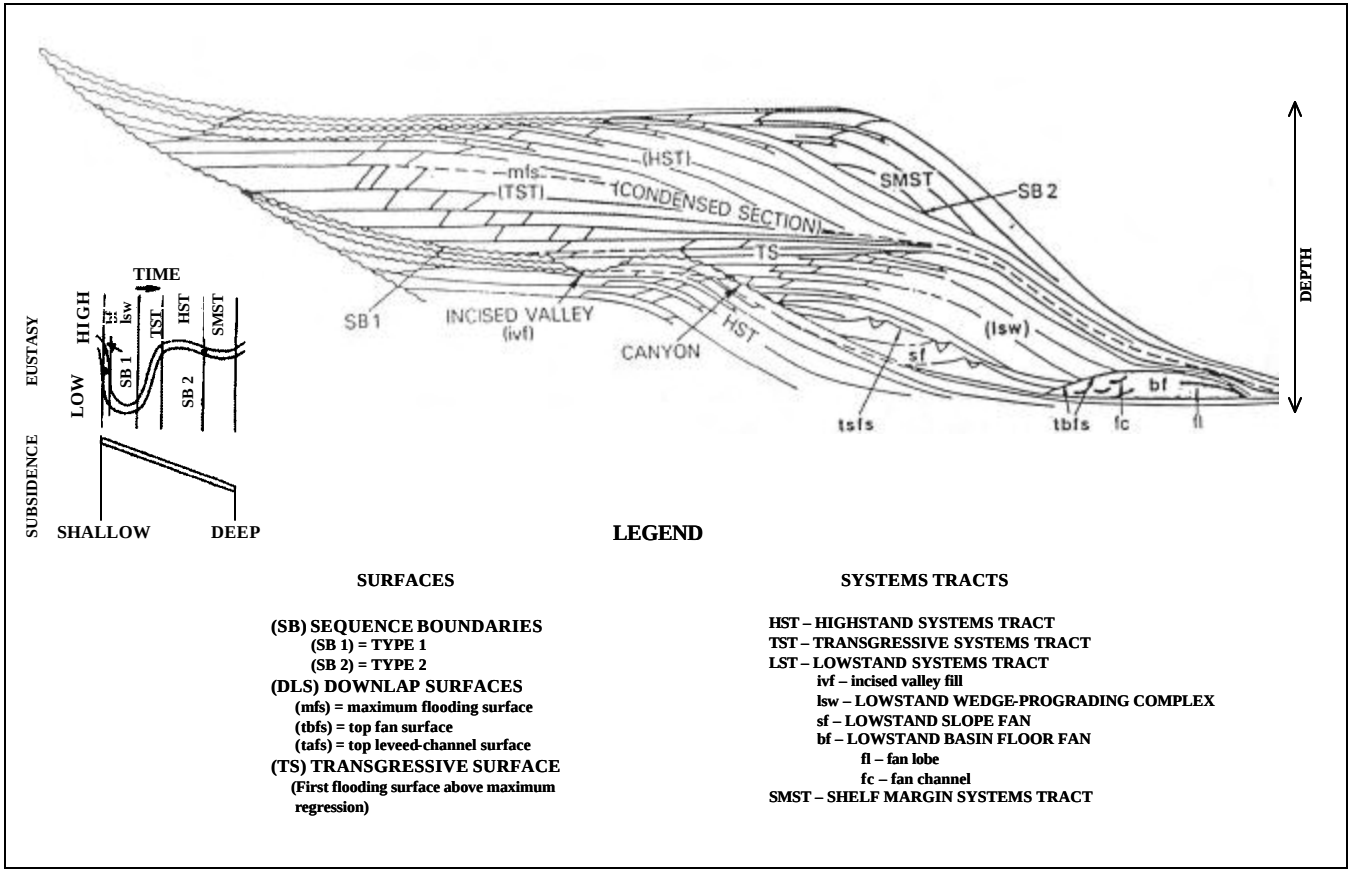

Figure 3.3. Schematic illustration of systems tract, sequence boundaries and corresponding sea level changes (from Vail, 1987).

Two types of sequence boundaries can be distinguished by the nature of changes of sea-level (Figure 3.3). A Type 1 sequence boundary is characterized by subaerial exposure and associated erosion from downcutting streams, a basinward shift in facies, a downward shift in coastal onlap and onlap of overlying strata. It forms when the rate of sea-level fall exceeds the rate of subsidence at the depositional shoreline break. A Type 2 sequence boundary is characterized by subaerial exposure and a downward shift in onlap landward of the depositional shoreline break. Type 2 sequence boundaries lack the subaerial erosion associated with the downcutting of streams and lack a basinward shift in facies. They form when the rate of sea-level fall is less than the rate of subsidence at the depositional shoreline break (Van Wagoner et al., 1987).

Sequences can be divided into system tracts, which are linkages of contemporaneous depositional systems (Brown and Fisher, 1977). System tracts are defined by their position within a sequence, types of bounding surfaces, and parasequence set stacking patterns (Van Wagoner et al., 1987). Each sequence consists of three system tracts: a highstand system tract (HST), a transgressive system tract (TST), and a lowstand system tract (LST) or shelf margin system tract (SMST). Figure 3.3 shows systems tracts and corresponding sea-level changes. The HST consists of an aggradational to progradational set of parasequences that overlies the maximum flooding surface and that is overlain by the next sequence boundary. During the HST, the rate of relative sea-level rise begins to slow and relative sea level eventually begins to fall prior to the next sequence boundary. The TST consists of a retrogradational set of parasequences. It is underlain by the transgressive surface and overlain by the maximum

flooding surface. The TST is deposited during a rapid sea-level rise. The LST is the set of depositional systems active during the time of relatively low sea level following the formation of the sequence boundary. It lies on a Type 1 sequence boundary and is bounded at the top by the transgressive surface. The LST may include three distinct parts, the basin-floor fan, the slope fan, and the lowstand wedge. The SMST is deposited during a time of slow sea-level fall. It is characterized by one or more weakly progradational to aggradational parasequence sets, which onlap onto the sequence boundary in a landward direction and downlap onto the sequence boundary in a seaward direction. The SMST lies on a Type 2 sequence boundary and is bounded at the top by the transgressive surface.

CHAPTER IV

SEISMIC FACIES ANALYSIS

Seismic facies are defined as three-dimensional seismic units composed of groups of reflections whose parameters are distinguished from those of adjacent seismic reflection patterns (Mitchum et al., 1977). Analysis of seismic facies provides the basis on which depositional processes and environmental settings can be interpreted.

This study follows the nomenclature and the techniques of seismic facies analysis described by Sangree and Widmier (1977). Thirteen different seismic facies were identified in the study area through the interpretation of reflection configuration, continuity, amplitude, frequency and variation of the facies laterally and vertically. Seismic facies characteristics and their geological interpretation are listed below:

(1) High-amplitude, parallel, horizontal, high-continuity facies. These facies have deposited on the shelf; therefore, they represent the shelf seismic facies (Figure 4.1a). High-amplitude reflections suggest interbedded deposition of shales with relatively thick sandstones (Sangree and Widmier, 1977). High-continuity reflections are interpreted as sediment deposition in a relatively uniform environment.

(2) Variable amplitude, parallel to subparallel, low-continuity facies. These facies have been observed in the northern part of the study area and associated with shelf deposition (Figure 4.1b). Sediments have been deposited by fluvial currents characterized by poor lateral continuity reflection and bursts of high amplitude (Sangree and Widmier, 1977).

(3) Oblique-progradational facies. These seismic facies are associated with shelf margin and slope deposition (Figure 4.1c). Steeper dipping strata, with toplap against the sequence boundary, indicate the oblique-progradation configuration. Oblique-progradational facies develop during periods of relatively rapid supply of sediments and a stillstand or low subsidence/slow rise of sea level. Truncation of reflectors at the upper boundary of the sequence suggests erosion; therefore their classification as tangential oblique-progradational facies.

(4) Sigmoid-progradational facies. Sigmoid-progradational clinoform is characterized by gentle sigmoid (S-shaped) reflections along the depositional dip (Figure 4.1d). This type of progradational facies formed during rapid basin subsidence and/or rise of sea level with low sediment supply (Sangree and Widmier, 1977).

(5) Low- to moderate-amplitude, parallel to subparallel, moderate- to high-continuity facies. Low- to moderate-amplitude typically corresponds with the dominant shale content of the prodelta facies (Sangree and Widmier, 1977, Figure 4.1e). This seismic facies is related to the highstand systems tract.

(6) Moderate- to high-amplitude, parallel and high-continuity facies. Moderate- to high-amplitude facies are interpreted to indicate thinly interbedded sands with relatively thick shales (Figure 4.1f). Parallel patterns of continuous reflections created by widespread parallel strata are probably the expression of low-energy deposits. This seismic facies is related to the transgressive systems tract.

(7) Moderate- to high-amplitude, parallel to subparallel, variable continuity facies. Moderate- to high-amplitude facies are interpreted to indicate thinly

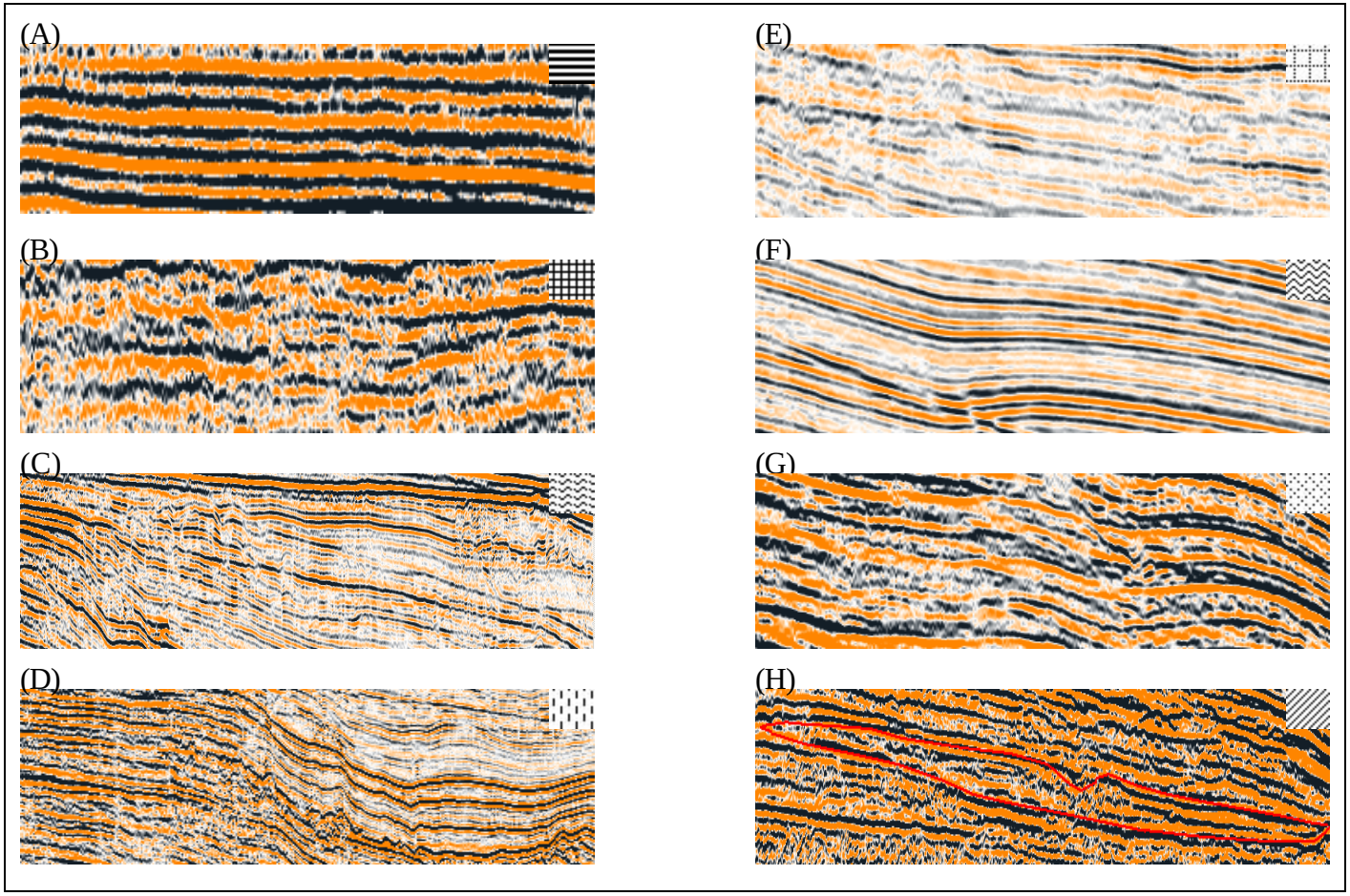

Figure 4.1. Examples of the seismic facies identified within the study area with map symbol, respectively. (a) high-amplitude, parallel, and high-continuity, (b) variable amplitude, parallel to subparallel, and low-continuity, (c) oblique-progradational, (d) sigmoid-progradational, (e) low- to moderate-amplitude, parallel to sub-parallel and moderate- to high-continuity, (f) moderate- to high-amplitude, parallel and high-continuity, (g) moderate- to high-amplitude, parallel to subparallel, and variable continuity, (h) high-amplitude, semi-continuous, concave-down, bi-lateral downlap reflection configuration.

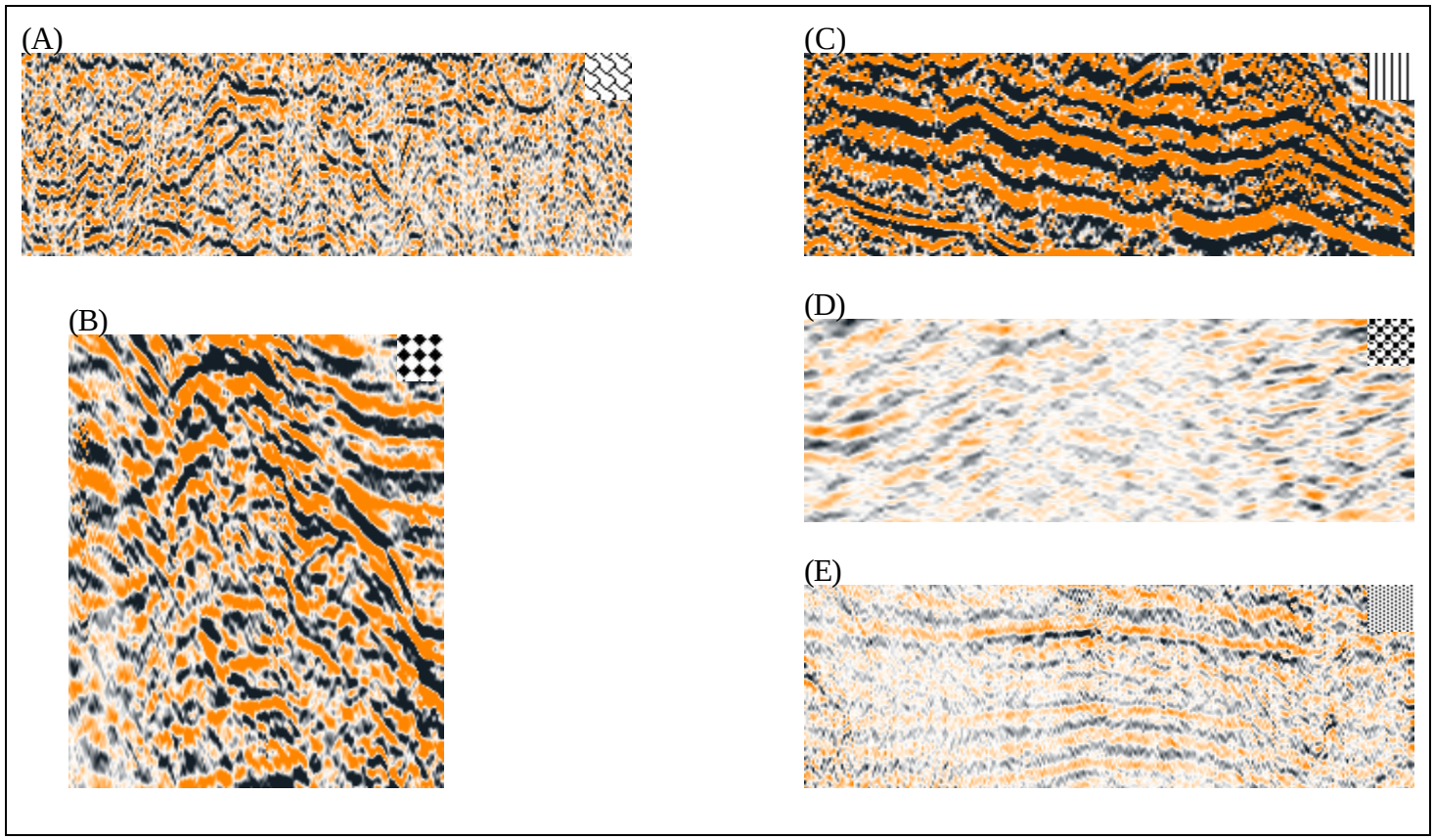

Figure 4.2. Seismic facies examples identified within the study area with map symbol, respectively. (a) high- to low-amplitude, disorganized, discontinuous, nonparallel, (b) moderate- to high-amplitude, quasi-continuous, (c) anomalously high-amplitude, (d) low-amplitude, acoustic wipeout and poor internal coherency, (e) acoustic blanking.

interbedded sand with relatively thick shales (Figure 4.1g). This seismic facies is characterized by an internal seismic reflections package of the lowstand wedge sediments that were deposited during relative lowstand and the beginning of the relative rise of sea level.

(8) High-amplitude, semi-continuous, concave-down, bi-lateral downlap reflection configuration facies. This facies is interpreted as a slope fan as it develops on the lower-middle slope (Figure 4.1h). High-amplitude reflections are associated with dominantly shale deposits.

(9) High- to low-amplitude, disorganized, discontinuous, nonparallel facies. These facies are associated with mass-transport processes (Figure 4.2a). These can include slides, slumps, and debris flow resulting from instability of the sediments.

(10) Moderate- to high-amplitude, quasi-continuous facies. This facies is interpreted as mud volcano flows and cone-like volcanic buildups (Figure 4.2b). The high amplitude indicates a distinct acoustic impedance contrast between the mudflow and the surrounding sediments.

(11) Bright spots or anomalously high-amplitude facies. High-amplitude anomalous zones associated with the presence of gas-charged sediments (Figure 4.2c) appear as a high-amplitude event as a result of the large impedance contrast between gas and surrounding shallow sediments.

(12) Low-amplitude, acoustic wipeout, poor internal coherency facies. This type of chaotic seismic facies is associated with mud volcanoes (Figure 4.2d).

(13) Acoustic blanking facies. This is a type of seismic anomaly created by shallow gas, which appears as a diffuse and chaotic seismic facies masking nearly all other reflections (Murphy et al., 2002, Figure 4.2e). Acoustic blanking most likely occurs when interstitial gas bubbles in the sediment absorb seismic energy, resulting in the rapid attenuation of the seismic wave energy (Anderson and Bryant, 1990).

CHAPTER V

SEQUENCE STRATIGRAPHIC ANALYSIS

Analysis of high-resolution seismic reflection profiles in this study involved the identification of six sequences. The description of each sequence begins with an identification and interpretation of sequence boundary, isochron map (including directions of sediment transport), followed by an analysis of the depositional environments and discussion of seismic facies distribution. To represent the sequence stratigraphy of the sequences, four seismic sections were selected over the study area. Figure 5.1 shows the location of the seismic sections.

Sequence I

Sequence I, the oldest sequence recognized in the study area, is an interval between Sequence Boundary I and Sequence Boundary II. The age range of Sequence I is from 117,000 years B.P. to 71,000 years B.P. It therefore represents the late Pleistocene epoch or Upper Khazar stratigraphic unit. This sequence is distributed throughout the study area.

Sequence Boundary I, the base of the first seismic sequence, can be recognized throughout the study area. This seismic sequence boundary is characterized by variable amplitude and continuous to discontinuous reflection. As an erosional surface, this boundary can also be recognized by truncation of the older strata below and onlap of the younger strata above the surface. In the shelf this surface occurs at depths of 500 ms to

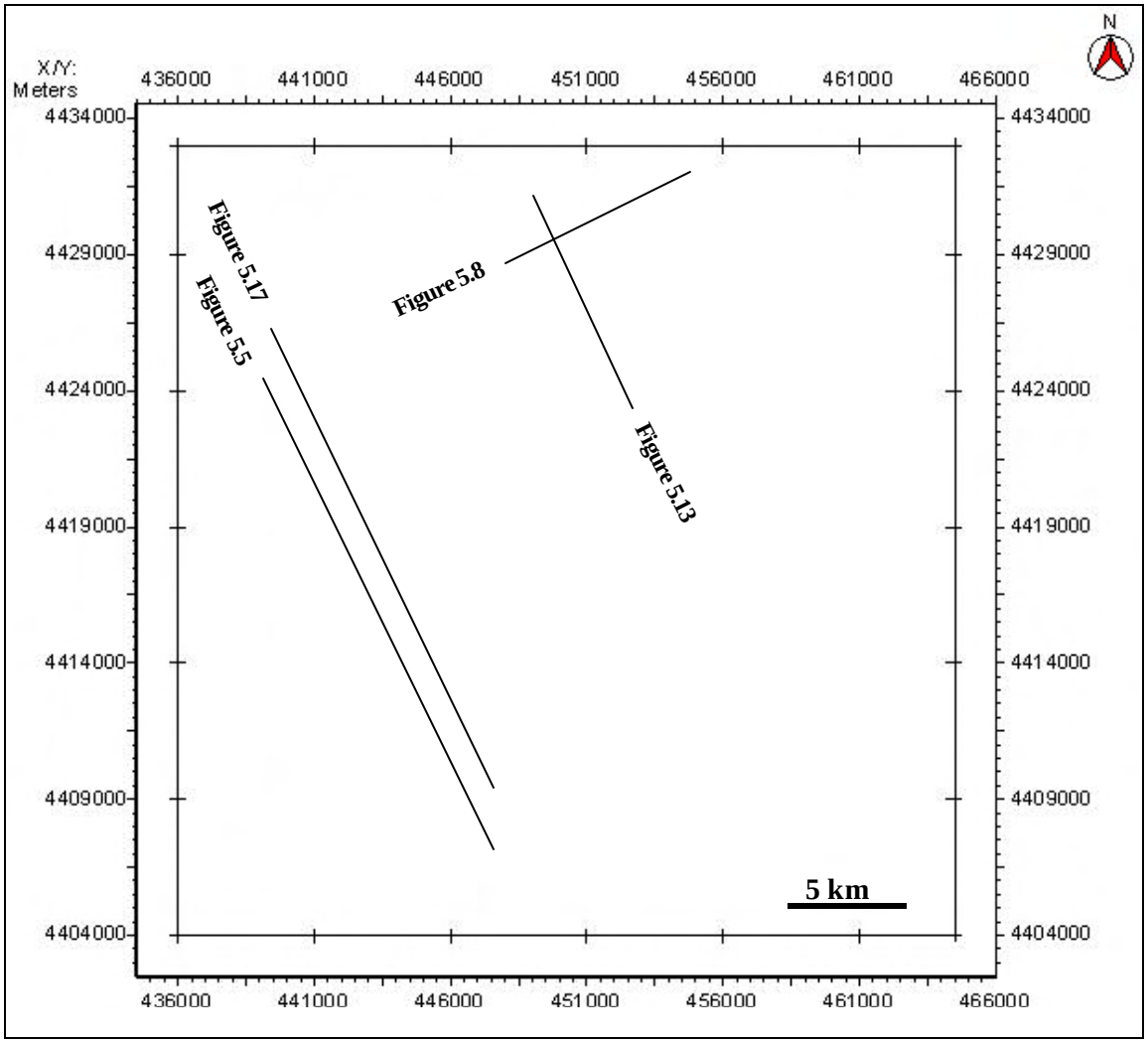

Figure 5.1. Seismic sections to be used to discuss sequences.

1200 ms in the slope areas. The position of the shelf edge is observed at 600 ms. A two-way time structure map of Sequence Boundary I reveals the significant subsidence into the dormant central mud volcano (Figure 5.2).

The Isochron map in Figure 5.3 represents the interval between Sequence boundaries I and II. The thickness of Sequence I ranges from 20 ms to 250 ms. The general pattern of the package is one of thickening to the southeast and southwest from the central area. The central part of the study area shows dramatic thinning of this package to the south over the fold, indicating continued uplift. This suggests that deposition of Sequence I occurred during a period of fold growth. The isochron map clearly shows that the sediment transport direction is from northwest to southeast. Uplift of the central part along with mud volcano pulses resulted in an increase of terrigeneous input on the flanks of the tectonically active zone. Another explanation for thicker sediment accumulation on the flanks of the fold may be as a result of more active slumping and other mass-movement processes off the sides of the fold during tectonic uplift. The sequence is almost entirely absent on the northwest corner of the study area as a result of erosion caused by slumping from the shelf edge or the steep shelf-slope transition zone.

In general, faults are more numerous in the northwestern half of Sequence I. The major faults trend east - west and most are downthrown to the south. These faults are results of gravity mass movement processes that occur on the upper slope area.

The most prevailing feature of Sequence I is the large central mud volcano. The associated caldera extends approximately 5 km along the fold axis and 3.5 km in an

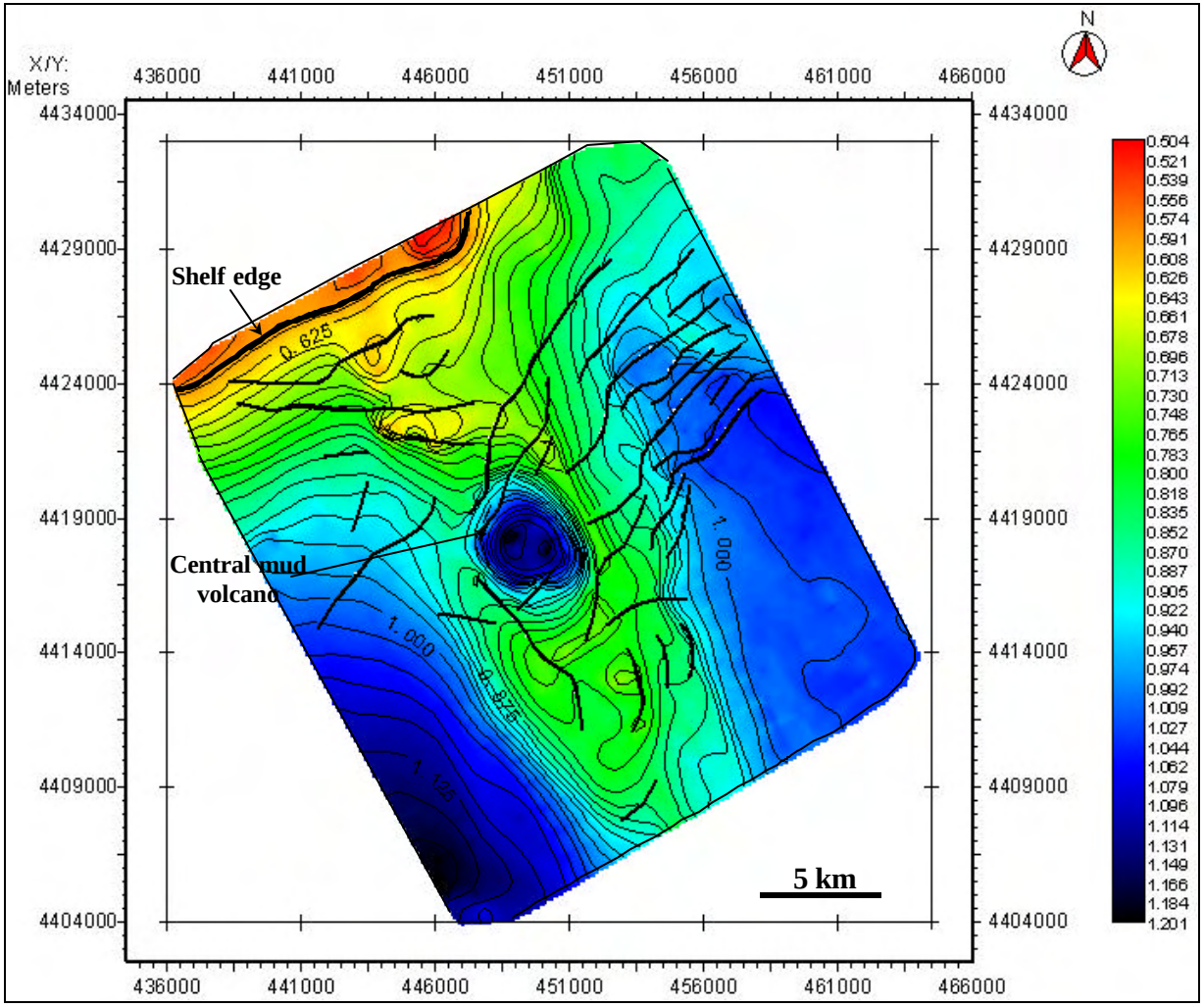

Figure 5.2. Two-way travel time structure map of Sequence Boundary I. Position of the shelf edge at 600 ms. The contour interval is 25 ms.

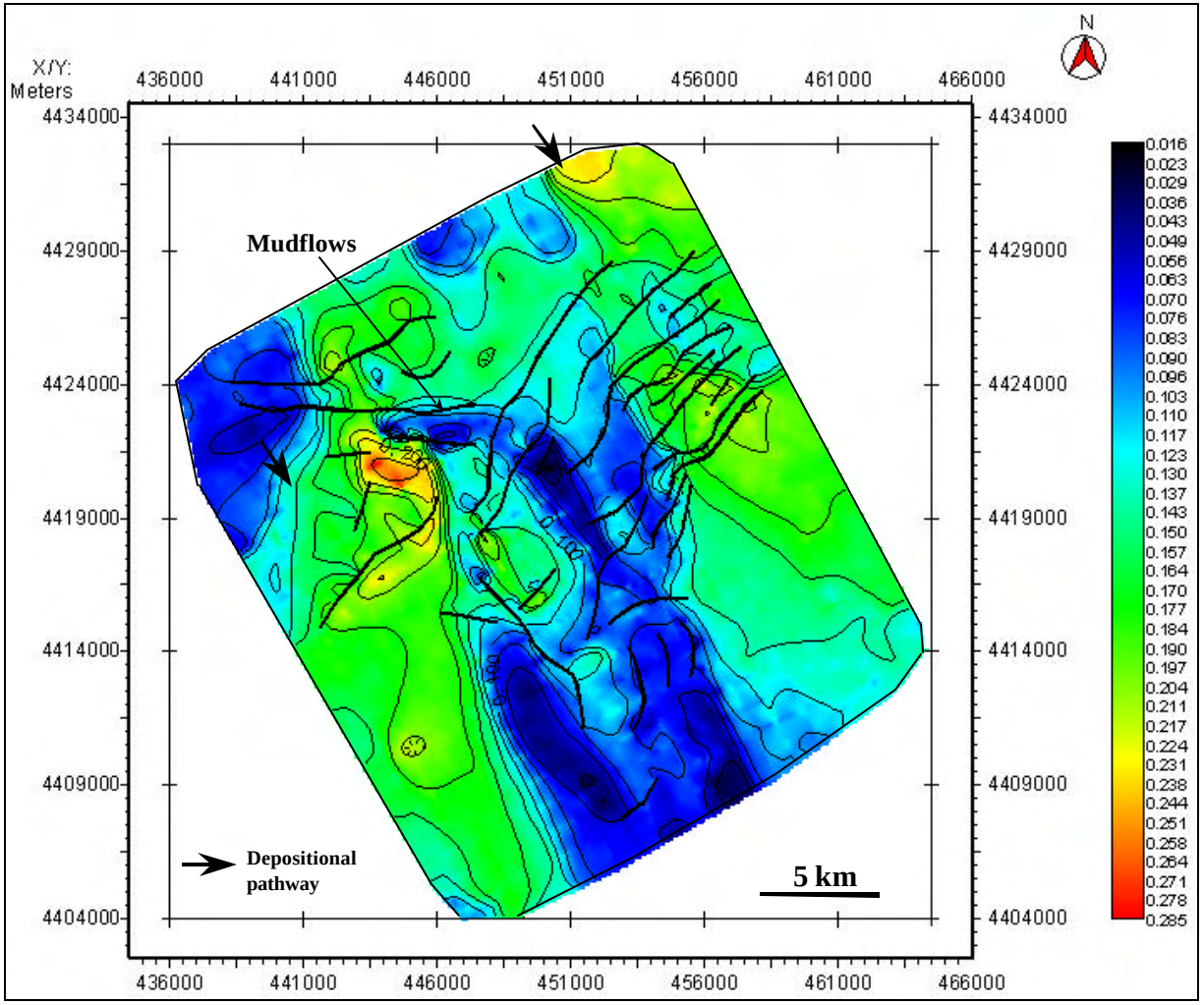

Figure 5.3. Isochron map showing three depocenters and depositional pathways of Sequence I. The mudflows are directed northward. The contour interval is 20 ms in two-way travel time.

orthogonal direction. The caldera-like appearance indicates that the central mud volcano was active at some point of its history, creating a caldera-type feature that has been infilled by mud volcano material and sediment material (Fowler et al., 2000). This mud volcano appears to have been active during deposition of Sequence I, as evidenced by the mudflows and cone-like buildups. The conical buildups are interpreted as mud volcano, and the high-amplitude reflectors as the mudflows from volcano during periods of activity. The isochron map also clearly shows the north-northwest track of mudflows from the central mud volcano, which is opposite the main sediment transport direction. The mudflows also create a minibasin in the hanging wall of the counter regional fault. The counter regional fault along the minibasin margin trends northwest-southeast.

Sequence I consists of seven seismic facies (Figure 5.4). Variable amplitude, parallel to subparallel and low-continuity reflection in the northern part of the study area represent the shelf seismic facies. Sediments deposited by fluvial currents are characterized by poor lateral continuity reflection and bursts of high amplitude (Sangree and Widmer, 1977). In the depositional dip direction, the shelf seismic facies grades basinward into a moderate- to high-amplitude, parallel to subparallel, variable continuity seismic facies. Moderate- to high-amplitude indicates interbedded sand with relatively thick shales. I interpreted this seismic facies as lowstand wedge sediments that were deposited during relative lowstand and the beginning of the relative rise of sea level. The lowstand wedge overlies a channel-levee-overbank system (CLS), which is observed in the toes of the clinoform wedge within sequence I in the southwestern area (Figure 5.5). A CLS is represented by a high-amplitude, semi-continuous, concave-down, bi-lateral

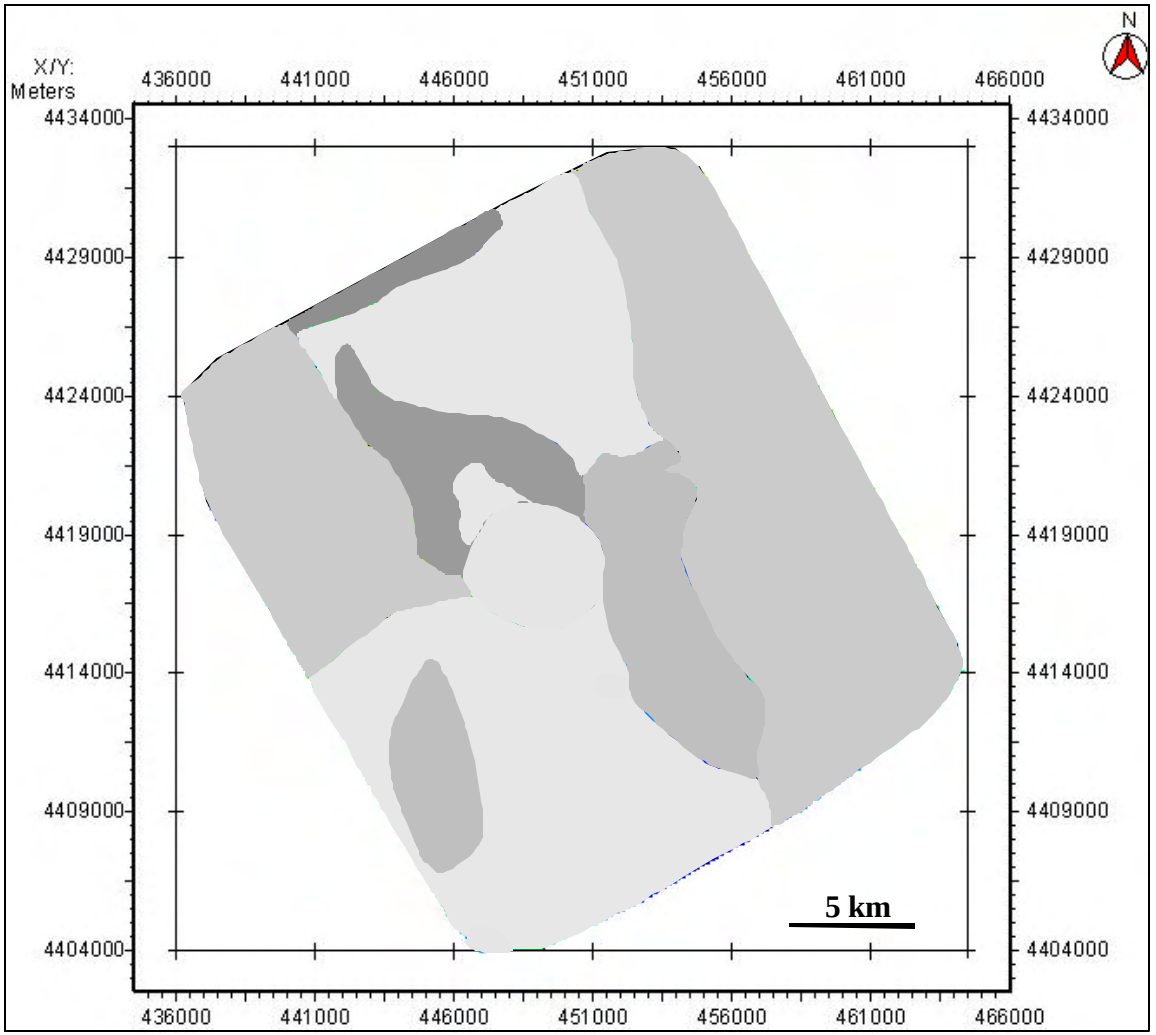

Figure 5.4. Seismic facies distribution map of Sequence I. See Chapter IV for legend and text for detailed discussion.

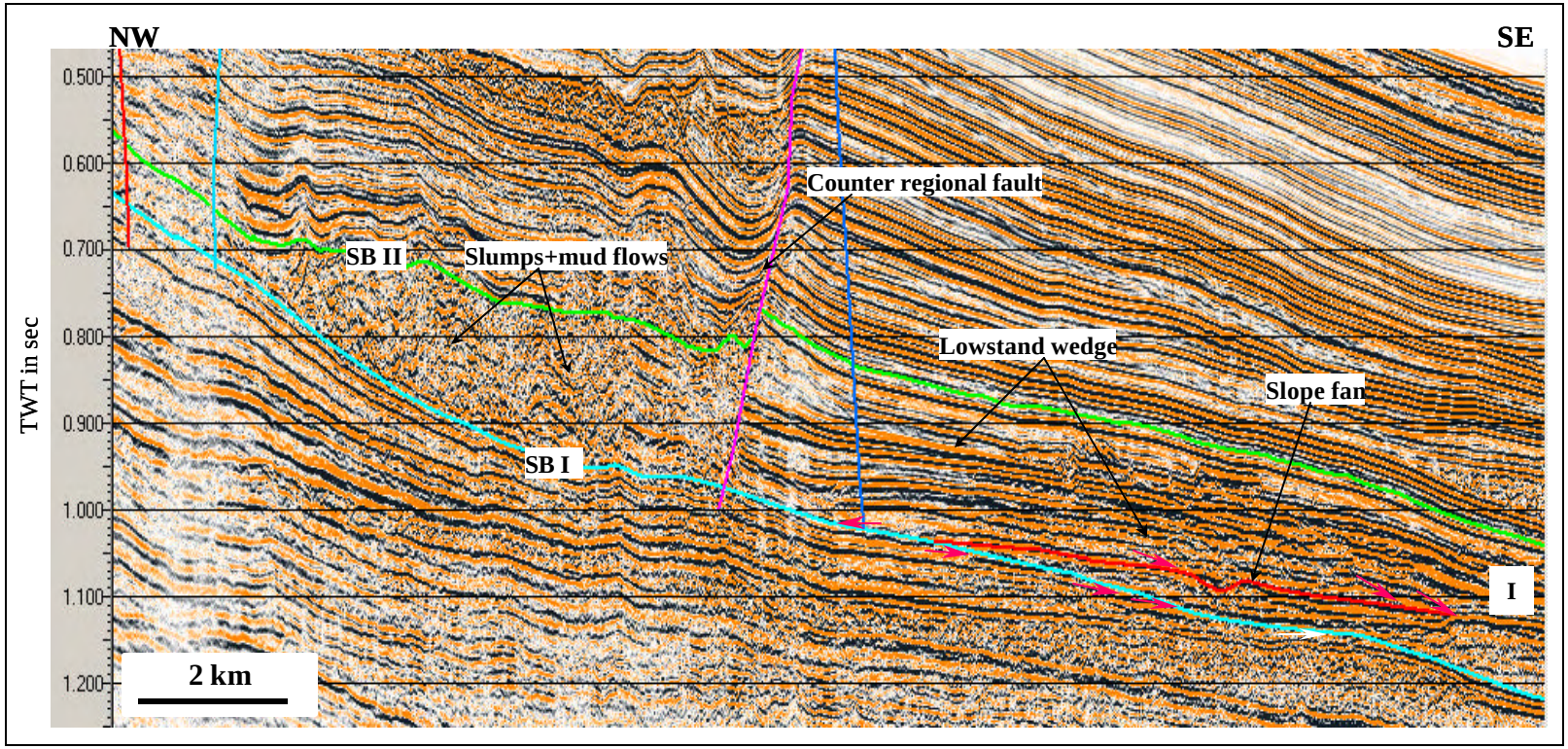

Figure 5.5 Seismic section showing lowstand deposits and slumps resulting from sediment instability along the shelf edge within Sequence I. See Figure 5.1 for the location and text for detailed discussion.

downlap reflection configuration. This CLS is “gull-wing” shaped and mounded in form with aggrading and migrating channels. Its levees and overbank are more developed, and it is characterized by high-amplitude, continuous facies, with high-amplitude, discontinuous channel facies. This suggests that high-amplitude reflections are associated with dominantly shale deposits. The CLS is relatively small (< 3 km radius) and thin (<100 ms of sediment). The CLS on the southwestern slope may be referred to as a slope fan as it has developed on the lower-middle slope. A slope fan is formed “when the rate of eustatic fall exceeds the rate of subsidence at the depositional shoreline break and when the depositional shoreline break is located at, or close to, the physiographic shelf slope break” (Van Wagoner et al., 1988). In the eastern part of study area the large zone of chaotic facies represented by high- to low-amplitude, disorganized, discontinuous, nonparallel reflection has been interpreted to be represent extensive sediment movement from the fold during the period of tectonic activity. The same seismic facies, but different in origin, is also observed in the northeastern part of Sequence I. This chaotic facies formed from sediment instability along the shelf edge. Acoustic blanking is a type of seismic anomaly created by shallow gas, which appears as a diffuse and chaotic seismic facies masking nearly all other reflections. This facies was identified to the southeast of the study area. Moderate- to high-amplitude, discontinuous seismic facies represent mud volcano flows and cone-like volcano buildups. The high amplitude indicates a distinct acoustic impedance contrast between the mudflow and the surrounding sediments. This seismic facies is observed to extend up to 10 km to north, northwest and west directions from the central mud volcano. A seismic facies that is

characterized by the low-amplitude, acoustic wipeout and poor internal coherency can be associated with a mud volcano. An impressive 1 km diameter mud volcano is still a positive feature on the seafloor (Figure 2.8).

Based on the seismic facies that I identified within this sequence and reflection configuration, I interpreted the sediments within Sequence I as a lowstand deposits, accumulated during the lowstand systems tract.

Sequence II

Sequence II is an interval between Sequence Boundary II and Sequence Boundary III. The age range of Sequence II is from 71,000 years B.P. to >51,000 years B.P. It therefore represents the late Pleistocene epoch or Lower Khvalyn stratigraphic unit. This sequence is distributed throughout the study area.

On the seismic sections, seismic Sequence Boundary II is characterized by strong amplitude and continuous reflection. Sequence Boundary II, which is the base of the second seismic sequence, occurs at the depth ranging from 400 ms at the shelf to more than 1000 ms in the slope areas. The dominant feature of the two-way time structure map (Figure 5.6) is a position of the shelf edge at 500 ms and a subsidence into the central mud volcano.

Figure 5.7 is an isochron map that represents the interval between Sequence Boundaries II and III. The thickness of this interval ranges from 40 ms to 400 ms. Three areas of maximum thickness can be recognized related to this interval. The first pathway is located in the northeastern part of the study area. It came from the northwest and

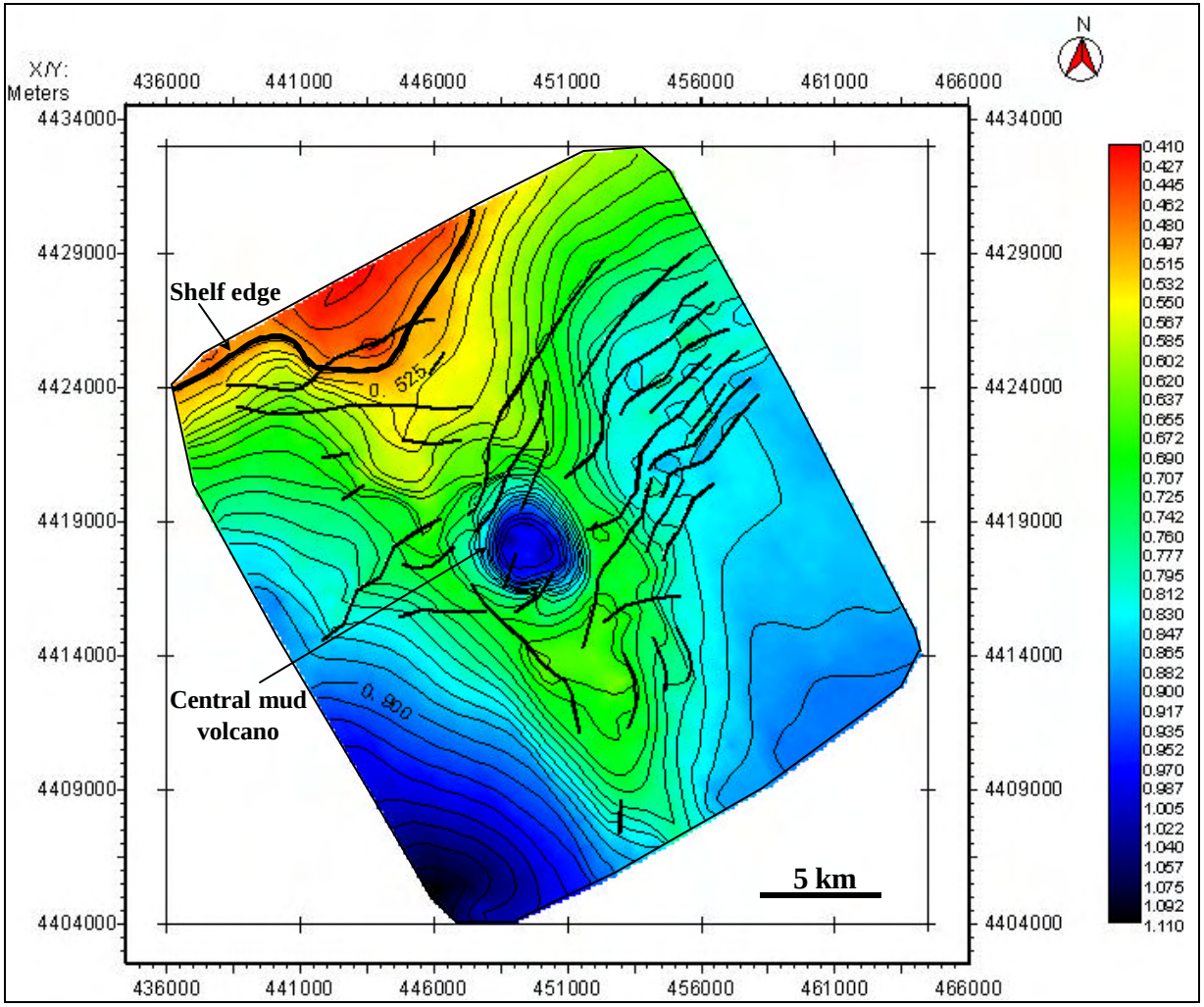

Figure 5.6. Two-way travel time structure map of Sequence Boundary II. Position of the shelf edge at 500 ms. The contour interval is 25 ms.

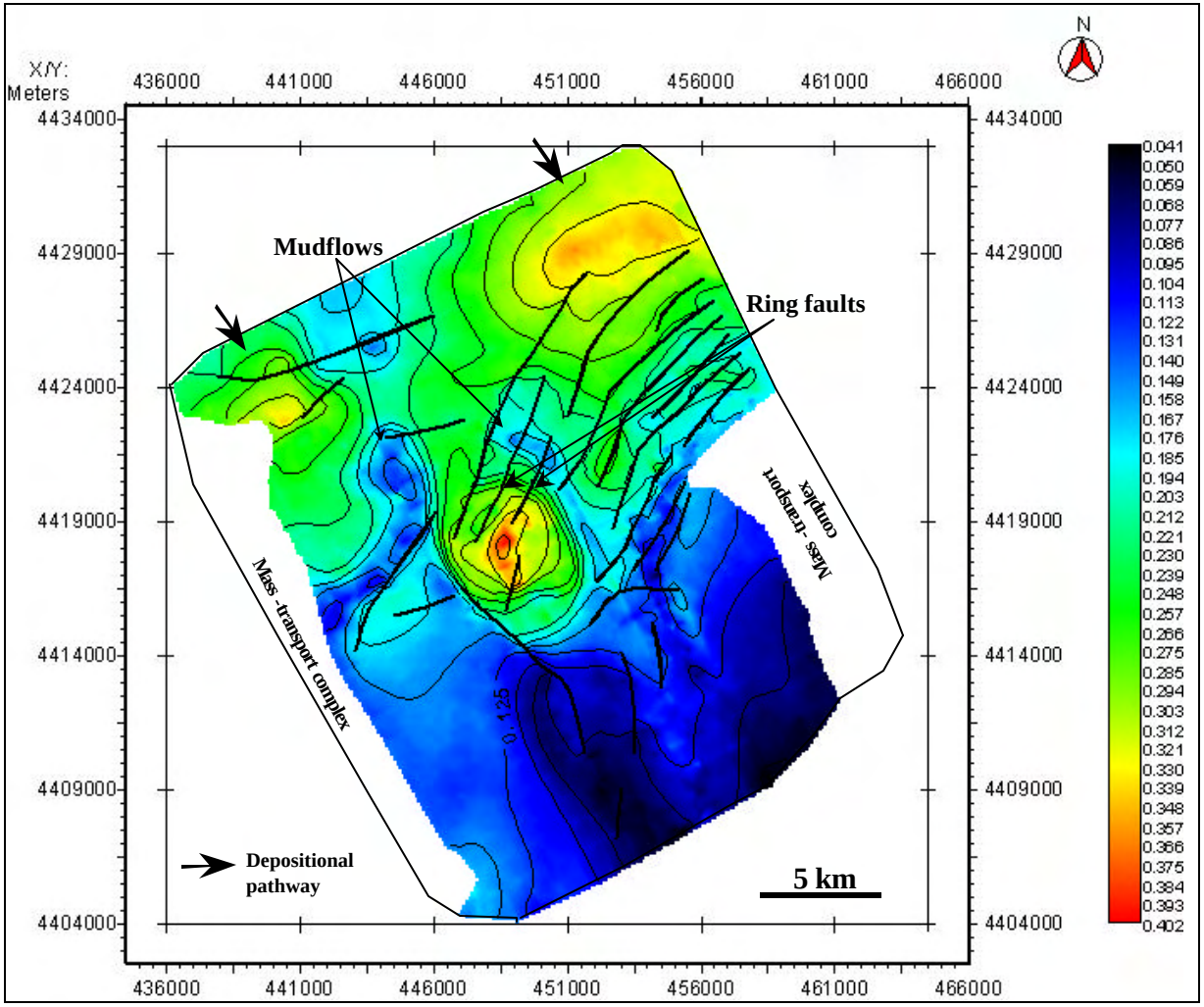

Figure 5.7. Isochron map showing three depocenters and depositional pathways of the Sequence II. Ring faults cut sequence around mud volcano. The mudflows are directed to northwards. The contour interval is 20 ms in two-way travel time.

connected with the depocenters where accumulation of the sediments reached 350 ms. The second pathway is located in the northwestern part and linked with relatively smaller depocenters than the previous one; here, accumulation of the sediments reaches only 300 ms. The third depocenter, with maximum thickness of 400 ms, occurs in the central part and is associated with a 5-km-diameter collapse structure. On the east and west sides from the central mud volcano, significant thinning of the interval is interpreted as paleo-mudflows during a period of intense mud volcano activity. These flows are directed to northward, rather than to the south. The north direction is opposite from the main sediment transport pathway, so it could only result from tectonic uplift and not a depositional slope. Several deep extensional faults called "ring faults" cut Sequence II around the collapsed caldera mud volcano. Evidence from the seismic data of a large amount of down-dropped sediment within the collapsed caldera and the elevation of paleo-mudflows above the top of the mud volcano suggests these faults are likely to have formed during volcano deflation and internal subsidence. In addition, since faults are associated with almost all mud volcanoes, they can provide efficient pathways for the upward migration of deeper gas to the upper intervals.

Sequence II can be divided into three subsequences bounded by erosional truncation surfaces associated with 2-km-wide canyons. These canyons can be recognized clearly in the slope area on the northeastern part as shown in the seismic section (Figure 5.8) with a north-south axis. This seismic section shows that the subsequences were truncated by canyons related to the younger subsequences and exhibit U-shaped profiles, gently upward concave. These erosional canyons usually

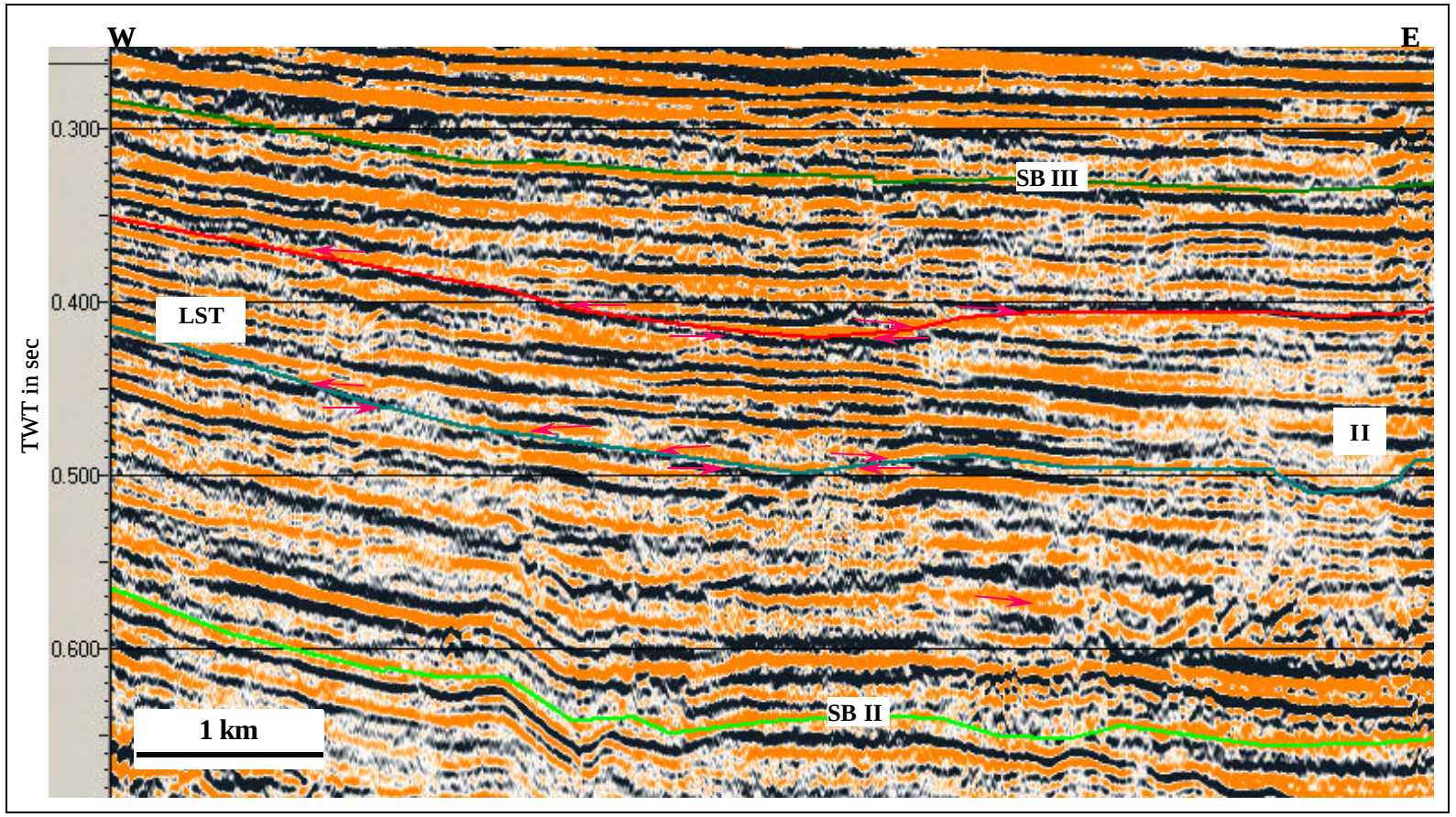

Figure 5.8. Seismic section showing subsequences cut by canyons related to the younger subsequences associated with Sequence II. See Figure 5.1 for the location and text for detailed discussion.

occur in the steepest areas of slope, where gravity flows are accelerating (Galloway, 1998). Toward the basin, canyons become broader most likely related to the creation of shelf-margin instability. Erosional canyons are interpreted as lowstand canyons that have been infilled as a result of initial rise of the relative sea level. Subsequences can be attributed to basinward downlapping progradation followed by the erosional upper surface. The onlap termination pattern of the facies above erosional surfaces of subsequences can also be recognized, especially in the shelf-slope area. Based on the reflection configuration, I interpreted the sediments within these subsequences as a lowstand deposits formed during the lowering of relative sea level to a position below the shelf edge.

Sequence II consists of six seismic facies (Figure 5.9). The shelf seismic facies is represented by a high-amplitude, parallel, high-continuity reflection configuration. High-amplitude reflection probably corresponds to interbedded shales with comparatively thick sandstones. High continuity reflections suggest deposition in a relatively equable environment (Sangree and Widmer, 1977). Internal seismic reflections packages of the lowstand deposits within Sequence II are represented by moderate- to high-amplitude, parallel to subparallel, and variable continuity seismic facies. These seismic facies are interpreted to indicate thinly interbedded sand with relatively thick shales. Parallel to subparallel reflectors pass laterally and suddenly into chaotic zones that are interpreted as redeposited material in the form of slumps and viscous debris flows. The chaotic facies is abundant along the eastern and western flank, represented by high- to low-amplitude, disorganized, discontinuous, nonparallel reflection. Rapid deposition and

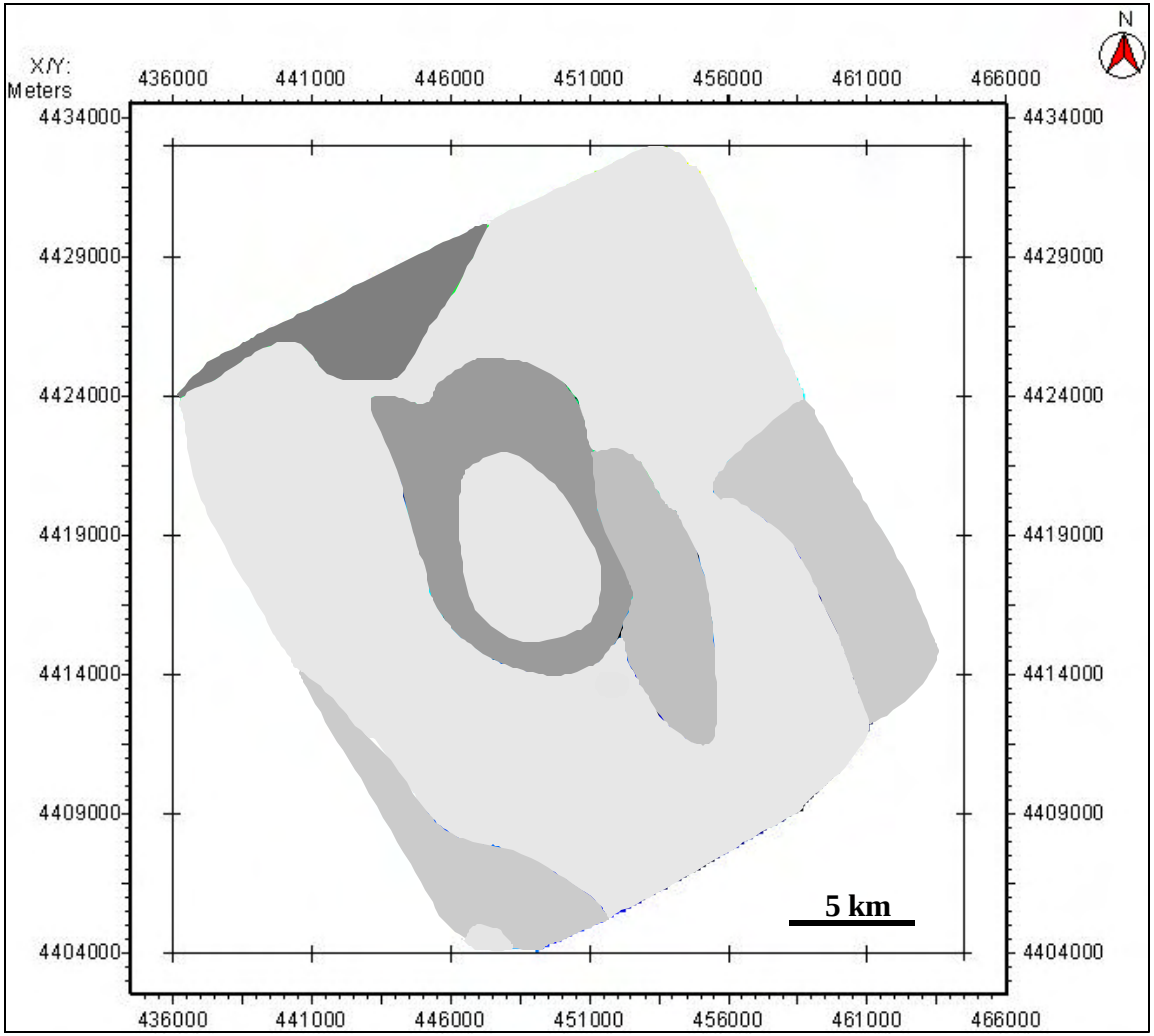

Figure 5.9. Seismic facies distribution map of Sequence II. See Chapter IV for legend and text for detailed discussion.

progradation of sediment over an unstable shelf margin may result in oversteepening and gravity sliding of shallow sediment layers. Suter and Berryhill (1975) believed that sediment instability may be greatest during lowstands of sea level. Acoustic blanking seismic facies is mainly observed in the southern part of the study area. Acoustic blanking most likely occurs when interstitial gas bubbles in the sediment absorb seismic energy, resulting in the rapid attenuation of the seismic wave energy (Anderson and Bryant, 1990). Moderate- to high-amplitude zones are associated with the presence of mud volcano flows and cone-like volcano buildups. These seismic facies are identified close to the largest mud volcano of the study area. Low-amplitude, acoustic wipeout and poor internal coherency seismic facies represent mud volcanoes.

Sequence III

Sequence III is an interval between Sequence Boundary III and Sequence Boundary IV. The age range of Sequence III is from >51,000 years B.P. to 51,000 years B.P. It therefore represents the late Pleistocene epoch or Lower Khvalyn stratigraphic unit. This sequence is distributed throughout the study area except in the southeastern flank and along the western flank as result of slope failure related to slope instability.

The seismic Sequence Boundary III is the base of the third seismic sequence. This boundary is characterized by a strong amplitude, continuous reflection. In the shelf, this surface occurs at depths of 250 ms to greater than 900 ms in the slope areas. As an erosional unconformity surface, this boundary can also be recognized by truncation of the older strata below and onlap of the younger strata above the surface. The two-way

time structure map shows that the regional dip of this surface is to the south (Figure 5.10) and a subsidence into the dormant central mud volcano collapse caldera. Its Seismic Boundary III was cut by a series of faults on the eastern side. The position of the shelf edge is observed at 350 ms.

Figure 5.11 is an isochron map representing the interval between Sequence Boundaries III and IV. The thickness of this interval ranges from 10 ms to 280 ms. Two maximum thicknesses in this area can be interpreted as the depocenters or paleotopographic lows. Based on this isochron map, I interpreted that source of sedimentation during this period was from the northeast and northwest toward a southern direction. The first depocenter on the northeast part is associated with the shelf-edge deltaic outbuilding and the second one is adjacent to a cone-shaped feature. The overall sequence thins to the south.

Sequence III contains seven seismic facies (Figure 5.12). On the shelf, seismic facies is represented by a high-amplitude, parallel, high-continuity reflection configuration. High-amplitude reflections probably indicate interbedded shales with comparatively thick sandstones. High-continuity reflections propose sediment deposition in a relatively equable environment (Sangree and Widmer, 1977). Repeated falls of sea level during Sequence III came together with a relatively high supply of sediment, resulting in the progradational stacking typical of the lowstand wedge (Figure 5.13). The oblique tangentional reflection patterns indicate rapid progradation during deposition of Sequence III. Outbuilding has been caused mainly by extension of the coastal plain across the shelf during lowstands and following progradation as a result of deposition of

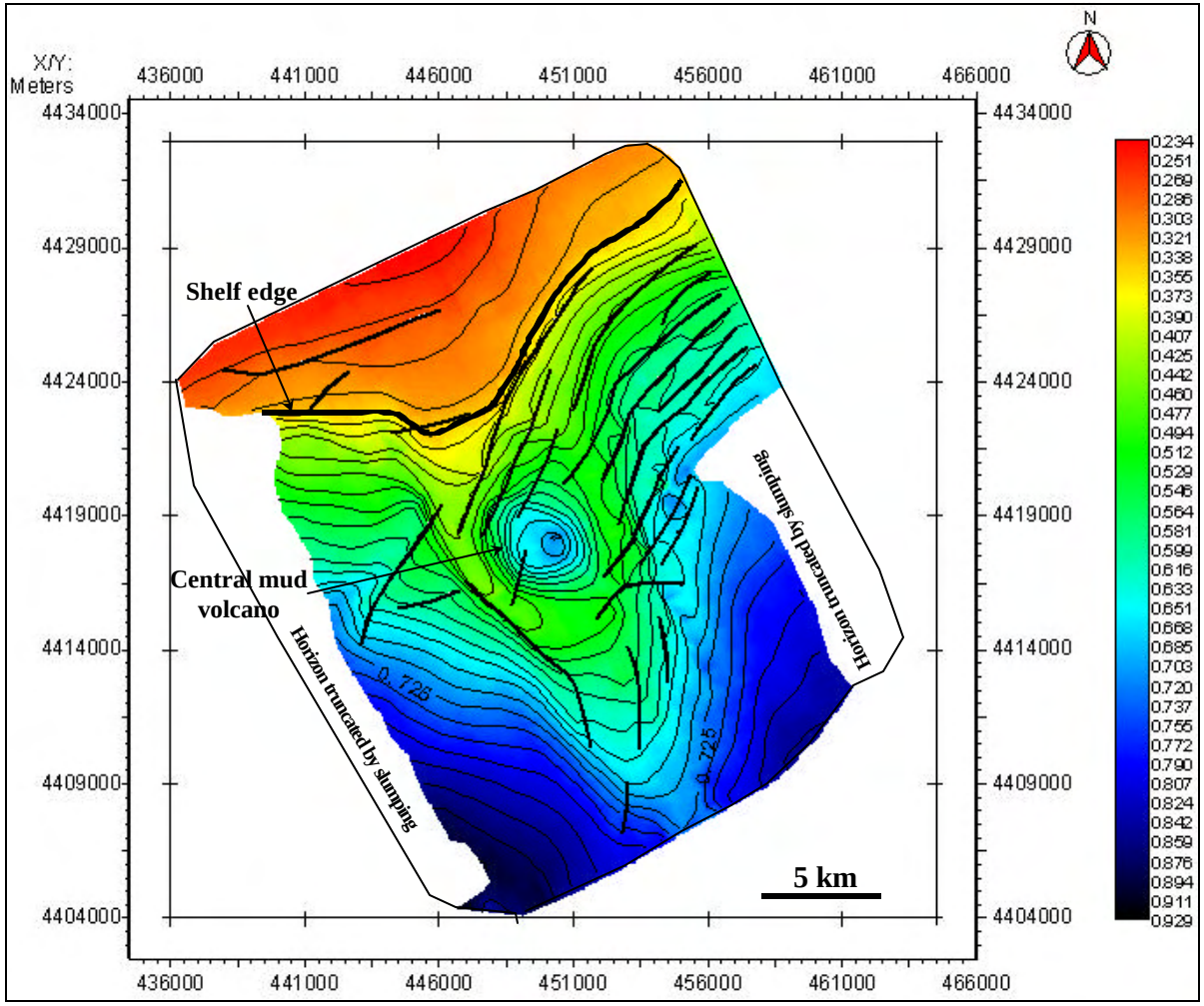

Figure 5.10. Two-way travel time structure map of Sequence Boundary III. Position of the shelf edge at 350 ms. The white polygon delineates the areas where the horizon has been truncated because of slumping. The contour interval is 25 ms.

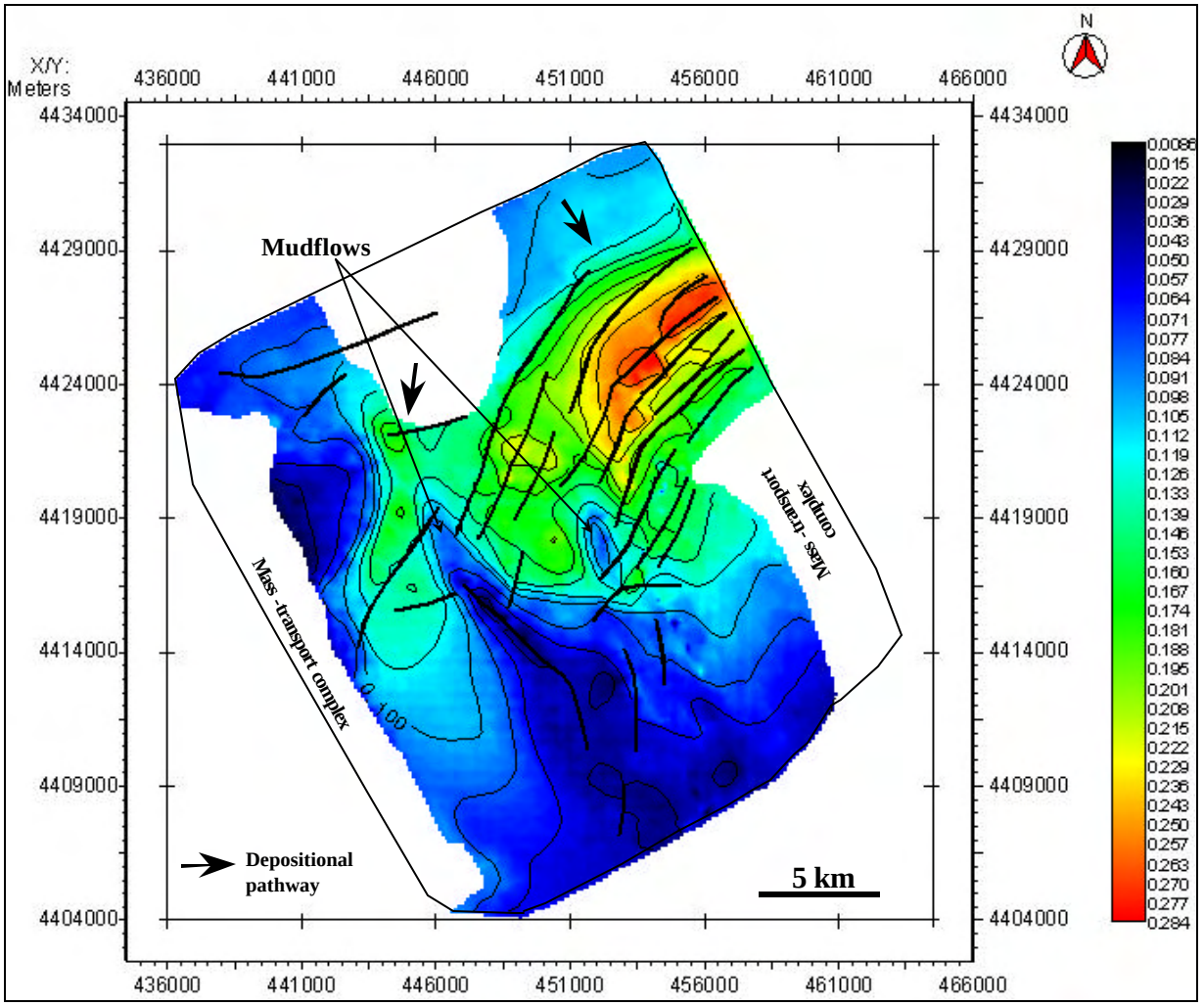

Figure 5.11. Isochron map showing two depocenters and depositional pathways of Sequence III. Progradation of shelf-edge delta in the northeastern part. The mudflows are directed northward. The contour interval is 20 ms in two-way travel time.

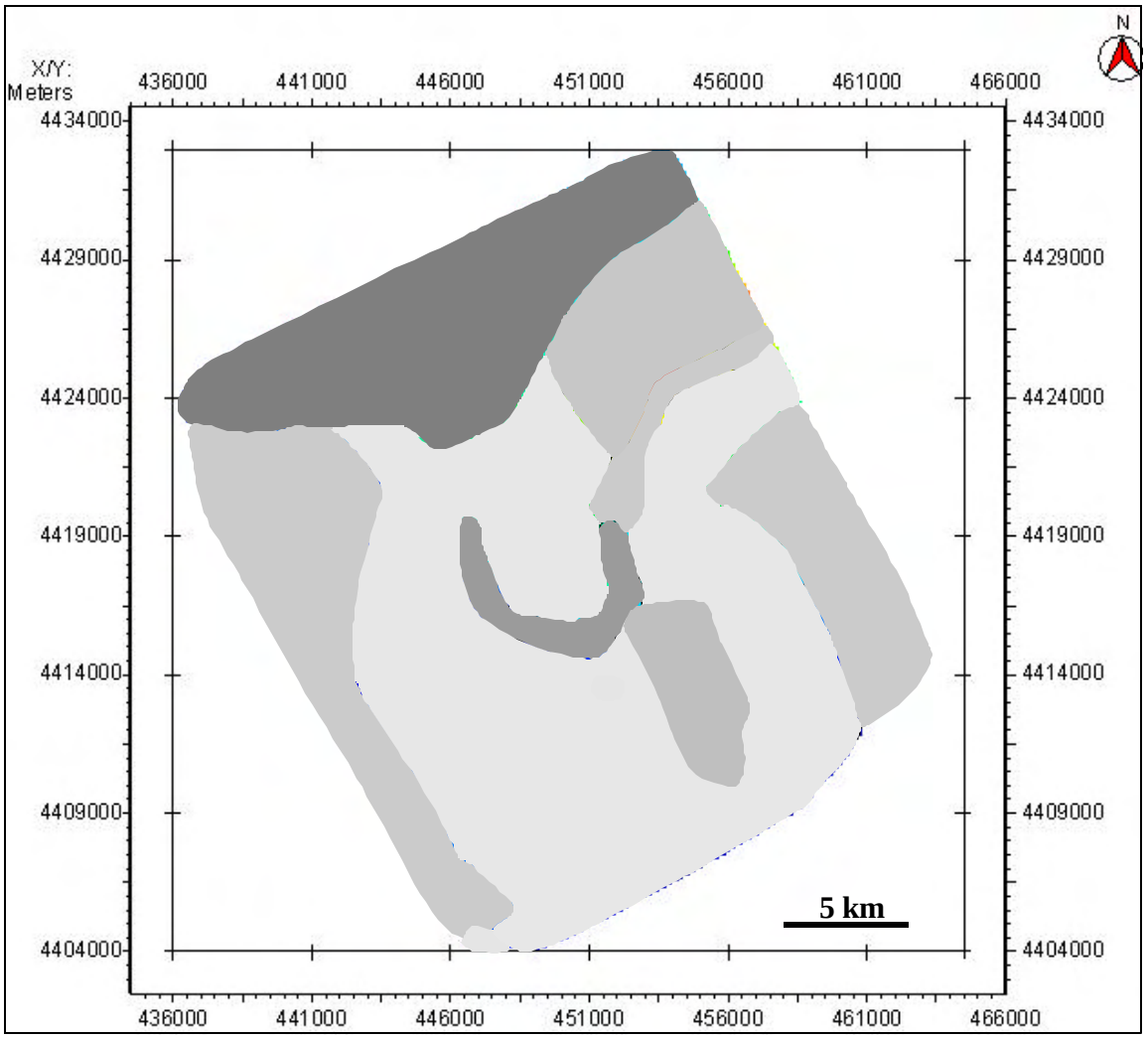

Figure 5.12. Seismic facies distribution map of Sequence III. See Chapter IV for legend and text for detailed discussion.

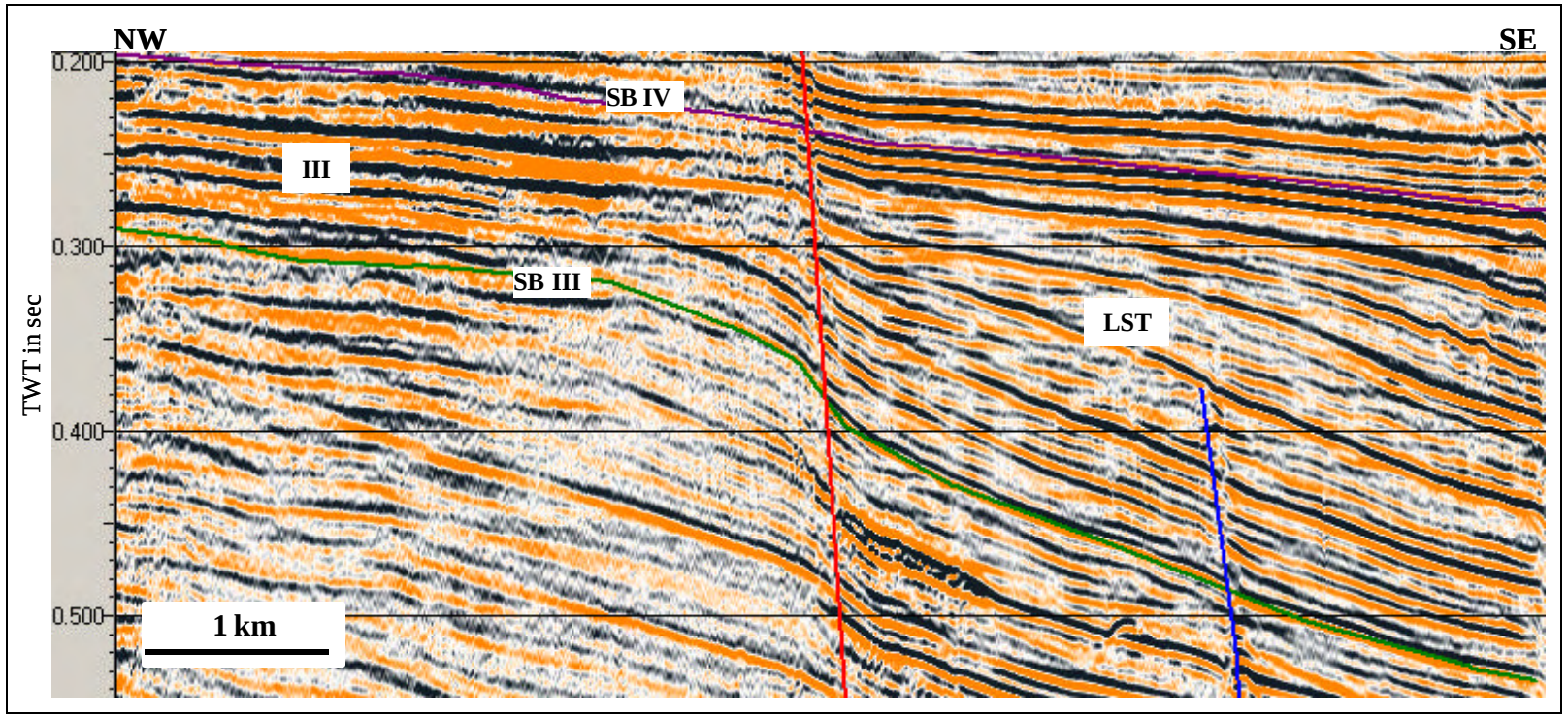

Figure 5.13. Seismic section showing deltaic clinoform within Sequence III. See Figure 5.1 for the location and text for detailed discussion.

the delta at the shelf break. The position of bygone channels leading into the shelf-edge delta cannot be plotted because data for the shelf are insufficient .A moderate- to high-amplitude, parallel to subparallel, variable continuity seismic facies is characterized by an internal seismic reflections package of the lowstand systems tract. Moderate- to high-amplitude is interpreted to indicate thinly interbedded sands with relatively thick shales. In such high-energy environments the upper strong amplitude horizontal reflection is coincident with the surficial layer of sand (Suter and Berryhill, 1975). The high depositional rates combined with enhanced subsidence rates and rapid progradation over the unstable continental shelf margin resulted in the initiation and formation of a massive slope failure at the shelf edge along the eastern part of study area. Slope failure in the form of slides, slumps and viscous debris flow are represented by chaotic facies as a continuing process during the rapid delta outbuilding. The chaotic facies are depicted by high- to low-amplitude, disorganized, discontinuous, nonparallel reflections. The chaotic seismic facies is also observed along the western flank. This facies appears to represent sediment that has slumped during the uplift of an adjacent topographic high. Sequence III contains very bright reflectors that are laterally continuous for up to several kilometers to the south. This type of widespread seismic anomalies indicate the presence of shallow gas in the sediment, which most likely came from mud volcanoes during periods of activity. This appears as a high-amplitude event, as a result of the large impedance contrast between gas and surrounding shallow sediments. Mud volcanoes are characterized by low-amplitude, acoustic wipeout and poor internal coherency seismic

facies. A moderate- to high-amplitude, discontinuous facies is preserved around the central mud volcano, which can be associated with mud volcano flows.

Sequence IV

Sequence IV, the thinnest layer in the study area, is an interval between Sequence Boundary IV and Sequence Boundary V. The age range of Sequence IV is from 51,000 years B.P. to 26,350 years B.P. It therefore represents the late Pleistocene epoch or Lower Khvalyn stratigraphic unit. The sequence is distributed throughout the study area except in the southeastern flank and central south part, where it was truncated by a younger sequence.

Sequence boundary IV is the base of the fourth seismic sequence, which was likely formed by fluvial erosion and deposition during a sea-level lowstand. This boundary is characterized by a strong-amplitude, continuous reflection that is recognizable on the seismic sections. The sequence boundary occurs at depths of shallower than 200 ms and greater than 800 ms in the lower slope area. The two-way time structure map (Figure 5.14) reveals a relatively gently southward dipping and a subsidence into the dormant central mud volcano with faults that cut the eastern part and shelf edge to the northeast. These subparallel faults form numerous narrow horst and graben structures related to basin subsidence and slope instability. The main feature of the two-way time structure map is a position of the shelf edge at 275 ms.

The isochron map in Figure 5.15 represents the interval between Sequence Boundaries IV and V. This interval is the thinnest one and is distributed over all the

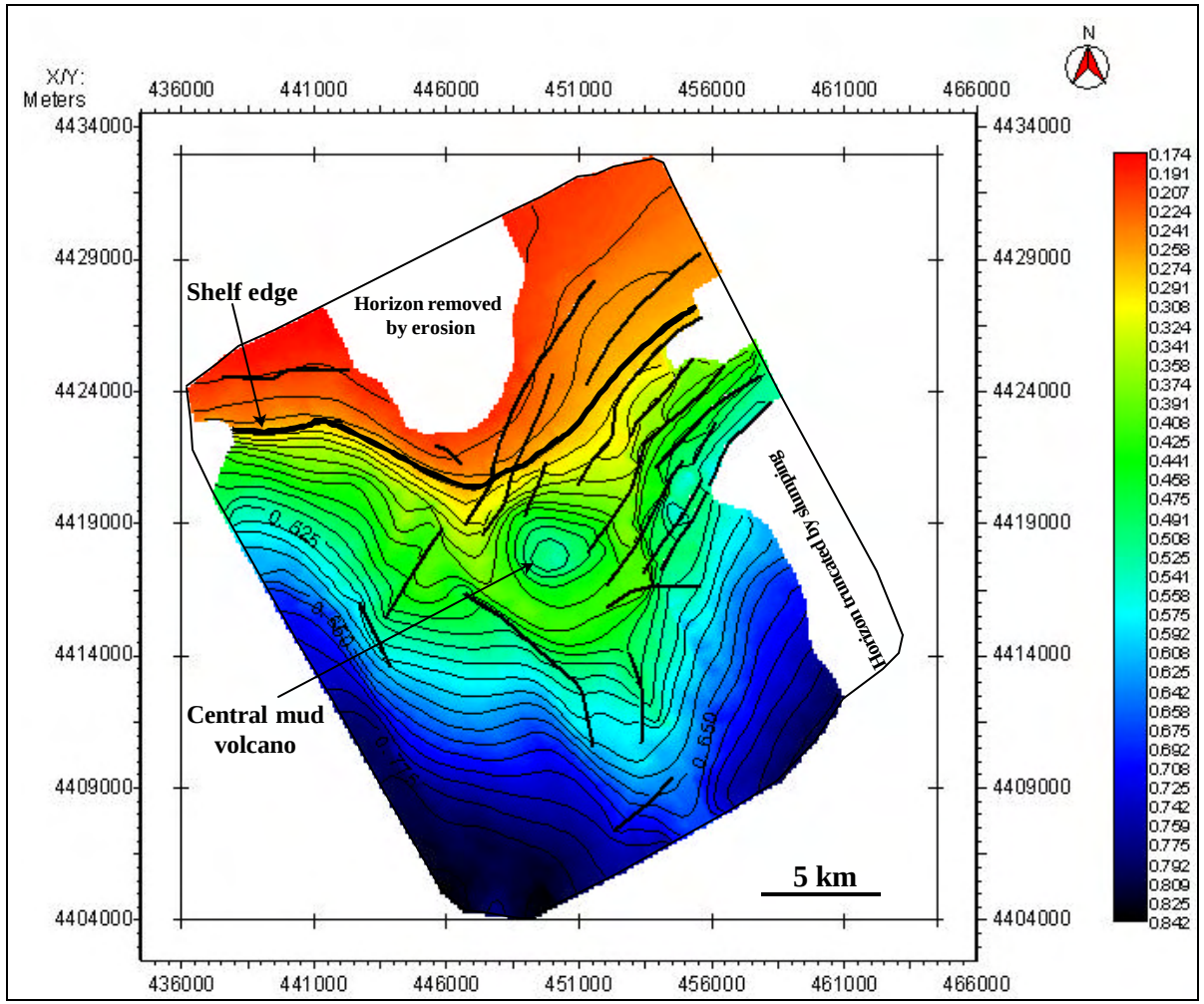

Figure 5.14. Two-way travel time structure map of Sequence Boundary IV. Position of the shelf edge at 275 ms. Northern part of the horizon has been removed by erosion and eastern part has been truncated by slumping. The contour interval is 25 ms.

study area, except the slope failure area in the southeastern part and central north part, where the interval was completely eroded by younger sequences. The thickness of this interval ranges from 10 ms to 120 ms. Three areas of maximum thickness, which represent depocenters, can be recognized in this interval. The first depocenter, which is located in the northwestern part, is associated with the shelf-edge delta and produced an accumulation of sediment with maximum thickness of 130 ms. The second depocenter is located in the central part and is related to subsidence of a mud volcano. Another different feature of Figure 5.15 is an abrupt thickening in the eastern part, as expression of increasing in thickness on the downthrown sides of the parallel step faults.

Sequence IV contains six seismic facies (Figure 5.16). A high-amplitude, parallel, high-continuity reflection configuration facies in the north part of the study area represents the shelf seismic facies. High-amplitude reflections indicate interbedding shales with comparatively thick sandstones facies. High-continuity reflections are interpreted as sediment depositions in a relatively consistent environment (Sangree and Widmer, 1977). Laterally, high-amplitude and high-continuity reflections grade into the undaform part of prograded slope facies. The major seismic facies is a sigmoid progradational clinoform. Sigmoid progradational clinoform is characterized by gentle sigmoid (S-shaped) reflection along the depositional dip. This type of progradational clinoform formed during rapid basin subsidence, and/or rise of sea level with low sediment supply (Sangree and Widmer, 1977). Major shifts of the delta complex from the east to the west may indicate that subsidence has been more significant in the western part of the study area. A moderate- to high-amplitude, parallel to subparallel,

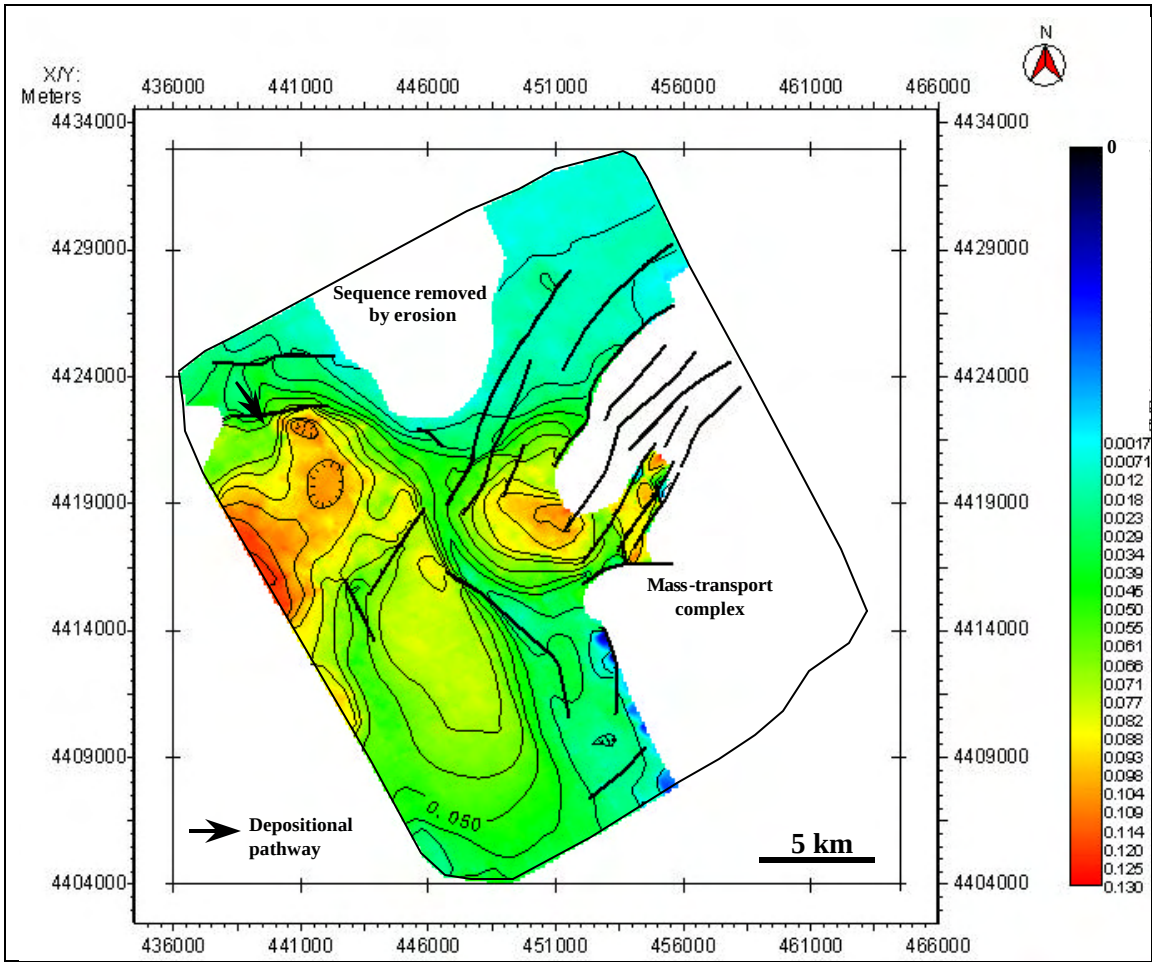

Figure 5.15. Isochron map showing two depocenters and depositional pathway of the Sequence IV. Progradation of shelf-edge clinoform in the northwestern part. Sequence has been removed by erosion in the north and integrated into mass-transport complex in the east. The contour interval is 10 ms in two-way travel time.

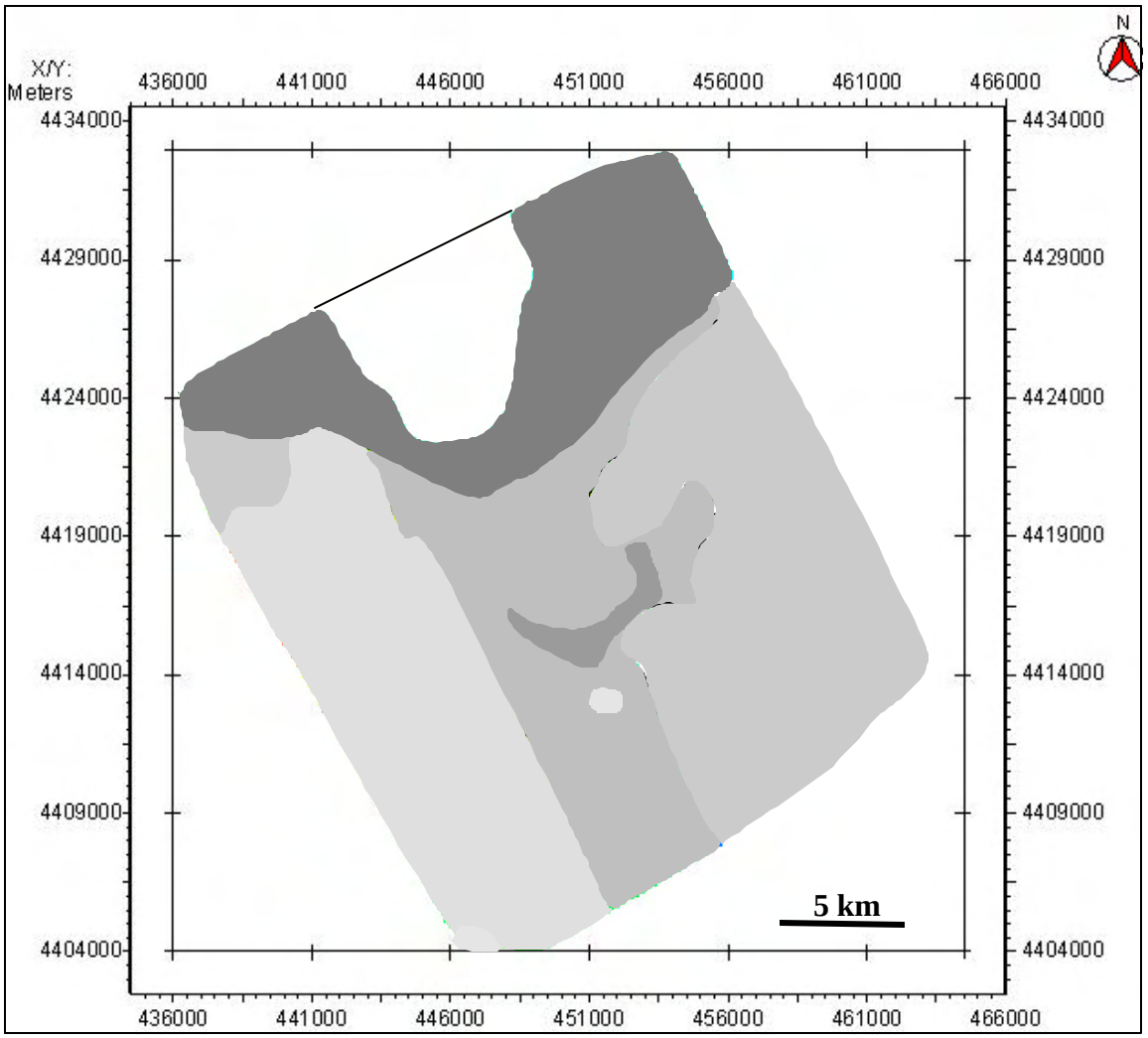

Figure 5.16. Seismic facies distribution map of Sequence IV. See Chapter IV for legend and text for detailed discussion.

high-continuity reflection configuration seismic facies characterizes Sequence IV. Moderate- to high-amplitude is interpreted to indicate low-energy turbidity currents. This sequence can be divided into three subsequences with identical internal seismic descriptions bounded by a series of minor sequence boundaries marked by widespread subaerial exposure but little truncation (Figure 5.17). The reason for development of minor sequence boundaries may be a rapid relative fall in sea level coupled with a low supply of sediment. This sequence shows a retrogradational stacking pattern; i. e., younger subsequences are successively displaced landward. The retrogradational stacking pattern indicates that the increase of accommodation exceeds the sediment supply (Van Wagoner et al., 1988). Little or no fluvial deposit is preserved at the base of the sequence; in this case a transgressive systems tract lies directly on the sequence boundary (Miall, 1996). Sequence IV can be interpreted as sequence, that includes three cycle of transgressive systems tract because of its retrogradational or backstepping character separated by lowstand systems tract. On the eastern part of study area, the large zone of chaotic facies has been interpreted to indicate of extensive development of slope failure. High- to low-amplitude, disorganized, nonparallel and discontinuous reflections characterize this facies. The same seismic facies are observed on the southwestern part. Slope failure deposits as a result of collapse, slide and slump processes are interpreted to have been derived from the shelf edge in the northwest toward the basin in the southwest. Massive slide, slumps, and debris flow over an area of 150 km^2 must be related to slope instability caused by high sedimentation rates combined with tectonic instability. A moderate- to high-amplitude, discontinuous facies

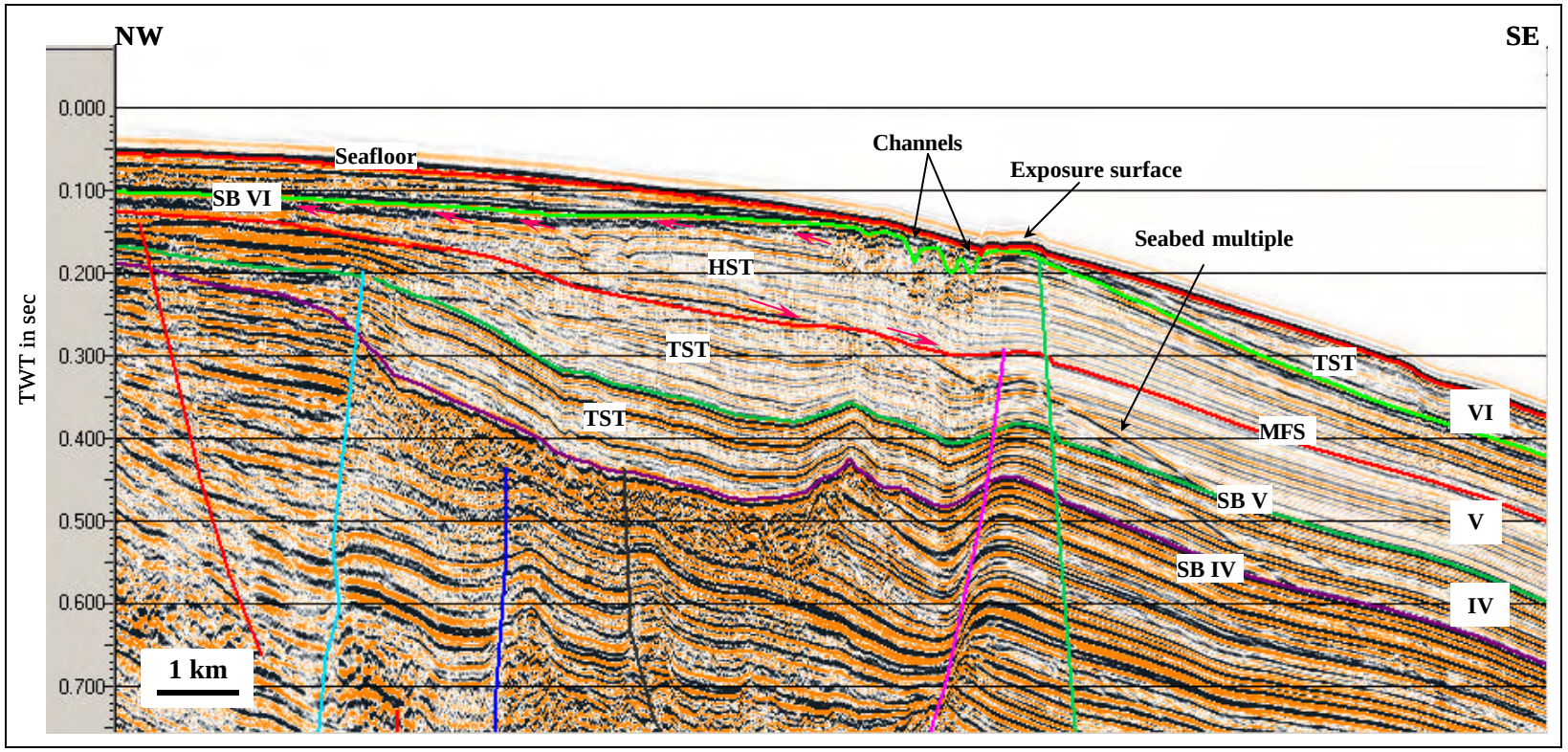

Figure 5.17. Seismic section shows development of a sigmoid progradational clinoform within Sequence IV, tangential oblique progradational facies within Sequence V, erosional channels and exposure surface associated with Sequence VI. See Figure 5.1 for the location and text for detailed discussion.

preserved around a central mud volcano can be associated with mud volcano flows. Mud volcanoes are characterized by low-amplitude, acoustic wipeout and poor internal coherency seismic facies.

Sequence V

Sequence V is an interval between Sequence Boundary VI and Sequence Boundary VI. The age range of Sequence V is from 26,350 years B.P. to 11,500 years B.P. It therefore represents the late Pleistocene epoch or Upper Khvalyn stratigraphic unit.

This sequence is distributed throughout the study area, except the southeastern flank. The southeastern part is defined as a slope failure area and interpreted as related to slope instability that has occurred during the period of deposition of Sequence V. On the seismic section this sequence can be recognized by its erosional bounded surfaces at the base and top.

Sequence Boundary V is the base of the fifth seismic sequence. This boundary is characterized by strong amplitude, continuous reflections. The event is obscured by strong sea-bed multiples. Sequence Boundary V occurs at a depth of 160 ms in the shelf areas and greater than 800 ms in the slope areas. Based on reflection configuration and erosion nature, this surface is interpreted to have been formed during a relative fall in sea level or lowstand systems tract. Figure 5.18 shows the two-way time structure map of the Sequence Boundary V. The two-way time structure map reveals the overall dip direction to the southwest resulting from depositional slope and subsidence into the

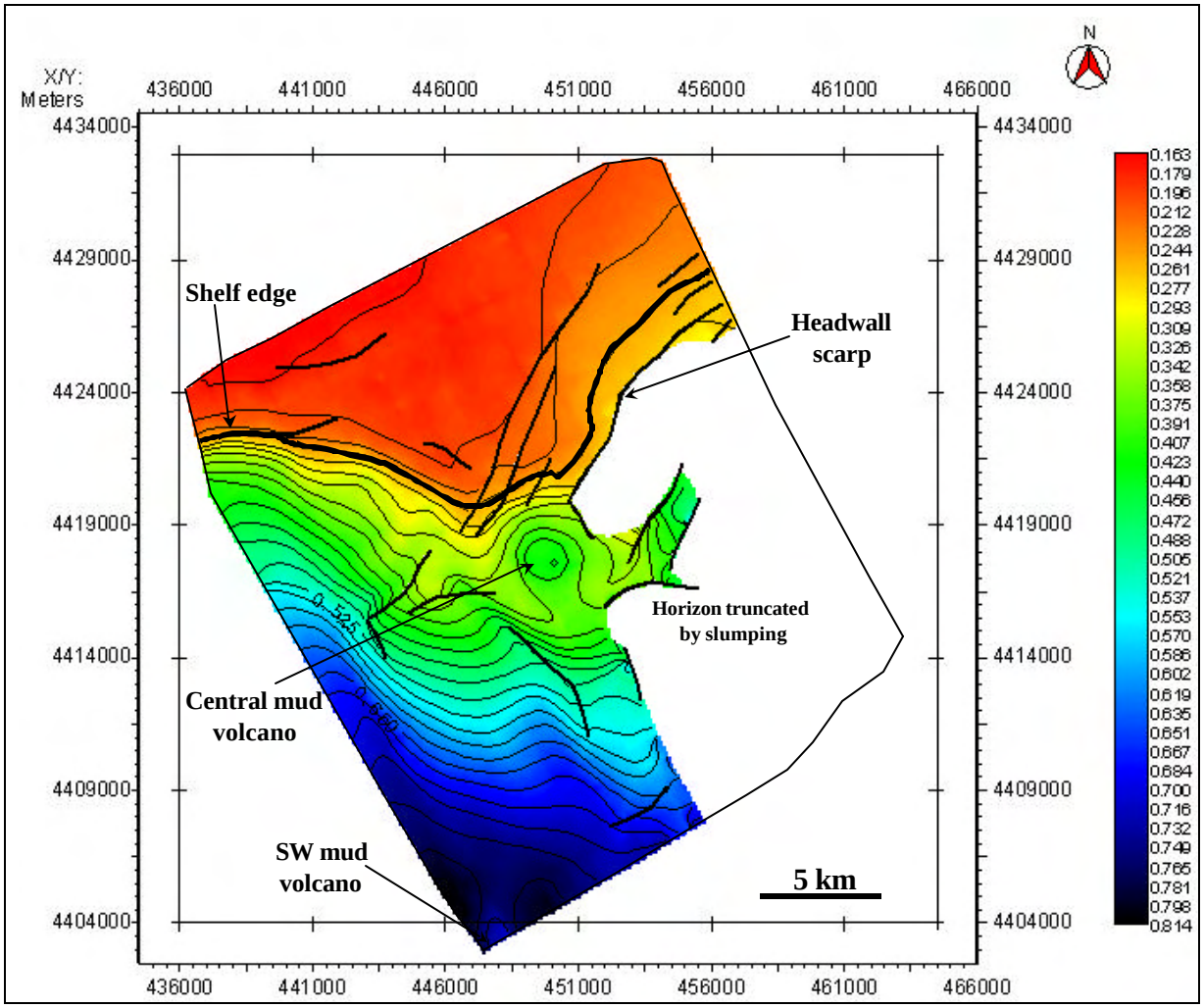

Figure 5.18. Two-way travel time structure map of Sequence Boundary V. Position of the shelf edge at 250 ms. The white polygon delineates the areas where the horizon has been truncated by slumping. The contour interval is 25 ms.

dormant central caldera mud volcano. Another dominant feature of the two-way time structure map is the position of the shelf edge at 250 ms.

The isochron map in Figure 5.19 represents the interval between Sequence Boundaries V and VI. I mapped this interval throughout the study area, except the slope failure area in the southeastern flank. The thickness of this interval ranges from 80 ms to 345 ms. Two areas of maximum thickness can be recognized. The first depocenter, which is located in the western part of the area, is related to the shelf-edge deltaic outbuilding and produced the accumulation of sediment with maximum thickness of 345 ms within 6 km of the shelf break. Isochron map patterns show the delta to be constrained by their position at the shelf edge. Figure 5.19 shows the areal extent and thickness distribution of sediments in the delta complex. The second depocenters, indicated by the accumulation of sediment with maximum thickness of 225 ms, is located in the central part of the area and associated with a mud volcano. Thickening of Sequence V into the caldera of the mud volcano is the result of increased accommodation space following subsidence. The reason for this subsidence after mud volcanism ceased probably reflects differential compaction of the underlying mud volcano.

Sequence V consists of seven seismic facies (Figure 5.20). High-amplitude, parallel, high-continuity reflection configuration facies in the north part of the study area represent the shelf seismic facies. High-amplitude reflections suggest interbedded shales with relatively thick sandstones facies. High-continuity reflections are interpreted as sediment deposition in a relatively uniform environment (Sangree and Widmer, 1977).

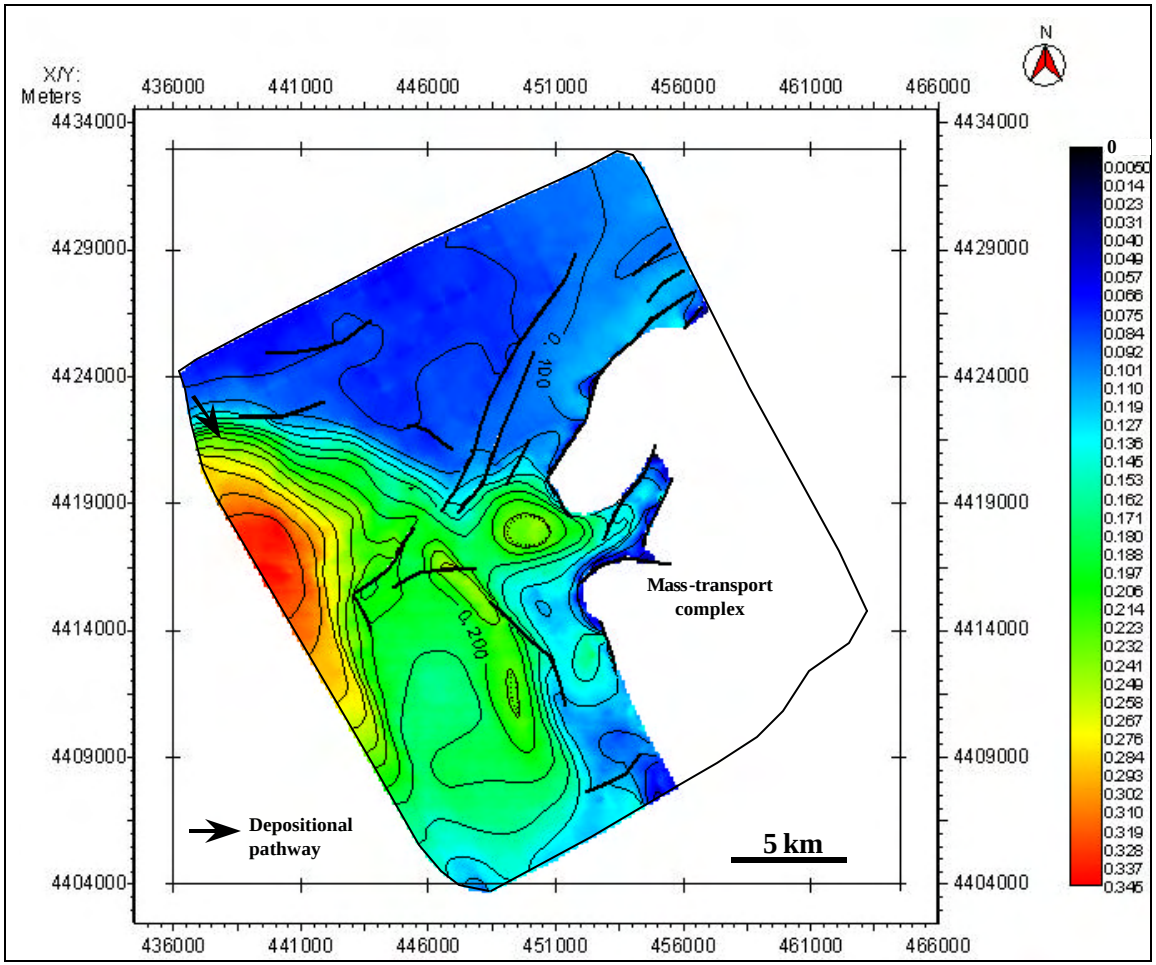

Figure 5.19. Isochron map showing two depocenters and depositional pathway of Sequence V. Progradation of shelf-edge clinoform in the northwestern part. Sequence has been integrated into mass-transport complex in the east. Mass-transport complex is limited to the north by headwall scarp. The contour interval is 20 ms in two-way travel time.

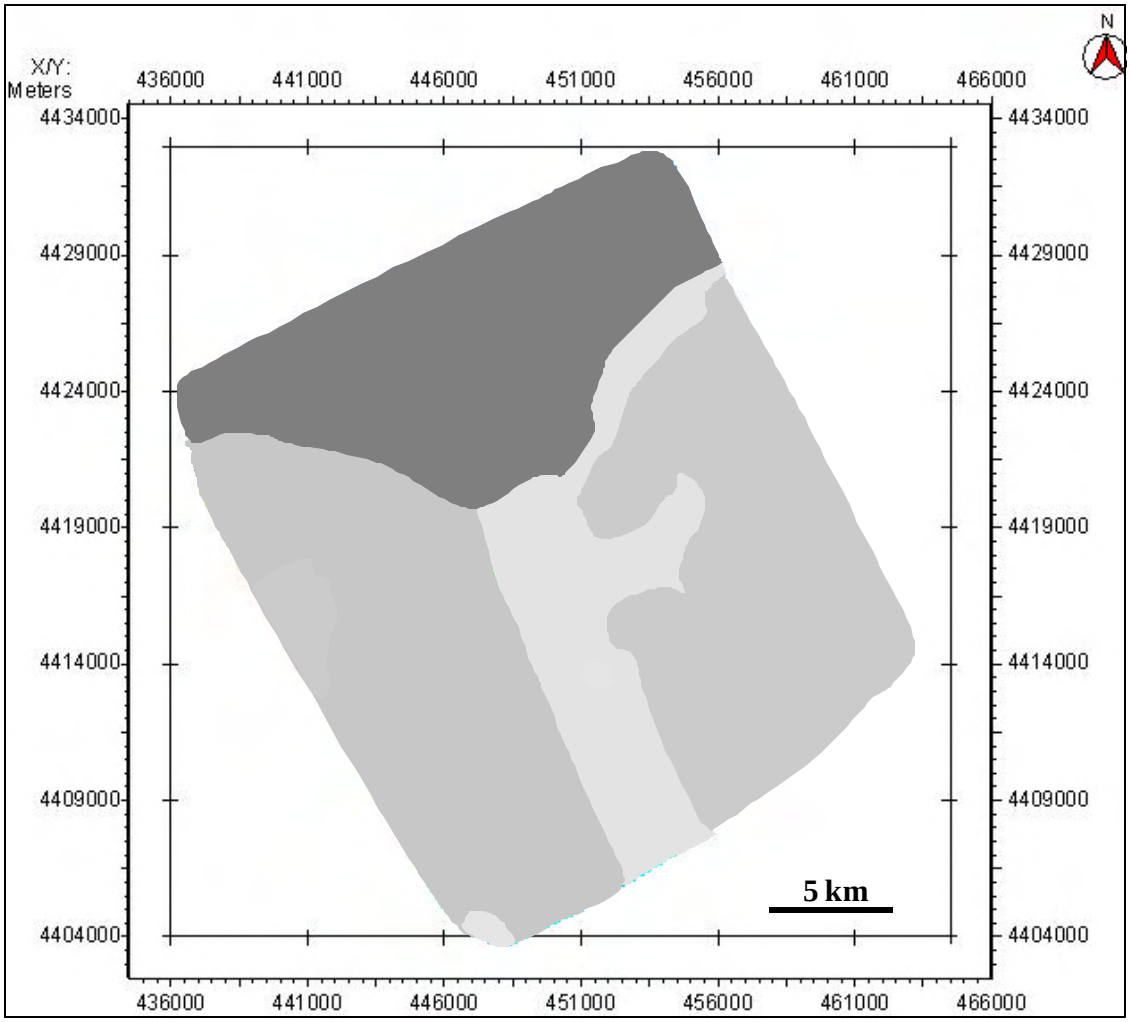

Figure 5.20. Seismic facies distribution map of upper portion of Sequence V. See Chapter IV for legend and text for detailed discussion.

The major seismic facies is an oblique-prograding clinoform. The truncation of reflectors at the upper boundary of the sequence suggest erosion and their classification as tangential oblique-progradational facies (Figure 5.17). In the study area, this seismic pattern occurs on the shelf edge; hence, it is characteristic of fluvial deltas. In a high-energy depositional environment such as tangential oblique-progradational facies, the upper horizontal reflection event is coincident with the surficial layer of sand (Berg, 1982). Seismic reflections within Sequence V indicate that this sequence can be subdivided into lower and upper portions because of the superposition of different seismic facies. A moderate- to high-amplitude, parallel, high-continuity seismic facies characterizes the lower portion. Moderate to high amplitudes are interpreted to indicate thinly interbedded sand with relatively thick shales. In contrast, the upper portion is characterized by a low- to moderate-amplitude, parallel to subparallel, moderate- to high-continuity reflection configuration; the portions are separated by a downlap surface, which is clearly recognizable as a high-amplitude, continuous reflector and easily followed throughout the area. Low to moderate amplitudes, typically correspond to a dominant shale content of the prodelta facies (Sangree and Widmer, 1977). Based on the bounding surface, their position within the sequence, and reflection packages, the lower portion of Sequence V is interpreted to have been deposited during a relative rise in sea level and defined as the transgressive systems tract. The upper portion of Sequence V is characterized by the time of maximum regression and an increasingly progradational stacking pattern rather than aggradational of the shelf edge and interpreted to be deposited during highstand sea level. The base of this systems tract is a downlap surface

or a maximum flooding surface that separates the transgressive and highstand systems tracts. The chaotic facies occurs along the eastern part and within the upper part of the sequence in a small, isolated area on the western flank. This facies are represented by high- to low-amplitude, disorganized, nonparallel and discontinuous reflections. They are interpreted as slope failures that suggest mass transport of sediment downslope (Sangree and Widmer, 1977). In the eastern part, slope failure has affected an area of at least 150 km^2 and probably a more extensive area to the east. This large-scaled slope failure is interpreted as a slump, and debris flow must be related to slope instability caused by rapid deposition and tectonic activity. The slope failure is clearly related to masses of sediment displaced from the shelf edge or the shelf-slope transition zone extending basinward. It also appears to represent sediment that has slumped during the uplift of an adjacent topographic high. The area of extensive slope failures is separated from the unfailed part by a headwall scarp that trends northwest. On the north, the main headwall scarp turns to the east and extends along the shelf edge to the eastern limit of the area. On the lower southwestern corner of the study area, another type of chaotic seismic facies is present. This seismic facies is characterized by the low-amplitude, acoustic wipeout and poor internal coherency associated with a mud volcano. A moderate- to high-amplitude, discontinuous facies is preserved around the central mud volcano associated with mud volcano flows.

Sequence VI

Sequence VI, the youngest sequence found in the study area, is an interval between Sequence Boundary VI and the sea floor. The age range of Sequence VI is from 11,5000 years B.P. to the present. It therefore represents the Holocene epoch or Novocaspian stratigraphical unit.

Sequence boundary VI is the base of the sixth seismic sequence. On the seismic sections, this boundary is characterized by strong amplitude, continuous to discontinuous reflections. As an unconformity surface, Sequence Boundary VI can be recognized by truncation of the older layers below and onlap above the seismic surface. This sequence boundary surface occurs at a depth of 90 ms in the shelf areas and greater than 700 ms in the slope areas. Figure 5.21 shows the two-way time structure map of Sequence Boundary VI. The time structure map reveals that this surface is greatly influenced by a depositional basin configuration. This sequence surface progressively deepens toward the southeast, its surface characterized by paleohighs and lows that can be recognized in the center and the northeastern part of the study area, respectively. The dominant feature of the time structure map of Sequence Boundary VI is a position of the shelf edge at 200 ms and a paleopromontory. A couple of phenomena could explain the origin and existence of the paleopromontory: local tectonic uplift related to central mud volcano activity, resistance to erosion. A sequence boundary surface is associated with incised, V-shaped erosional channels that cut down through the underlying sequence, clearly recognizable on the west side of the study area. To the south, the sequence boundary is truncated by the present-day sea floor. In the east parallel step normal faults cut this

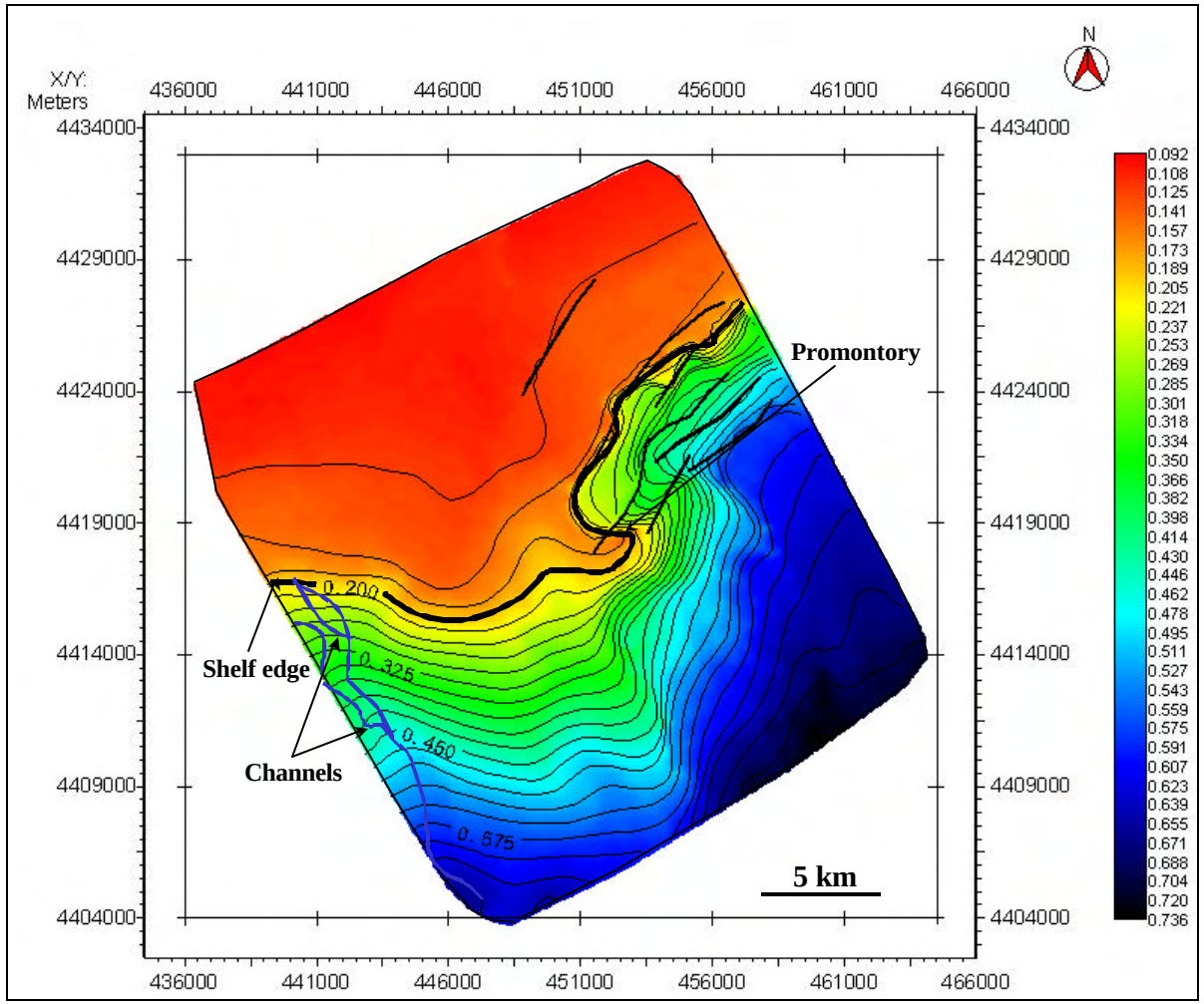

Figure 5.21. Two-way travel time structure map of Sequence Boundary VI. Position of the shelf edge at 200 ms. Erosional channels are observed in the western part. The contour interval is 25 ms.

sequence boundary. These faults are the same cut through Sequence Boundaries I to VI.

The isochron map in Figure 5.22 represents the interval between Sequence Boundary VI and the sea floor. This interval is the youngest layer in the study area and can be recognized in most parts of the study area, except in the central-southern portion where sequence is truncated by the seafloor. The thickness of this interval ranges from 0 ms to 160 ms. Two areas of maximum thickness, which represent depocenters, can be recognized related to this interval. The isochron map suggests that the depocenters, which are indicated by accumulation of the sediments, were related to two depositional pathways. The first pathway came from the north on the west side and mainly fed the depocenters caused by channel distribution that can be traced from the upper slope area down to the lower slope. Channels are best identified on seismic lines that run parallel to depositional dip. The second fairway came from the north on the east side and produced the accumulation of sediment with maximum thickness of 160 ms. The isochron map shows an increase in thickness to the south-southeast as abrupt thickening occurs on the downthrown sides of the parallel step normal faults.

Sequence VI contains three major seismic facies (Figure 5.23). A high-amplitude, parallel, high-continuity reflection configuration facies occurs in the north part of the study area. This type of seismic facies deposited on the shelf represents the shelf seismic facies. High-amplitude reflections suggest interbedded deposition of shales with relatively thick sandstones (Sangree and Widmer, 1977). High-continuity reflections are interpreted as sediment deposition in a relatively uniform environment. In the depositional dip direction, shelf seismic facies transit into moderate- to high-

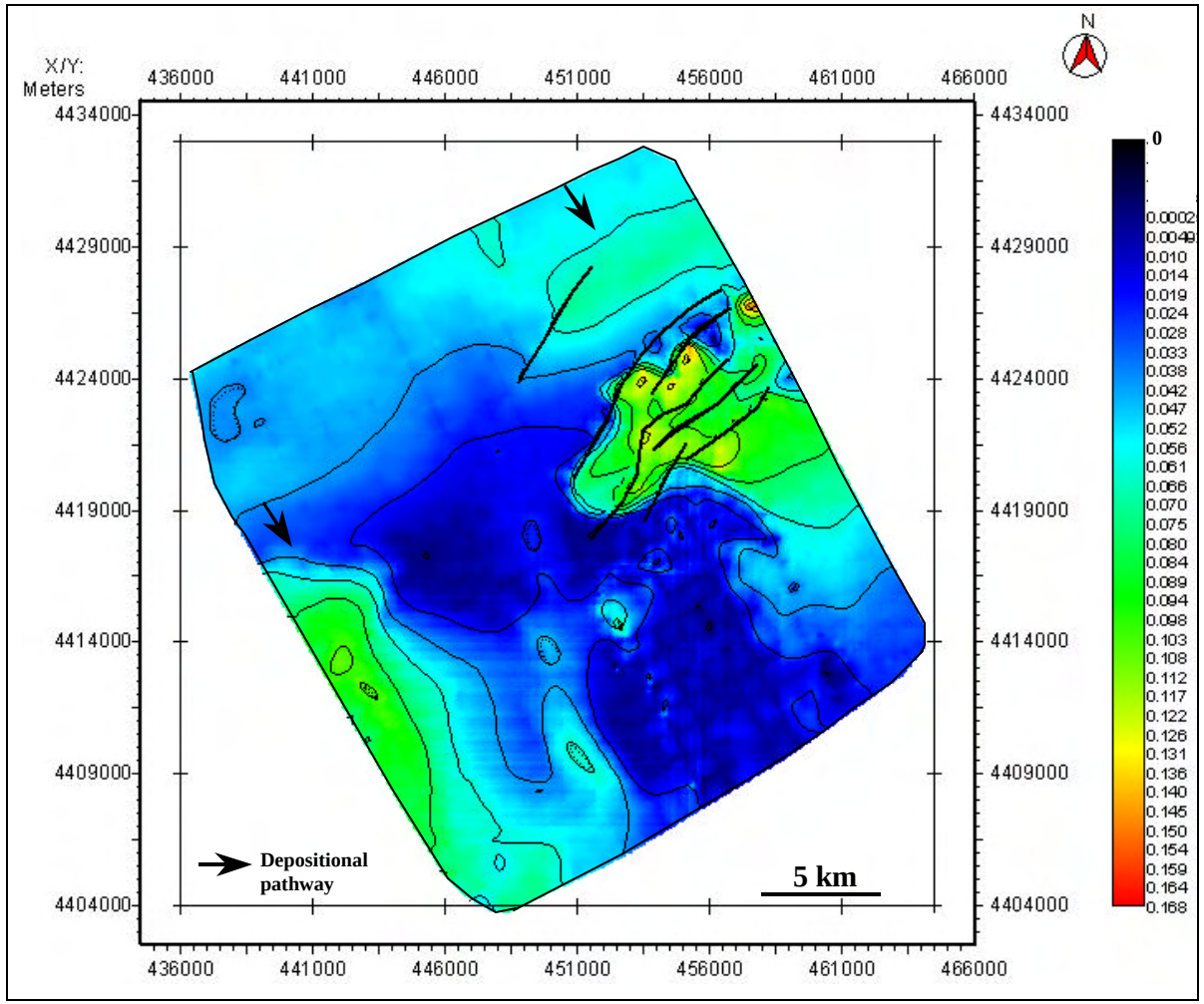

Figure 5.22. Isochron map showing two depocenters and depositional pathways of Sequence VI. The contour interval is 20 ms in two-way travel time.

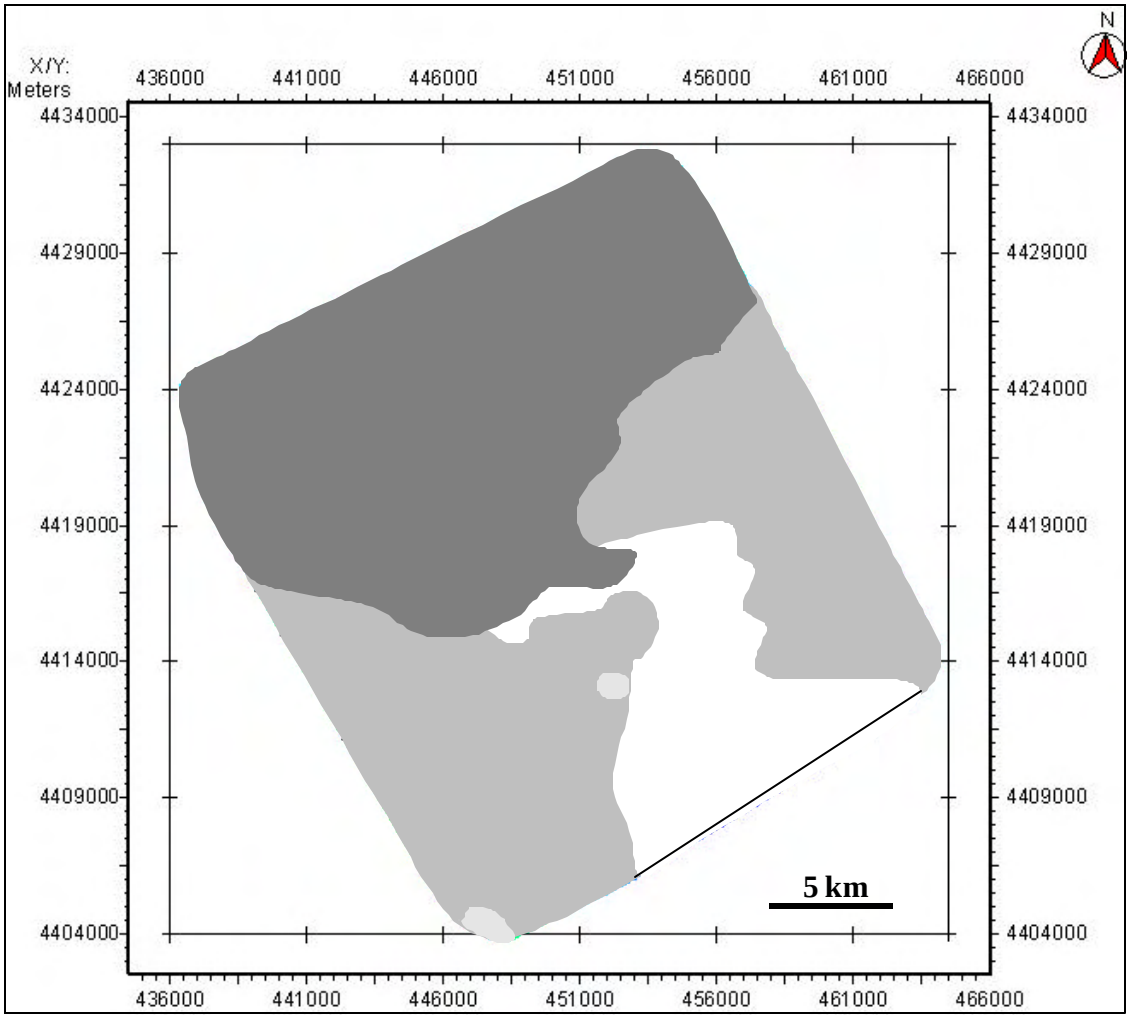

Figure 5.23. Seismic facies distribution map of Sequence VI. The white polygon delineates the areas where the sequence has been eroded. See Chapter IV for legend and text for detailed discussion.

amplitude, parallel to subparallel, and high-continuity reflection configuration slope seismic facies. Moderate to high amplitude are interpreted to indicate of thinly interbedded sands with relatively thick shales. These thin sands may indicate a series of small regressions in sea level during Holocene time (Kosarev and Yablonskaya, 1994), allowing coarser material to be carried downslope. Parallel patterns of continuous reflections created by widespread parallel strata are probably the expression of low-energy deposits. The upward shift of coastal onlap patterns of this seismic facies on the shelf indicates a relative rise in sea level. This package is therefore interpreted as the transgressive systems tract. On the western part of study area, this facies type overlies the incised erosional channels (Figure 5.17). The sides of the channel may consist of reflectors that dip toward the center of the channel. A high-energy depositional regime is suggested by the configuration of reflectors. This is therefore interpreted as the lowstand systems tract. If coarse sand is present at the source, these channels could perform as conduits for sand to be transported into the lower slope and basinward. Low-amplitude, acoustic wipeout and poor internal coherency seismic facies represent mud volcanoes.

CHAPTER VI

SUMMARY AND CONCLUSIONS

The results presented herein are believed to contribute to a better understanding of the depositional history of the late Pleistocene - Holocene on the northwestern margin of the SCB within a sequence stratigraphic analysis. The following main conclusions have been drawn from this study:

1. The late Pleistocene - Holocene strata in the study area were deposited in the continental shelf and slope on the northwestern margin of the SCB. The shelf dips gently to the north and west, and the slope region dips moderately to the south and southwest beyond the shelf edge.

2. Six late Pleistocene - Holocene sequence boundaries and downlap surface within Sequence VI, interpreted as flooding surface that separates the transgressive systems tract from the highstand systems tract, have been identified in this study.

3. It is clear from the two-way time structure map of sequence boundaries that shelf edges progradate basinward through time as a result of the large influx of clastic sediments.

4. The late Pleistocene - Holocene interval in the study area can be divided into six major seismic sequences bounded by erosional unconformities at their tops and bottoms.

5. Six isochron maps provide a detailed picture of the temporal and spatial distribution of the late Pleistocene - Holocene sedimentation on the northwestern margin

of the SCB. Analysis of isochron maps suggests that the areas of maximum thickness related to the depocenters include (1) large-scale slumping and other mass-movement processes, (2) shelf-edge deltaic outbuilding, (3) adjacence to cone-shaped mud volcano flows, (4) subsidence of mud volcano, (5) downthrown sides of parallel step faults. Isochron maps of each sequence reveal that the dominant direction of sediment transport is from the northwest to the southeast.

6. Growth faults, counter regional fault, parallel step faults, and ring faults associated with collapse structure mud volcano are the major fault types in the study area.

7. Numerous of geologic drilling hazards are present in the study area. These are mud volcanoes, sediment instability, and shallow gas.

8. Diverse depositional processes on the northwestern margin of the SCB are suggested by the thirteen seismic facies patterns recognized in the study area.

9. Sequence stratigraphy analysis of sedimentary strata from 117,000 years B.P. to present led to the identification of a highstand systems tract, two transgressive systems tract and six lowstand systems tracts. Each systems tract is characterized by the specific seismic facies associated with it. The highstand systems tract are characterized by low- to moderate-amplitude, parallel to subparallel, moderate- to high-continuity facies. Moderate- to high-amplitude, parallel, high-continuity facies characterize seismic facies of transgressive systems tract. The lowstand deposits within sequences can be recognized by moderate- to high-amplitude, parallel to subparallel, variable continuity facies.

10. Two distinct progradational complexes were interpreted within Sequence III and Sequences IV and V in the northeastern and northwestern parts of the study area, respectively. The progradational complex of Sequence III in the northeastern part is characterized by a tangential oblique-progradational clinoform; and the progradational complex in the northwestern part is characterized by a sigmoid-progradational clinoform (Sequence IV) developing into a tangential oblique-progradational clinoform (Sequence V) at later stages of its deposition.

11. The lake experienced abundant high-frequency and high-amplitude fluctuations in level. These lake-level changes are believed to have been controlled by an interaction of tectonic and climatic factors. Climate-driven fluctuations of the lake level may be related to Milankovitch-type climatic variations. Changes in lake level have a major impact on the rate of sediment supply, accommodation space and depositional environments. Rapid sedimentation rates on the northwestern margin of the SCB during the late Pleistocene - Holocene averaged more than 5 m/1000 years. Rapid fluctuations in the lake level, high rate and type of sediment supply, proximity to the shelf edge, tectonic dynamics and mud volcano activity are the principal factors for sedimentation on the northwestern margin of the SCB.

REFERENCES CITED

Abdullayev, N. R., 2000, Seismic stratigraphy of the Upper Pliocene and Quaternary deposits in the South Caspian Basin: Journal of Petroleum Science and Engineering, v. 28, p. 207-226.

Abrams, M. A., and A .A. Narimanov, 1997, Geochemical evaluation of hydrocarbons and their potential sources in the western South Caspian depression, Republic of Azerbaijan: Marine and Petroleum Geology, v.14, p. 451-468.

Anderson, A. L., and W. R. Bryant, 1990, Gassy sediment occurrence and properties: northern Gulf of Mexico: Geo-Marine Letters, v. 10, p. 209-220.

Belopolsky, A. V., and M. Talwani, 2000, Petroleum reserves and potential of the Greater Caspain region: AAPG International Conference and Exhibition, p. 49-51.

Berg, O. R., 1982, Seismic detection and evaluation of delta and turbidite sequences: their application to exploration for the subtle trap: AAPG Bulletin, v. 66, no. 9, p. 1271-1288.

Boulin, J., 1991, Structures in southwest Asia and evolution of the eastern Tethys: Tectonophysics, v. 196, p. 211-268.

Bouma, A. H., 1981, Introduction to offshore geologic hazards, *in* Offshore geologic hazards: American Association of Petroleum Geologists, Education Course Notes Series No. 18, p. 1-1 – 1-101.

Bozkurt, G., D. Nummendal, and D. Eichen, 1997, Sequence stratigraphy of the Pleistocene Amu Darya Delta on the Turkmen sector of the Caspian Sea: SEG Annual Meeting Expanded Abstracts, p. 613.

Brown, Jr. L. F., and W. L. Fisher, 1977, Seismic stratigraphic interpretation of depositional systems: examples from Brazilian rift and pull-apart basins, *in* C. E. Payton, ed., Seismic stratigraphy-application to hydrocarbon exploration: AAPG Memoir 26, p. 213-248.

Burdick, D. J., and W. C. Richmond, 1982, A summary of geologic hazards for proposed OCS oil and gas lease sale 68, southern California: United States Department of the Interior, Minerals Management Service, and Geological Survey, Open-File Report 82-33, 38 p.

Buryakovsky, L. A., G. V. Chilingar, F. Aminzadeh, 2001, Petroleum geology of the South Caspian Basin: Boston, Gulf Professional Publishing, 442 pp.

Carlson, P. R., M. Golan-Bac, H. A. Karl, K. A. Kvenvolden, 1985, Seismic and geochemical evidence for shallow gas in sediment on Navarin continental margin, Bering Sea: AAPG Bulletin, v. 69, p. 422-436.

Edwards, M. B., 2000, Origin and significance of retrograde failed shelf margins; tertiary northern Gulf coast basin: Gulf Coast Association of Geological Societies Transactions, v. 50, p. 81-94.

Emery, D., and K. J. Myers, 1996, Sequence stratigraphy: London, Blackwell Science, 297p.

Fowler, S. R., J. Mildenhall, S. Zalova, G. Riley, G. Elsley, A. Desplanques, F. Guliyev, 2000, Mud volcanoes and structural development on Shah Deniz: Journal of Petroleum Science and Engineering, v. 28, p. 189-206.

Galloway, W. E., 1998, Siliciclastic slope and base-of-slope depositional systems: component facies, stratigraphic architecture, and classification: AAPG Bulletin, v. 82, no. 4, p. 569-595.

Guliyev, I. S., and A. A. Feizullayev, 1996, Geochemistry of hydrocarbon seepages in Azerbaijan, *in* D. Schumacher and M. A. Abrams, eds., Hydrocarbon migration and its near-surface expression: AAPG Memoir 66, p. 63-70.

Jones, R. W., and M. D. Simmons, 1997, A review of the stratigraphy of Eastern Paratethys (Oligocene – Holocene), with particular emphasis on the Black Sea, *in* Regional and petroleum geology of the Black Sea and surrounding region: AAPG Memoir 68, p. 39-51.

Kosarev, A. N., and E. A. Yablonskaya, 1994, The Caspian Sea: The Hague, SPB Academic Publishing, 259 pp.

Lebedev, L. I., I. A. Aleksina, L. S. Kulakova, Ye. A. Bars, V. A. Gorchilin, Z. P. Yedigaryan, A. A. Narimanov, A. V. Nikishina, N. V. Pashali, Z. M. Skulskaya, D. S. Turovski, V. N. Kholodov, Kh. B. Yusufzadeh, 1987, Kaspiyskoe More: Geologiya i Neftegazonosnost': Moscow, Nauka, 296 pp (in Russian).

Lerche, I., A. Ali-Zadeh, I. Guliyev, E. Bagirov, R. Nadirov, M. Tagiyev, A. Feizullayev, 1997, South Caspian Basin: stratigraphy, geochemistry and risk analysis: Baku, Nafta-Press, 429 pp.

MacDonald, I. R., D. B. Buthman, W. W. Sager, M. B. Peccini, N. L. Guinasso, 2000, Pulsed oil discharge from a mud volcano: Geology, v. 20, p. 907-910.

Mamedov, P. Z., 1992, Seismostratigraphicheskie issledovaniya v Kaspiyskom more: Avtoreferat, Baku, AzGNA, 40 p.

Mangino, S., and K. Priestley, 1998, The crustal structure of the southern Caspian region: Geophysical Journal International, v. 133, p. 630-648.

Miall, A. D., 1996, The geology of fluvial deposits: New York, Springer-Verlag, 582 p.

Mitchum, Jr. R. M., P. R. Vail, and J. B. Sangree, 1977, Seismic stratigraphy and global changes of sea level, Part 6: Stratigraphic interpretation of seismic reflection pattern in depositional sequences, *in* C. E. Payton, ed., Seismic stratigraphy-application to hydrocarbon exploration: AAPG Memoir 26, p. 117-133.

Murphy, S., T. Missiaen, L. Loncke, J.-P. Henriet, 2002, Very high-resolution seismic mapping of shallow gas in the Belgian coastal zone: Continental Shelf Research, v. 22, p. 2291-2301.

Narimanov, A. A., 1990, Late Pliocene stage of geologic development of western shelf of South Caspian Sea: Petroleum Geology, v. 25, p. 344-346.

Narimanov, A. A., 1993, Basin modeling, *in* A. Dore et al. eds., Advances and aplications: NPF Special publication, v. 3, p. 599-608.

Narimanov, A, A., N. A. Akperov, and T. A. Abdullayev, 1998, The Bahar oil and gas condensate field in the South Caspian Basin: Petroleum Geoscience, v. 4, p. 253-258.

Nichols, J., T. Scoular, and P. Hagger, 1998, Development of drilling facilities for a field development in the Caspian Sea: SPE Annual Technical Conference and Exhibition, 741-754.

Nummedal, D.,1999, The Paleo-Volga delta and lacustrine sequence stratigraphy of the South Caspian Basin: Houston Geological Society Bulletin, p. 14-15.

Philip, H., A. Cisternas, A. Gvishiani, and A. Gorshkov, 1989, The Caucasus: an actual example of the initial stages of continental collision: Tectonophysics, v. 161, p. 1-21.

Posamentier, H. W., and P. R. Vail, 1988, Eustatic controls on clastic deposition II-sequence and systems tract models, *in* C. K. Wilgus, B. S. Hastings, C. G. St. C.

Kendall, H. W. Posamentier, C. A. Ross, J. C. Van Wagoner, eds., Sea level changes: an integrated approach: SEPM Special Publication No. 42, p. 125-154.

Rahmanov, R. R., 1987, Mud volcanoes: Moscow, Nedra, 174 pp (in Russian).

Reynolds, A. D., M. D. Simons, M. B. J. Bowman, J. Henton, A. C. Brayshaw, A. A. Ali-Zade, I. S. Guliyev, S. F. Suleymanova, E. Z. Ateava, D. N. Mamedova, and R. O. Koshkarly, 1998, Implications of outcrop geology for reservoirs in the Neogene Productive Series: Apsheron Peninsula, Azerbaijan: AAPG Bulletin, v. 82, no. 1, p. 25-49.

Ruehlman, J. F., M. A. Abrams, and A. A. Narimanov, 1995, The petroleum systems of the West South Caspian Basin: AAPG Covention Abstracts, p. 117.

Sangree, J. B., and J. M. Widmier, 1977, Seismic stratigraphy and global changes of sea level, Part 9: seismic interpretation of clastic depositional facies, *in* Charles E. Payton, ed., Seismic stratigraphy-application to hydrocarbon exploration: AAPG Memoir 26, p. 165-184.

Suter, J. R., and H. L. Berryhill, Jr., 1975, Late Quaternary shelf-margin deltas, northwest Gulf of Mexico: AAPG Bulletin, v. 69, no. 1, p. 77-91.

Vail, P. R., R. M. Mitchum, Jr., and S. Thompson, III, 1977, Seismic stratigraphy and global changes of sea level, Part 3: the depositional sequence as a basic unit for stratigraphic analysis, *in* C. E. Payton, ed., Seismic stratigraphy – applications to hydrocarbon exploration: AAPG Memoir 26, p. 63-81.

Vail, P. R., 1987, Part 1: seismic strartigraphy interpretation procedure, *in* A. W. Bally, ed., Atlas of Seismic Stratigraphy: AAPG Studies in Geology, no. 27, p. 1-10.

Vail, P. R., and W. W. Wornard, Jr., 1991, An integrated approach to exploration and development in the 90s: well log-seismic sequence stratigraphy analysis: Gulf Coast Association of Geological Societies Transactions, v. 41, p. 630-650.

Van Wagoner, J. C., R. M. Mitchum, K. M. Campion, H. W. Posamentier, and P. R. Vail, 1987, Part 2: key definition of sequence stratigraphy, *in* A.W. Bally, ed., Atlas of Seismic Stratigraphy: AAPG Studies in Geology, no. 27, p. 11-14.

Van Wagoner, J. C., H. W. Posamentier, R. M. Mitchum, P. R. Vail, J. F. Sarg, T. S. Loutit, and J. Hardenbol, 1988, An overview of sequence stratigraphy and key definitions, *in* C. K. Wilgus, B. S. Hastings, C. G. St. C. Kendall, H. W. Posamentier, C. A. Ross, J. C. Van Wagoner, eds., Sea level changes: an integrated approach: SEPM Special Publication no. 42, p. 39-45.

Zonenshain, L. P., and X. Le Pichon, 1986, Deep basins of the Black Sea and Caspian Sea as remnants of Mesozoic back-arc basins: Tectonophysics, v. 123, p. 181-211.

APPENDIX A

Determination of vertical seismic resolution

Dominant frequency for the study area was calculated by extracting the wavelet from the seismic line using the TracePak tool of Kingdom Suite software (Figure A-1).

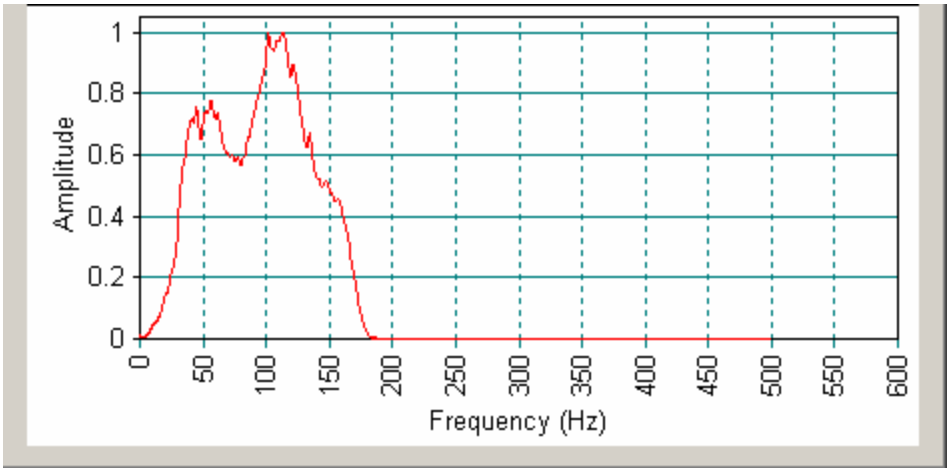

Figure A-1. Frequency spectrum of the study area.

The dominant wavelength of seismic waves is given by the equation $\lambda = v/f$, where v is the velocity and f is the dominant frequency. From Figure A-1, the dominant frequency is approximately 110 Hz. Average seismic velocity is 1800 m/sec. Applying the previous equation, the dominant wavelength is equal 16 m and the acceptable vertical resolution for seismic data is approximately 4 m.

VITA

Name	Ogtay Rasim Rahmanov
Education	B.S. in Geophysics, Azerbaijan State Oil Academy, 1994. M.S. in Geophysics, Texas A&M University, 2003.
Experience	June-August, 2002, Geoscientist, BP Azerbaijan Exploration BU, Sunbury, U.K. June-August, 2001, Geoscientist, BP GoM Deepwater Exploration BU, Houston, U.S.A. August, 1998 – August, 2000, Geophysicist, Reservoir Modeling Center/ State Oil Company of Azerbaijan Republic (SOCAR). January, 1993 – August, 1998, Geophysicist, Azerbaijan Scientific Research Institute of Geophysics/ SOCAR.
Permanent Address	11 Nakhichivanski str., Apt. 12, Baku 370003, Azerbaijan